Université d'Ottawa • University of Ottawa

Université d'Ottawa · University of Ottawa

FACULTÉ DES ÉTUDES SUPÉRIEURES ET POSTDOCTORALES

FACULTY OF GRADUATE AND POSTDOCTORAL STUDIES

John BOUGADIS

AUTEUR DE LA THÈSE - AUTHOR OF THESIS

M. A. Sc. (Civil Engineering)

GRADE - DEGREE

Department of Civil Engineering

FACULTÉ, ÉCOLE, DÉPARTEMENT - FACULTY, SCHOOL, DEPARTMENT

TITRE DE LA THÈSE - TITLE OF THE THESIS

Detection of Trends in Extreme Rainfall in the Province of Ontario

K. Adamowski

DIRECTEUR DE LA THÈSE - THESIS SUPERVISOR

CO-DIRECTEUR DE LA THÈSE - THESIS CO-SUPERVISOR

EXAMINATEURS DE LA THÈSE - THESIS EXAMINERS

R. Frenette

D. Townsend

J.-M. De Koninck, Ph.D.

LE DOYEN DE LA FACULTÉ DES ÉTUDES SUPÉRIEURES ET POSTDOCTORALES

SIGNATURE

DEAN OF THE FACULTY OF GRADUATE AND POSTDOCTORAL STUDIES

Detection of Trends in Extreme Rainfall in the Province of Ontario

by

John Bougadis

M.A.Sc thesis
submitted to the School of Graduate Studies and Research
under the supervision of

Dr. Kaz Adamowski

in partial fulfilment of the requirements for the degree of
Master of Applied Sciences, Civil Engineering*

at the

University of Ottawa
Ottawa, Ontario, Canada

The Master of Civil Engineering Program is a joint program
of the Ottawa-Carleton Institute for Civil Engineering

Your file Votre référence
ISBN: 0-612-90037-1
Our file Notre référence
ISBN: 0-612-90037-1

Abstract

Information on intensity-duration-frequency (IDF) of rainfall is commonly required for the design, construction, and management of many water resources projects involving natural hazards, due to extreme rainfall events. Design storms (DS) are determined from IDF relationships. Many hydraulic structures (dams, weirs, culverts, storm sewer systems, etc) are designed to serve 50 years or more into the future. Yet, these structures are being sized for the climatic conditions based on the past records, before climate change. Thus, new design methods accounting for climatic change are needed to prevent potential losses and damages resulting from under-design. This research addresses the issue of the effect of climate change on design storms. The major objectives of this study is to detect trends in extreme rainfall, and to estimate anticipated changes in return periods of extreme rainfall events due to trends.

In this study, trends (which might be attributed to climate change) are estimated for different durations of annual extreme rainfall using the regional average Mann-Kendall's S trend test. The method of L-moments was employed to delineate homogeneous regions. The trend test was modified to account for observed autocorrelation, and a bootstrap methodology was used to account for the observed spatial correlation. IDF estimates were computed for different combinations of durations and frequencies (return periods) for rainfall stations experiencing significant increasing trends. These estimates were compared to existing and climate change-induced precipitation extremes and its affect on the frequency (return period) of extreme rainfall events

Numerical analysis was performed on 44 rainfall stations from the province of Ontario, Canada for a 20 and 25 year time frame. This was done using data from homogeneous regions established using L-moments procedure for the annual maximum observations for the following duration: 5, 10, 15, 30 minute, and 1, 2, 6, and 12 hour, respectively. Depending on different rainfall durations, 4 to 6 homogeneous regions were delineated. Numerical analysis was performed for 63 meteorological stations to estimate the magnitude (rate) and direction of trend. Estimates from 15 stations were used to quantify the effect of trend on the frequency of design storms. Significant trends were detected for all durations.

Based on a 5% significance level, approximately 22% of the regions tested had a significant trend, predominantly for short duration storms. Serial dependency was observed in 2.3% of data sets and spatial correlation was found in 19% of the regions. The presence of serial and spatial correlation had a significant impact on trend determination. It was determined that due to the existence of trends the design storms of a given duration might occur more frequently in the future by approximately 31 years depending on the duration and return period.

Acknowledgments

I am truly grateful to my supervisor, Dr Adamowski for his knowledge, time, support, and interests in my thesis research topic. I also would like to thank him for his support in nominating me for a part-time teaching position, and for the amount of time he spent guiding me on my journal papers and presentations, class work, and other projects. Without his assistance, my thesis could not have been completed.

I would also like to thank my family: Patricia, George, Peter and Nikki Bougadis. Their patience and support in me to complete my thesis is much appreciated. I would like to thank my office mates and fellow graduate students: Jocelyn Paquette, Istemi Ozkan, Ayman Dabbas, Farhood Nowzartash, and Patrick Brisson. Their company, encouragement, time, and general advice during my Master's program was greatly needed and appreciated. I would also like to thank my friends for their encouragement and support during my academic studies, and undergraduate students I met along the way for their encouraging words and wisdom. I would also like to thank Maynard James Keenan who taught me to look at issues in a different angle and under a different light.

I would also like to thank professors and administration staff at the University of Ottawa for their support, time, and knowledge. Assistance was also provided by Dr. Cynthia Bocci (geostatistics) and Dr. Ellen M Douglas (bootstrapping). Their technical assistance on my thesis is gratefully appreciated.

Funding for part of this work was provided by NSERC and this is gratefully acknowledged.

Contents

List of Figures

List of Tables

Notation

Greek Characters:

α	=	Constant term in linear regression analysis.
$\hat{\alpha}$	=	Method of moment estimate for the Gumbel distribution..
β	=	Slope term in linear regression analysis.
$\hat{\beta}$	=	Method of moment parameter the Gumbel distribution.
β_r	=	Probability weighted moment.
$\gamma(h)$	=	Variogram ordinate at lag h.
ε	=	White noise error.
θ	=	Measures some aspect of the frequency distribution which is constant in a homogeneous region.
$\hat{\theta}$	=	Parameter of interest in bootstrap procedure.
$\hat{\theta}^{*B}$	=	Estimates of $\hat{\theta}$ based on bootstrap samples Y*.
$\hat{\theta}^{(i)}$	=	At-site estimate of θ based on the data for site i.
$\hat{\theta}^{R}$	=	Regional estimate of θ.
λ	=	Weights in the BLUE procedure.
λ_1	=	First sample L-moment, analogous to the mean.
λ_2	=	Second sample L-moment, analogous to the standard deviation.
λ_3	=	Third sample L-moment, analogous to the coefficient of skewness.
λ_4	=	Fourth sample L-moment, analogous to the coefficient of kurtosis.
μ	=	Mean of a distribution.
ρ_k	=	Population autocorrelation coefficient
ρ_{kk}	=	Population cross correlation coefficient
σ	=	standard deviation of a distribution.
τ_2	=	Ratio of the L-moments λ_2/λ_1. Also termed L-CV.
τ_3	=	Ratio of the L-moments λ_3/λ_2. Also termed L-skew or L-skewness.
τ_4	=	Ratio of the L-moments λ_4/λ_2. Also termed L-kurtosis.

Roman Characters:

a	=	Range of a variogram in geostatistical analysis.
b	=	Estimate of a probability weighted moment.
B	=	Bootstrap samples.
c	=	Coefficient related to exceedance probability to determine rainfall intensity (i).
C_0 & C	=	Used to express the nugget effect (C_0) and sill (C_0 + C) of a variogram.
D	=	Discordance statistic.
e	=	Coefficient in log-linear regression to determine rainfall intensity (i).
f	=	Coefficient in log-linear regression to determine rainfall intensity (i).
F(x)	=	Cumulative distribution function. Also abbreviated as CDF.
$\hat{F}_y$	=	Empirical distribution function. Also abbreviated as EDF
h	=	Lag used to evaluate auto or cross-correlation in geostatistical analysis.
H_i	=	Heterogeneity statistics based on observed and simulated regions.
i	=	Rainfall intensity.
k	=	Lag used to evaluate auto and cross correlation.
K	=	Frequency factor related to design storms or station number.
m	=	Rank of a data set or total number stations in a region.
N, n	=	Sample length of data set.
P	=	Probability.
r	=	Order of a moment or L-moment or number of successes in the Binomial distribution.
r_k	=	Sample autocorrelation coefficient.
r_{kk}	=	Sample cross correlation coefficient.
$\overline{r}_m$	=	Regional average cross correlation coefficient.
s	=	Measuring the difference between at-site $\left(\hat{\theta}^{(i)}\right)$ and regional estimates $\left(\hat{\theta}^{R}\right)$
S_i	=	Sample covariance matrix based on vector containing L-moment ratios (u).
S	=	Mann-Kendall trend test statistic.
$\overline{S}_m$	=	Regional average Kendall's S.
T	=	Return period.
t	=	Rainfall storm duration or time interval.
u	=	Vector containing the first three L-moment ratios ($t^{(i)}$, $t_3^{(i)}$, $t_4^{(i)}$).
V_i	=	Variability of L-parameter groupings with respect to simulation results.
W_t	=	Pre-whitening of a data set due to significant autocorrelation.
x	=	Random variable or design storm estimate.
Y_t	=	Regression variable at time t.
Y*	=	Bootstrap sample.
Z_s	=	Test statistic to determine significance for trend test
Z	=	Goodness of fit statistic for various parametric distributions.
$\hat{z}$	=	Estimate of z at an unmeasured station (x_o) from known observations ($z(x_1)$.....$z(x_n)$) in the BLUE procedure.

Abbreviations

ACF	=	Autocorrelation function.
AES	=	Atmospheric Environmental Services
AM	=	Average annual maximum precipitation.
BLUE	=	Best linear unbiased estimator.
CDF	=	Cumulative distribution function.
CEI	=	Climate Change Indices.
CV	=	Coefficient of variation.
EDF	=	Empirical distribution function.
EV	=	Extreme Value Type I (Gumbel distribution), II, III distribution.
GEV	=	Generalized extreme value distribution.
GIS	=	Geographical information system.
IDF	=	Intensity-duration-frequency relationships.
IFD	=	Intensity-frequency-duration relationships.
IID	=	Independently and identically distributed.
IPCC	=	International Panel on Climate Change.
Lat	=	Latitude in decimal degrees.
L-moment	=	Linear moment statistics.
LN	=	Log Normal Distribution.
Long	=	Longitude in decimal degrees.
LP	=	Log Pearson Distribution.
MAP	=	Mean annual precipitation.
PDF	=	Probability density function.
PDS	=	Partial duration series.
PWM	=	Probability weighted moment.
RI	=	Rainfall Index.
RF	=	Russian Federation territory.
RPF	=	Russian Permafrost Free territory.
WMO	=	World Meteorological Organization.

Chapter 1

INTRODUCTION

1.1 Motivation

The Intergovernmental Panel on Climate Change (IPCC) (1996) reported changes in temperature extremes that can be attributed to the increase of concentration of carbon dioxide (greenhouse gases) into the atmosphere. Past studies of climate trends (Nicholls et al., 1996), indicate that the global mean surface temperature has increased by approximately 0.3 to 0.6°C since the late 19th century and by 0.2 to 0.3°C over the last 40 years. Zhang et al. (2000) found an annual mean temperature increase between 0.5 and 1.5°C in Canada (south of 60°N) from the period of 1900 to 1998, in which the greatest warming occurred in the spring and summer periods of western Canada. From 1950 to 1998, Zhang found warming in southern and western Canada, while northeast Canada generally experienced cooling. Climate change trends may be easier to detect in northern countries, such as Canada (Nicholls et al., 1996), since anthropogenic climate change signal is projected to be stronger in the high-latitude countries.

Recent studies (Nicholls, 1995; Karl and Knight, 1998) suggest that the hydrological cycle could intensify due to the increase in temperature extremes. Trenberth and Shea (1996), using a conceptual model (shown in figure 1.1), found that an increase in greenhouse gases and temperature extremes (global warming) will cause surface heating to increase. The theory of global climate change, endorsed by many scientists (Bard, 2002), holds that industrial activity is causing a build

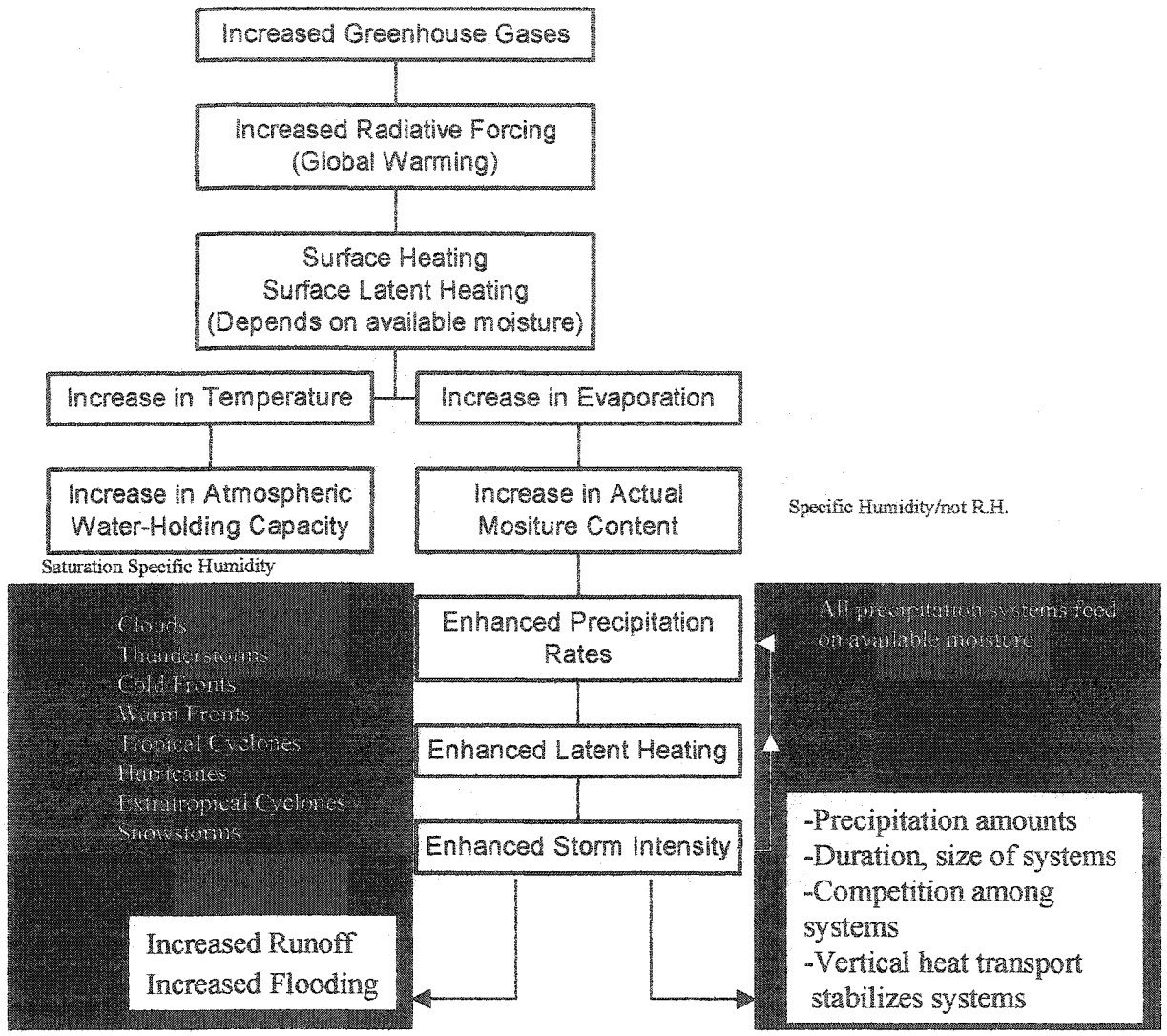

Figure 1.1: Conceptual Model developed by Trenberth and Shea (1996)

up of carbon dioxide in the atmosphere, trapping the sun's heat close to the Earth and creating a hotter, more turbulent atmosphere that will lead to more extreme weather events like droughts, storms, heat waves, and floods. There are many studies and research initiatives (International Research Institute, 2001, and others) concerned with better predictions and understanding of the complexity of climate change and its possible consequences.

Potential impacts of climate change effects in Canada could include the following (Bruce et al.2002): an increase in the frequency and severity of extreme weather events including short-duration/high intensity rainfalls; a change in precipitation distribution, amounts and types; polar ice and permafrost melt in northern Canada; and sea level rise. Such changes might have multiple national, regional and municipal consequences. Urban areas, having large populations and expensive infrastructure are particularly vulnerable to climate change impacts. However, no analysis of Canadian data has been reported in literature dealing with estimation of trends in extreme short duration rainfall events. Zweirs et al. (1998) reported that frequency of heavy one-day rains could occur with return periods halved e.g. a 20 year return period rainfall becomes a 10 year event. Information on trends in extreme short-duration rainfall is needed to determine climate change impacts on design, management, and operation of urban infrastructure, and to prepare adaptation measure to deal with extreme events. One of the main objectives of this thesis is to detect trends in extreme rainfall, and to estimate anticipated changes in return periods of extreme rainfall events due to trends.

Several studies (Guttman et al., 1992; Karl and Knight, 1998; among others) have found increases in precipitation amounts across the USA and Canada in recent years, which can be attributed to climate change. Zhang et al (2000) found that annual precipitation totals in Canada have changed by -10% to 35%, with the northern regions generally experiencing the strongest increases. Dai et al. (1997) have found an increase in precipitation in the mid and high latitude land areas, which contribute to enhanced evaporation and more runoff.

It has been found that hydrological variables associated with precipitation are also experiencing significant trends. Lambert (1996) discovered an increase in extra tropical storm severity in the Northern hemisphere during the period of 1899 and 1991, while an increased in atmospheric and water vapor was found in North America, China, and tropical regions (IPCC, 1996; Ross and Elliott, 1996; Zhai and Eskridge, 1997). Adamowski and Bocci (2001) have found significant trends in annual mean, monthly, and minimum stream flows in various regions of Canada.

All of these studies provide evidence suggesting that the conceptual model developed by Trenberth and Shea (1996) is supported by findings using observed data. However, there are regions in the world where there are no signs of climate change. For example, Zhai et al. (1999) found no increasing trends in 1 and 3 day precipitation extremes in China, and Kumar et al. (1997) found no significant trends in 1, 2, and 3 day precipitation totals in India. There are also potential problems with precipitation data sets, such as a short record length and incomplete global coverage (Karl and Easterling, 1999) to make a conclusions that the conceptual model is 100% accurate. However, it is clear that the hydrological process is not stationary, which leaves problems for engineers who use design charts to estimate rainfall intensity for various frequency and events that will occur in the future.

Rainfall information is required for many theoretical and practical reasons. One of the most common uses of rainfall information in engineering is in developing design storms which are used in calculating design storm runoff (Maidment, 1993). Design storm rainfall is defined as a relationship between rainfall intensity (depth, mm), duration (time, minutes), and frequency (probability or return period, years). Such relationships are known as IDF curves or equations and are usually derived using observed annual maximum (AM) series at one site (at-site) or several sites (regional analysis). In developing these relationships, the estimates of rainfall intensity for a given duration and frequency can be obtained from statistical analysis employing various probability distributions (such as Gumbel distribution) and parameter estimation methods (such as method of moments).

These IDF relationships are used in the design, construction, and management of many water resources projects involving natural hazards, due to extreme rainfall events. For example, many hydraulic structures (culverts, storm sewer systems) are designed to control surface runoff. In the absence of adequate stream flow data, rainfall data is used extensively in the synthesis of peak flows. Many methods (such as: rational method, synthetic unit hydrographs, etc.) require IDF inputs to determine peak flows. It is therefore very important to have reliable estimates of IDF relationships which would reflect possible future conditions.

When IDF relationships are needed for ungauged locations, or for stations with a short rainfall record, then use is made in Canada (Hogg and Carr, 1985) and the United States of America (USA) (Hershfield, 1961) of regionalized information mapped in the form of a rainfall frequency atlas. More recently, generalized IDF relationships have been expressed by equations (Adamowski et al., 1997). These maps and equations have been developed subject to various assumptions, which unfortunately give rise to many uncertainties. Also, they were developed without examining whether rainfall events are subject to climate change (trends).

Of all previous studies on trend detection in extremes of precipitation, the influence of serial and spatial correlation was not investigated (Zhai et al., 1999; Plummer et al., 1999). It is perhaps because the assumption of independent observations is required in many trend tests. However, the effect of spatial and/or temporal correlation among data sets may lead to misleading interpretations of trends (Douglas et al., 2000) and furthermore, correlation reduces the effective sample size of the data set.

Precipitation data at various sites in a homogeneous region are intercorrelated because of the physical proximity of the sites. The effect of such cross correlation in regional flood analysis has been investigated in only a few studies, although not in precipitation. Hosking and Wallis (1997) showed that interstation correlation can have a dramatic effect on the variance of the average of the unbiased estimators. It drastically reduces the information content of the data.

The main purpose of this study is to: a) investigate the evidence of trends in the annual maxima precipitation data for various durations, b) evaluate the effect of serial and spatial correlation of precipitation on the detection of trends, c) detect trends in regional data, d) evaluate the effects of trends on IDF estimates, and e) determine and quantify the consequences of trends on return periods of design storms.

1.2 Objectives

The objectives of this thesis are as follows:

1) To review and modify the methodologies used in trend detection including:
   - Review of IDF relationships and regional approaches for estimating design storms.
   - Adapt the techniques used to delineate homogenous regions.
   - Modify trend detection techniques for a single site and a regional basis for time/space correlated data.

2) To perform a single site analysis on rainfall stations in the province of Ontario to determine:
   - Significant trends in annual maximum rainfall data for the 5, 10, 15, 30 minute and 1, 2, 6, 12 hour storm durations for various record lengths.
   - Significant autocorrelation in the rainfall data sets.
   - IDF estimates for sites experiencing a significant increasing trend.
   - To quantify the effect of trends on the return periods of design storms.

3) To investigate and estimate the existence of trends at a regional scale involving:
   - Determination of homogenous regions by the method of L-moments for a 20 and 25 year time for the 5, 10, 15, 30 minute and 1, 2, 6, 12 hour rainfall durations.
   - Introducing a new methodology to define homogeneous regions based on the direction (plus, minus, no trend) of trend.
   - Evaluate the effect of serial correlation of precipitation on the detection of trends.
   - Evaluate the effect of spatial correlation by using L-moments, cross-correlation and variograms on the detection of trend.
   - Determine trends in the annual maximum precipitation data for various durations and regional data sets.

1.3 Scope

Annual maximum rainfall data for the 5, 10, 15, 30 minute and 1, 2, 6, 12 hour storm durations are analysed for 63 stations in the province of Ontario. To the author's knowledge, no tests have been performed on different storm durations of extreme rainfall. The stations have record lengths ranging from 18 to 73 years, and periods ranging from 1926 to 1998. The Mann-Kendall S statistic (Mann, 1945; Kendall, 1962) is applied to determine if trend in the rainfall time series data for each station and duration is significant at a 5% level. Record lengths of 20, 25, and 30 years (when applicable) along with the total existing record length of the station are used to investigate the sensitivity of record lengths selection on the magnitude and significance of trend. Serial correlation in the precipitation data sets will be examined and it's affects on the Mann-Kendall trend test, since the test requires the data to be time independent. Significant autocorrelation is detected by using Anderson's (1942) confidence interval. IDF curves are generated, based on recent rainfall data, for station duration's experiencing a significant increasing trend. The IDF estimates were compared for stations with and without trend, and the differences in intensity were used to compare its impact on the return period of the rainfall event.

Homogeneous regions were delineated based on the L-moment procedure developed by Hosking and Wallis (1993) enabling the determination of a proposed region to be accepted as homogeneous. A heterogeneity measure is used to test proposed regions based on summary statistics of the at-site data. The summary statistics are in the form of L-moments, a method to estimate statistical properties of hydrological data. The procedure uses at-site characteristics (geographical location, and mean annual precipitation), along with the at-site measurement (annual maximum precipitation), to determine if a group of stations can be grouped as one homogeneous region. The direction of trends (plus, minus, no trend) was also used as an additional information in delineating the homogeneous

At a regional scale, the Mann-Kendall statistic is modified to incorporate the amount of stations in a region, assuming the rainfall data is serial and spatially independent. As for single sites, the data

sets are examined to determine if significant autocorrelation is evident, therefore, nullifying the assumption that the data is independent. Average cross correlation was computed to examine the dependency between stations in a region. Regions with high cross correlations nullify the assumption of the data to be identically distributed implying the region to be spatially dependent.

In order to explore the correlation structure of the regionalized precipitation field, a geostatistical method is employed (Chilès and Delfiner, 1999). The sample variogram is used to plot the squared differences of rainfall observations between stations in a region. The correlation structure in a region vanishes when the separation distance, h, between stations is greater than the range (distance at which the variogram reaches the plateau). Several types of models exist to model the sample semivariogram. The model used in this paper is the spherical model (Brooker, 1991). Therefore, a region was labeled spatially correlated if (a) a range, or correlation, existed in the variograms for a region and (b) if the heterogeneity measure and cross correlation values suggested spatial correlation.

For regions that are found to be spatially dependent, the bootstrap method (Efron, 1979) can be used to estimate a statistical parameter of interest (i.e. trend). The null hypothesis is for the data to show no trend, be serial independent and spatially correlated. The bootstrap samples are used to create an empirical cumulative distribution function (CDF) for the regional average Mann-Kendall statistic. Using the bootstrap procedure 5000 regional average Mann-Kendall S statistics were calculated, then ranked in ascending order and given a non-exceedance probability (P) using the Weibull plotting formula.

1.4 Publication of Results

The results from this research resulted in the following publications/presentations:

1) Adamowski K, Bougadis J. Detection of trends in annual extreme rainfall. *28th Annual Meeting of the Canadian Geophysical Union*, Banff, Alberta, May 18-21, 2002.

2) Adamowski K, Bougadis J. Regional estimation of temporal trends in rainfall. *5th International Conference on Hydro-science and Engineering*, Warsaw, Poland, September, 2002.

3) Adamowski K, Bougadis J. Detection of trends in annual extreme rainfall. *Journal of Hydrological Processes*, (in press).

4) Adamowski K, Bougadis J. Influence of trend on short durations design storms. Submitted to the Journal of the Canadian Water Resources, 2003.

1.5 Outline of the Thesis

Chapter 2 presents the literature review outlining past research methodologies on homogeneous region delineation, climate change and spatial analysis.

Chapter 3 presents the theories and equations applied in this thesis. This chapters discusses how to classify a group of sites as a homogeneous region, trend tests for single sites and regional analysis, intensity-duration-frequency relationships, the effect of serial and spatial correlation on precipitation data and trend tests, and bootstrapping techniques for spatially correlated regions .

Chapter's 4 and 5 present the summary of research findings, and gives recommendations for future research.

Appendices A and B present additional tables and figures of the findings presented in Chapter 4. Appendices C and D present the rainfall stations used in this thesis and the computer programs developed to determine the findings presented in Chapter 4.

Chapter 2

LITERATURE REVIEW

2.1 Single Sites Rainfall Frequency Analysis

Design storms are used in various engineering applications including determination of peak rainfall intensity for a given duration and return period. The annual maxima (AM) series is commonly used because it is has a theoretical basis in extrapolating beyond the period record (Hogg and Carr, 1985). Generally, AM rainfall data applies to the months of April till October, since rain gauges are taken out of service in the winter months.

In developing the IDF relationships, for each daily rainfall measurement recorded for a site with durations ranging from 5 minutes to 1 day, is used from which the largest rainfall depth of the year is extracted from the records. The maximum rainfall depth is transformed into an intensity (knowing the duration) for each year and ranked in descending order and assigned a rank (m), where the rank of 1 is assigned to the largest depth, rank of 2 is assigned to the second largest depth and so on. The intensities are then assigned a return period (T) or frequency using the Weibull plotting-position formula (Singh, 1992)

$$T = \frac{n+1}{m} \tag{2.1}$$

For each duration, the series of intensities and return periods are plotted on probability paper, and the distribution is fitted often using the extreme value Type I (EV I) distribution developed by

Gumbel (1954). The World Meteorological Organization (WMO)(1981) indicates that the Gumbel distribution is most often used by national meteorological services in the world to describe rainfall events. The intensity-frequency-duration (IFD) relationships are then transformed into IDF curves by selecting intensities based on the return period of interest (ranging from 2 year to 100 year), and re-plotting the intensities versus duration for all return periods.

The IDF curves can also be expressed in a mathematical form, in which rainfall intensity (i) is defined by

$$i = \frac{c}{t^e + f} \tag{2.2}$$

where t is the duration of storm, c is related to the exceedance probability, and e and f are coefficients. The coefficients can be determined by log-linear regression, however, these constants vary with station location and return period.

Frequency analysis can be performed numerically using the mean, standard deviation, and skewness of the rainfall intensities with the storm duration being fixed. Various probability distributions, such as lognormal (LN), and log-Pearson (LP) III, have been investigated, however, EV I is most often used. Often, the frequency factor method (Maidment, 1993) is used, such as

$$x = \mu + K\sigma \tag{2.3}$$

in which x is the design storm, μ and σ are the mean and standard deviation of the data, and K is the frequency factor specific for a given distribution and annual return period.

In summary, design storm estimates from IDF curves and relationships are derived using single site frequency analysis in which the annual time series is assumed to be independent (free of correlation and trends). The impact of human activities on the weather, such as climate change, is ignored. In this study, the assumption of independency is questioned based on an autocorrelation analysis, which examines correlation in the time domain of the rainfall series. To determine if precipitation data is affected by climate change, the Mann-Kendall test is applied on single sites to detect the

possibility of significant trends.

2.1.1 Distribution Selection and Parameter Estimation

In frequency analysis, there is no theoretical basis in selecting one statistical distribution over the other to describe the behaviour of extreme hydrologic variables (Alexander et al., 1969). In practise, many distributions are selected to 'best' fit the raw data. A variety of goodness-of-fit tests are applied to determine which distribution is to be selected, based on an agreement between the distribution and the extreme variables.

Many goodness-of-fit tests have been applied to annual extreme rainfall data. A graphical approach applied by Dalrymple (1960) and Farmer and Fletcher (1972) uses probability papers and plotting positions to plot the observed data for comparison with the theoretical distribution. Other statistical tests, such as the Chi-Square, and Kolmogorov-Smirnov (Keeping, 1966), compare the discrepancy between the frequency distribution as observed in the data and the hypothesized distribution. Matalas and Wallis (1973) have doubted the use of these tests due to their subjectivity of the index of fit and the plotting position.

A suitable distribution can be based on moment ratio diagrams (Wu and Goodridge, 1974; Watt and Nozdryn-Plotnicki, 1980). The coefficients of skewness and kurtosis are computed for the sample and compared with the coefficients of the parent distributions. However, sampling errors exist in estimating higher order moments associated with existing ranges of record length (Hazen, 1924; Wallis et al., 1974).

The lack of a firm theoretical procedure for selecting an appropriate statistical distribution in rainfall analysis leads national meteorological agencies to adapt a policy of standardizing IDF analysis (Gupta, 1970). The most frequently used probability distribution in the analysis of rainfall data is the two-parameter EV I distribution (WMO, 1981), with constant skewness and kurtosis of 1.14 and 5.4, respectively. The WMO (1981) indicated the second most used distribution is the two-

parameter LN with a constant theoretical skewness and kurtosis of 0.0 and 3.0, respectively.

Even though the EV I is used in Canada, other studies have found problems with the distribution based on climate, geographical regions, and storm durations. Wurtele and Roe (1978) suggested the use of the EV I in regions with moderate to high rainfall intensity characteristics, while desert regions were better fitted with the EV II. Uppala (1978) found the rainfall data in western Finland was best fit with the EV II distribution, while the EV III was more appropriate in Eastern Finland. Sneyers (1977 and 1978) found a discrepancy of distribution selection for different storm duration in annual rainfall maxima in Belgium. The EV I distribution was fit for storm durations less than 30 minutes and the GEV II distribution for storm durations ranging from1 to 24 hours. Pilon et al. (1991) found that the rainfall data in Ontario, Canada are best fitted by the general extreme value (GEV) distribution, the parameters of which depend on storm duration.

Once the appropriate probability distribution is chosen to describe the observed data, the parameters of the distribution must be estimated. Two common approaches used for parameter estimation are the method of moments and maximum likelihood methods. Both parameter estimation methods have shown to produce nearly unbiased results in fitting to the two-parameter EV I distribution (Watt and Nozdryn-Plotnicki, 1980; among others). However, the method of moments is simpler to compute, and is often used for this distribution. In three-parameter distributions, there is no general agreement in which technique should be used. The efficiency in the method of maximum likelihood is dependent on the sample size. Matalas and Wallis (1973) have shown that the method of maximum likelihood is efficient for large samples, while Bobee and Robitaille (1977) found the efficiency to decrease as the sample size decreases. The efficiency of the method of moments is affected by the presence of outliers (high or low) in the data set (Klemes, 1987). This issue has not been further investigated in this thesis.

An alternate approach for parameter estimation was introduced by Greenwood (1979) in the form of probability weighted moments (PWM). Landwehr et al. (1979) found the PWM to be an unbiased parameter estimator for data samples drawn from purely random samples in comparison with the

method of moments and the method of maximum likelihood. Hosking (1990) used the PWM through the development of linear moment statistics (L-moments). This topic is further discussed in Chapter 3.

In summary, single site frequency analysis and IDF relationships are prone to errors, often occurring from the assumptions of (i) selection of probability distribution and (ii) method used in fitting the observed data to the distribution. The EV I distribution is used in IDF analysis, however, it is usually used based on administrative and standardization considerations. Regional approaches have been recognized to significantly reduce quantile estimates relative to that in single site approach (Pilon and Adamowski, 1992, among others). Regional techniques also have the ability to extend gauging networks to ungauged sites, allowing design storms to be estimated in regions with no rainfall data. In this thesis, a regional approach was applied to the province of Ontario to determine regions experiencing trends (increasing or decreasing). This method also allows us to estimate changes in trends for sites with no rainfall data.

2.2 Identification of Homogeneous Regions

For a group of sites to be considered as one homogenous region, it is often assumed that the meteorological and physiographic characteristics governing the generation processes of the hydrologic extreme variable should be similar. The process of identifying a homogeneous region is usually difficult and requires a great amount of subjective judgement. The benefits in regional analysis is transferring information between sites within a homogeneous region allowing estimates to be made at ungauged sites.

The delineation of homogeneous regions consists of two steps: (i) grouping mechanisms and (ii) homogeneity test. The first step in forming regions is to find a procedure to group together sites with similar characteristics. The newly formed region is then tested to determine if it is actually homogeneous, if not, then the process is repeated by regrouping sites.

2.2.1 Grouping Mechanisms

Site characteristics are used to initially group sites into one region, which would describe geographical location, elevation, and other physical properties of the site. Site characteristics can also be estimates that are known before any data are measured at the site, such as the mean annual precipitation, or estimates from the data measured at the site, such as the time of year which a flood occurs. The following are general grouping methods performed by authors in regional analysis:

a) Geographic Location

A subjective and simple approach in forming regions is choosing sites that neighbour each other, based on administrative areas (National Environmental Research Council, 1975) or major physical grouping of sites (Matalas et al., 1975). Acreman and Sinclair (1986) indicate that neighbouring stations and basins can be physically and hydrologically different, along with their generation mechanism of the extreme event. Aron et al. (1987) performed a study in Pennsylvania State, USA, in which IDF curves were developed using the LP 3 distribution for five geographically defined regions. The regions were not tested statistically if in fact the regions formed were homogeneous.

a) Subjective Partitioning

Homogeneous regions may be defined based on the similarity of site characteristics between stations. In analysing annual maximum precipitation data in Washington State, USA, Schaefer (1990) formed regions based on sites with similar mean annual precipitation. In the analysis of annual maximum stream flow data in the provinces of Ontario and Quebec, Canada, Gingras et al. (1994) formed regions by grouping sites corresponding to the time of year at which the largest flooding event typically occurred. Gingras and Adamowski (1993) delineated regions in the province of New Brunswick, Canada by grouping basins with probability density functions of similar shape, which reflected similar flood generating mechanisms.

b) Objective Partitioning

Homogeneous regions are developed based on a threshold value of a chosen site characteristic to minimize a within-group heterogeneity criterion, such as likelihood-ratio statistic (Wiltshire, 1985), sample coefficient of variation (Wiltshire, 1986a), or sample L-CV and L-skewness (Pearson, 1991a). The sites are then assigned into one of two groups depending on whether the statistic does or does not exceed the threshold value. The groups are then further subdivided until a final set of acceptable homogenous regions is achieved. Regionalization of streamflow data for drainage basins was performed by Pearson (1991b) in New Zealand using this approach.

c) Cluster Analysis

In regional frequency analysis, the cluster analysis is a standard procedure to divide data sets into groups to form homogeneous regions. Data vectors, composed of at-site statistics, site characteristics, or the combination of the two, are associated with a specific site. All sites in the analysis are separated into groups according to the similarity of their data vectors.

De Coursey (1973) applied this procedure to form groups having similar flood response, based on site characteristics of streamflow gaging sites in Oklahoma. Acreman and Sinclair (1986) formed five regions, four being homogeneous, for annual maximum streamflow data of 168 gaging sites in Scotland. Burn (1989) used this approach to form regions for flood frequency analysis, though his clustering variables included at-site statistics. Guttman et al. (1993) formed 104 regions, 101 being homogeneous, for annual precipitation totals for 1119 sites in the USA. Farhan (1984) used cluster analysis to form regions for stream gaging sites in Jordan on the basis of four principal components formed from a matrix of site characteristics.

d) Other Multivariate Analysis Methods

Other statistical methods, such as factor analysis and principal components, have been used to group similar sites. The factor analysis approach was applied by White (1975) to classify drainage basins in Pennsylvania, while Burn (1988) used principal component analysis on series of annual maximum streamflow data.

In this thesis, regions were initially formed based on the geographical approach by placing neighbouring sites together. This approach alone is quite subjective, therefore, similar sites were grouped together based on the mean annual precipitation (MAP), and direction of trend (plus or minus). Such an approach is unique and has not been reported elsewhere in the literature. This method implies that neighbouring sites with similar MAP should experience the same increase or decrease in extreme rainfall due to climate change.

2.2.2 Tests for Regional Homogeneity

Once a set of sites have been grouped to form a region, it is then required to test if the region can be accepted as homogeneous. The test consists of examining whether the at-site frequency distributions are the same except for a site-specific scaling factor (Hosking, 1997). The hypothesis of homogeneity is ultimately based on the data at the N sites in the region and whether it is consistent with the relation between the at-site frequency distribution.

One methodology that can be used in determining homogeneous regions in regional flood frequency analysis is the regression approach. Peak flood estimates are related to physiographic and climatic parameters, which govern the generation mechanisms of the flooding event, and ordinary least square approaches is used to estimate regression parameters. Important physiographic and climatic variables in regression analysis are basin slope, basin area, and mean annual precipitation. However, homogeneous region are obtained through visual assessment of the mapped regression residuals (Stedinger and Tasker, 1985).

Another method in flood frequency analysis to test for homogeneity is the index flood (Dalrymple, 1960). This approach develops a regional frequency curve for a homogeneous regions which consists of two steps: the development of basic dimensionless frequency curves relating the ratio of the flood (of any frequency) to an index flood (the mean annual flood). The second step is relating characteristics of drainage area and the mean annual flood in order to predict the mean annual flood at any location within the region. The homogeneity test determines if the individual frequency curves from each station can justifiably be combined by examining if the records from each site differ from one another by amounts attributed to chance. The test utilizes the 10 year flood estimates from the frequency curves of each station in the proposed region, and confidence limits are set to determine if the differences are accepted statistically. However, Benson (1962) indicated the test was not sensitive to a wide variety of extreme value characteristics.

The majority of tests involve a quantity, θ, that measures some aspect of the frequency distribution which is constant in a homogeneous region. Various researchers have used different statistics for the quantity of θ: Dalrymple (1960) utilized the 10-year flooding event scaled by the mean, Wiltshire (1986a) used the coefficient of variation, Chowdhury et al.(1991) used a combination of L-CV and L-skewness, and Hosking and Wallis (1993) used the L-CV or some combination of the L-CV, L-skewness, and L-Kurtosis. The test consists of determining the at-site estimate, $\hat{\theta}^{(i)}$, based on the data for site i, and the regional estimate, $\hat{\theta}^{R}$, using data from all the sites in the region. A test statistic, s, measuring the difference between the at-site and regional estimates is employed and expressed as (Hosking, 1997)

$$s = \sum_{i=1}^{N} \left(\hat{\theta}^{(i)} - \hat{\theta}^{R} \right)^2 \qquad (2.4)$$

The observed value of s for the region is compared with the "null distribution" that s would have if the region were homogeneous. The theoretical s found from the null distribution usually involves an assumption in selecting the frequency distribution for the sites in the region. The distribution is assumed to be Gumbel by Dalrymple (1960) and Fill and Stedinger (1995), generalized extreme

value by Chowdhury et al. (1991) and Lu and Stedinger (1992), and kappa by Hosking and Wallis (1993). Wiltshire (1986a) used a nonparametric jackknife approach to estimates the null distribution. The assumption of homogeneity in a region is rejected if the observed value of s lies far in the tail of its null distribution, indicating that it is unlikely that such an extreme value occurred by chance in a homogeneous region.

Another approach to test homogeneity in a region utilizes the likelihood-ratio tests that compare the fit of regional and at-site generalized extreme-value distributions fitted to the data by the method of maximum likelihood (Acreman and Sinclair, 1986; Buishand, 1989). Wiltshire's (1986b) test is based on the observation that if site i has data $Q_{ij}, j = 1,.....n_i$, and a frequency distribution with cumulative function $F_i(.)$, then the "G-statistics", $G_{ij} = F_i(Q_{ij})$, form a random sample from a uniform distribution on the interval (0,1) and should take an average value of 0.5. When F_i is replaced by a fitted distribution obtained from regional analysis, the G-statistics should remain constant if the region really is homogeneous, but nor otherwise. Wiltshire obtained the statistic that tests the similarity of the average deviation from 0.5 of each site's G-statistics calculated from the fitted regional distribution

The most rigorous and powerful approach was developed by Hosking and Wallis (1993) with the use of L-moments. The procedure first introduces a discordancy measure to identify sites whose at-site L moments are significantly different then the rest of the sites to form the proposed region. Then a heterogeneity measure is introduced which compares the difference between the weighted standard deviation of the at-site sample L-CV for the proposed region from the mean of 500 simulated homogeneous regions produced from the kappa distribution. Alila et al. (1994), applied this approach to test regions delineated by map and L-CV to determine regional IDF relationships for Canada.

The L-moment procedure developed by Hosking and Wallis (1993) is used in this thesis to delineate regions for the 5,10,15,30, minute and 1, 2, 6, 12 hour storm durations for the 20 and 25 year time frame. The discordancy measure was used to find irregular sites in a proposed regions, while, the

heterogeneity measure was used to determine if the grouped sites were actually homogeneous. The theoretical development for this procedure is outlined in Chapter 3.

2.3 Review of Climate Change Studies

During the past century, the presence of trends in precipitation has been detected over many regions of the world (Groisman and Legates, 1995; IPCC, 1998), especially in mid-to-high latitude land areas (IPCC, 1996). The occurrence's of large flooding events has increased since the 1990's (Karl and Easterling, 1999) in Asia, Europe, and the United States, suggesting a change in precipitation extremes. Global studies have been performed to find evidence of an increase in precipitation totals and how it will affect precipitation extremes (Groisman et al., 1999).

In climate change studies, various characteristics are chosen in the analysis, such as days with severe droughts, flooding events, daily and annual precipitation, and extreme precipitation. After such characteristics have been chosen, a methodology is used in order to determine if it is actually susceptible to climate change. This section will outline various characteristics, methodologies and results from recent climate change studies around the world.

2.3.1 Indicators for Climate Change

Extreme climate indices have been developed to examine the effect of the injection of greenhouse gases into the environment on climatic variables (temperature and precipitation). In the United States, Karl et al. (1996) introduced the climate change indices (CEI). The CEI is the annual arithmetic averages composed of the following factors based on the percentage of area of the US: (1) maximum temperature above and below normal; (2) minimum temperatures above and below normal; (3) severe drought and severe moisture surplus; (4) twice the percent area of the US with much greater than normal proportion of precipitation derived from extreme (more than 2 inches) 1- day precipitation events; and (5) much greater than normal number of days with and without precipitation. The definition for above/below normal conditions as those falling in the upper/lower

tenth percentile of the record period. The lower limit of the CEI index is 0%, meaning that no portion of the country is subject to any of the extremes of temperature or precipitation. The upper limit is the value of 100%, indicating the entire country is under extreme conditions throughout the year for each of the five indicators.

In Canada, Zhang et al. (2000) presented abnormal and extreme climate indices, abnormal being defined as percentages of the nation affected by cold (dry) and warm (wet) conditions, respectively, and represent precipitation below the 34th and above the 67th percentiles in the time series. Extreme indices represent precipitation below the 10th and above the 90th percentile, respectively. Zhang gridded the station's rainfall data using a technique developed by Hogg et al. (1997). In the extreme dry indices analysis, Zhang counted the number of grids in that season when the precipitation was below the 10th percentile. The extreme dry indices was then obtained by dividing the number of grids below the 10th percentile by the total number of grids. The same procedure was repeated for the other indices. Plummer et al. (1999) applied extremely wet and dry indices for the continent of Australia. Extremely dry and wet was defined as the percentage of Australia below the 10th and higher than the 90th percentile of the annual total. The annual percentile's were computed for individual stations and area weighting were determined using the Thiessen polygon approach.

Zhai et al. (1999) created his own rainfall index (RI) to define regional droughts and floods in China. His analysis focussed on the summer months (June-August) for the period of 1961 to 1990, His RI index consists of the mean total rainfall, the number of stations in the region and the number of stations with positive summer rainfall anomalies. If the RI is higher than 25% and 35% then a flood and severe flood conditions are defined. If the index was below -25% and -35% than a drought and severe drought conditions are defined.

Precipitation totals are often used to determine if a higher quantity of precipitation is being achieved in recent decades. Zhang et al. (2000) used annual precipitation totals to determine if increasing or decreasing trends are found in Canada, while Groisman et al. (1999) used summer daily precipitation data to determine if an increase would affect heavy precipitation rates. Gruza et al.

(1999) used mean annual precipitation and precipitation totals in the cold and warm seasons in Russia as an indicator for climate change.

Maximum 1-day and 3-day rainfall events have been often used in recent studies. Heino et al. (1999) utilized heavy 1-day totals in Northern and Central Europe, due to their role in flooding in small watershed in urban areas. Zhai et al. (1999) utilized maximum 1-day and 3-day rainfall totals in China.

Thresholds are utilized in studies to determine if the number of days of precipitation are frequently exceeding the arbitrarily chosen limit. Heino et al. (1999) applied this techniques to determine the number of days precipitation exceeded 10 mm in Northern and Central Europe, while Zhai et al. (1999) selected three threshold values, 10 mm, 50 mm, and 100 mm/day, for the 1-day rainfall event in China. Groisman et al. (1999) selected a threshold value based on the geographical location of the region. A threshold of 2 inches (50.8 mm) was selected for mid-latitude countries (USA and Mexico) and 1 inch (50.8 mm) for high latitude countries (Canada, Russia and Norway). Other researchers (Gruza et al., 1999; Groisman et al., 1999) used the number of days with measurable precipitation over a selected value. The value was also dependent on the country studied, where as 0.1mm/day was used China and 1 mm/day was chosen for Canada and Russia.

After the characteristic data set has been chosen, a trend analysis is performed to determine if the variable is changing over time. The trends are often assumed to be linear and found by performing simple linear regression. The statistical model used is

$$Y_t = \alpha + \beta t + \varepsilon_t \tag{2.6}$$

where Y_t is the variable at time t, α is a constant term, β is the slope of the regression line, and ε_t is the noise at time t. The constants α and β are regression parameters and the noise can be described by a pth order autoregressive model of the order 1. Zhang (2001) used a method to incorporate serial correlation in the trend computation. However, authors (Groisman et al., 1999) often simplify

the analysis by assuming independent precipitation events and do not explore the temporal correlation which may exist in precipitation data sets.

The magnitude of trend can be estimated by linear regression and its significance with a two-sided t-test. Another approach is to use Sen's estimate of the slope (Gilbert, 1987) and the significance with the non-parametric Mann-Kendall test (Sneyers, 1990). Heino et al. (1999) estimated the magnitude of trend using linear regression and Sen's estimate and found very similar results. Significance levels of trend are usually chosen at 5, 1, and 0.1 % levels.

In this thesis, the annual maximum 1-day event (often referred as the annual maximum series) was used as the characteristic for the trend analysis. The magnitude of trend was estimated using linear regression techniques, and serial correlation was used in the analysis to account for time dependence. The significance of the trend was estimated using the non-parametric Mann-Kendall trend test at a 5% level. This procedure was applied to single sites and in the regional approach.

2.3.2 Results of Previous Climate Change Studies

Groisman et al. (1999) applied a statistical model to determine the effects of climate change on heavy daily precipitation in the summer months for 8 countries: USA, Mexico, Canada, Russia, Norway, Poland, Australia and China. For North America, the daily precipitation data was accumulated at the National Climatic Data Center where 93 and 202 stations were used for Canada and Mexico, spanning the years 1900-1995 and 1950-1990, respectively. A total of 134 stations from the US Historical Climatology Network was used for the US with century long records. In Europe, 13 century long stations for Norway and 10 stations with data available after the world war II were used for Poland. In China, 198 stations spanning from 1951 to 1994 were used, while 379 stations were available in Australia with records startling as early as 1891 till 1994. In Russia, 223 stations were available ranging from 1943 to 1994.

The gamma distribution was used to model daily rainfall with three parameters: (1) shape (which remains relatively stable), (2) scale (which is most variable spatially and temporally), and (3) probability of daily precipitation. Groisman et al. (1999) found the strongest change in heavy precipitation occurred with variation of the scale parameter, indicating that changes in mean monthly precipitation totals tend to have the most influence on heavy precipitation rates.

For the USA, Australia and Norway, Groisman et al. (1999) searched for century long trends in precipitation frequency. In the USA, no significant trends in the summer and winter seasons were found, however, the spring and autumn trends had an annual increase of 5 to 6 precipitation days relative to the beginning of the century and the linear trends were significantly different than zero. In the summer season of the southeast region of Australia, a century-long statistically significant increase of 20% in precipitation frequency was detected. However, there was no significant changes in the frequency of rainy days in the winter season of Australia. In a related study, Hennessy et al. (1998) found significant increases in the number of rain days in all seasons, except winter, from 1910 to 1995. In Norway, century long trends in annual precipitation was found by Hanssen-Bauer and Førland (1994). The probability of daily precipitation exceeds 50% and the increase in summer total precipitation was followed by an increase in precipitation frequency.

For Canada and Russia, Groisman et al. (1999) analysed the probability of days with measurable precipitation above 1 mm. In southern Canada (south of 55°N) no significant trends were found, however, the number of days with rainfall has increased after the mid 1970's. There is also no trend in the number of days with summer precipitation. The number of summer days with precipitation greater than 1 mm has not changed over the European part of Russia, however, significant trends were found in the frequency of summer precipitation events above 20 mm. A statistically significant decreasing trend in precipitation frequency was observed over Siberia, the Asian part of Russia

Researchers (IPCC, 1996; among others) found at least a 5% increase in mean summer precipitation in all of the eight countries analysed. Groisman et al. (1999) applied this 5% increase in mean summer precipitation to the statistical model to determine its affect on heavy precipitation. Heavy

precipitation was defined as daily precipitation exceeding 2 inches for mid-latitude countries (USA and Mexico) and 1 inch for high-latitude countries (Canada and Norway).

In regions in the eastern USA, a 5 % increase in mean daily precipitation causes the probability of daily precipitation above 2 inches to increase by approximately 20%. In Mexico, an increase of 5% in summer precipitation yields a 20 to 30% increase in the probability of daily summer precipitation above 2 inches (excluding the desert regions). In this scenario, more than 70% of the increase in mean summer precipitation over the tropical regions of Mexico is caused by heavy rains.

For Canada, Russia, Poland and Norway the mean summer precipitation increased by 20% in the probability of days with precipitation above 1 inch. Heavy rainfall events cause a 30% increase in Russia, Canada, and Northern Norway and more than 40% in Southern Norway, and Poland of the increase of mean daily precipitation.

Zhang (2000) analysed precipitation totals in Canada for daily rainfall totals from 489 stations. The stations were subjected to rigorous quality and control and the data covers the majority of the country with a time period from 1900 to1998.

Zhang (2000) found abnormally dry conditions (precipitation less than 34th percentile) have been gradually decreasing, while abnormally wet conditions (precipitation greater than the 66th percentile) have increased from the period of 1900 till 1998. Extreme climate indices generally follow the same changes as the abnormal indices. One significant change is that summer precipitation, extreme dry and wet conditions, have increased in comparison with the abnormal index. The indices from 1950 till 1998 gradually decreased for the abnormal dry condition, while abnormal wet conditions gradually increased decade by decade. Both extreme indices generally displayed the same pattern as the abnormal indices for this time period.

Zhang (1999) found that total annual precipitation has increase by 12% in southern Canada from the time period of 1900 till 1998, with a steady increase found during 1920 till 1970. In some areas

of Southern Canada, the increase in precipitation is as high as 30%. Significant increasing trends were found in each province, with the exception of Alberta and Saskatchewan. In terms of percentages, eastern Canada experienced the greatest increase in all four seasons, although Quebec did not experience significant trends in the winter and spring seasons. British Columbia also experienced significant increases in all four seasons, while the Prairies experienced the least increases in precipitation with only the winter have significant trends.

Annual precipitation increased by 5% to 35% during the period of 1950 till 1998 in different areas of Canada. In general, increasing trends were found in all seasons for precipitation totals, and some area of decreasing trends were found in the winter season. Significant increasing trends were found in the Arctic (north of 60°N), while winter precipitation generally decreased in some areas of southern Canada.

Gruza et al. (1999) performed a climate change study within the Russian Federation (RF) territory as a whole and for its western part labelled the Russian Permafrost Free (RPF) territory. The data set contains monthly precipitation totals from 455 meteorological stations located within the former Soviet Union during the period of 1866 to 1995 and 202 precipitation stations contain data from 1901 to 1995. A data set composed of 41 stations with a time period of 1966 to 1995 was used in the analysis of extremes precipitation.

To test for regional climate change, Gruza et al. (1999) used an area-average technique to characterize the regional climate variability. This is composed of two steps: (i) averages in 5° latitude by 5° longitude boxes were calculated from the stations located within each box; (ii) area-weighted averaging was performed, based on the mean value of each box.

Annual mean precipitation, and precipitation for both warm and cold seasons experienced weak negative trends for the area-averaged RPF territory. Overall, the time series of the percentage of the area of the RPF covered by extreme anomalies showed a decrease of precipitation over Russian territory. The majority of decreases in the annual mean precipitation are found in the cold season.

For climate extremes during the winter seasons, a few stations displayed increasing number of days with precipitation exceeding the 95% percentile in European Russia (north of 55°) and in the center of Siberia. Decreasing trends were found in most of the other stations used in the analysis. For climate extremes during the summer seasons, there was an increase in summer precipitation at all stations in European Russia, however, negative linear trends in summer precipitation were generally obtained in other regions experiencing fewer days with heavy precipitation.

Heino et al. (1999) performed a long-term study on various extreme parameters in Northern and Central Europe. The northern countries consist of Finland, Sweden, and Norway, while the central countries are Poland, Germany, Switzerland, and Czech Republic. Record lengths for stations analyzed ranged from 1901 to 1995 and the data compiled were for an annual time series.

The researchers found no major trend in the maximum 1-day precipitation in the various countries in Europe. One station in Germany had the only significant trend, while insignificant increasing and decreasing trends are found in other countries. Heino (1999) indicates that 1-day precipitation totals from single stations is not a great indicator of climate change, however, regional trends of maximum precipitation should be used with a dense network of stations in a region.

Another method used by the researchers were the number of days with precipitation exceeding 10 mm, an important statistic in extremes analysis. One German station and a Norwegian station showed an increasing trend at a 5% significance level. Heino et al. (1999) mentions this statistic has its fault's, such as regions in the world where 10 mm of rain occurs often and some regions where 10 mm occurs seldom.

Plummer et al. (1999) performed a study on changes in climate extremes in the Australian regions using 379 stations in the analysis of precipitation with a time period beginning in 1910 and ending in 1995. Plummer followed the work performed by Salinger et al. (1996) where an increase in summer precipitation over Eastern Australia was found, while decreases were observed over parts of Southwestern Australia in the winter season.

Australia was separated into four quadrants (separated by 26°S and 135°E) using area-weighted averages for the indices based on rainfall and a modification to the Thiessen Polygon method (Lavery et al., 1997). Annual percentile values (Moore and McCabe, 1993) were calculated for individual stations and area weightings were derived from the Thiessen polygon procedure over the period 1910 to 1995. The percentage of Australia experiencing extreme dry conditions (below decile 1 or 10th percentile of annual total) has decreased slightly since 1910. Due to high rainfall totals in the mid-70's, a small increase in the area experiencing wet conditions (90th percentile) was found. At a 95 % level, neither trend is significant.

A number of authors (Yu and Neil, 1993; Lough, 1993 and 1997; Nicholls and Kariko, 1993; Suppiah and Hennessy, 1996) analyzed trends in heavy rainfall intensity in Australia revealing the results are dependent on the different definitions for heavy rainfall events and different statistical methods. In Plummer's work, heavy rainfall was defined as the 99th percentile of daily data for a period of 1910 to 1995. For changes in the intensity of heavy rainfall, the frequency of heavy rainfall are presented for a threshold of 1 inch. Heavy rainfall indices were computed at individual stations, then the Thiessen polygon method was used to develop area-averages for each quadrant.

For Australia as a whole, the 99th percentile rainfall intensity has experienced little change over the period of 1910-1995. More increasing trends were found for quadrants and seasons than decreasing, however, none significant at a 5% level. Southeast Australia in the autumn season had a 24% increase (significant at 6%) in precipitation and a 20% increase was observed in northwest winter and southwest summer. A decreasing trend of 20% was found in northeast winter and southwest autumn. In a related study, Hennessy et al. (1998) found a 31% increase in the 99th percentile in Southeastern Australia and a significant 13% decrease in Southwest Western Australia in the winter season. No significant trends were found at a 5% level in the annual number of days with rainfall over 25.4 mm. In general, small increases have been observed in summer and autumn seasons, while decreases have been seen in the winter season.

Zhai et al. (1999) performed a study on daily precipitation totals for 296 stations that had good spatial coverage of China. China was subjectively delineated into 8 regions, and the climate extreme indices were obtained by arithmetic means inside each region and weighted by area to give the trend.

For annual precipitation totals, a clear trend (increasing or decreasing) was not observed in the data sets, however large inter-annual variation are evident in the proportion of China affected by extreme annual precipitation totals. Increasing trends was seen in Western Northwest China, however the other regions experienced a negative trend (North China experiencing a significant negative trend at a 5% level). With the exception of Northwest China, the remaining regions covered by a much greater than normal number of rain days decreased significantly during 1951-1995. The discrepancy between trends in the extreme amount of annual precipitation and the number of rainy days suggests that rainfall intensity is changing.

For 1-day and 3-day maximum rainfalls, no significant trends were observed in China as a whole. North China was found to have statistically significant decreasing trends in both 1-day and 3-day rainfall extremes, while North West China had increasing trends, but not significant.

For amount and days of high intensity rainfall, decreasing trends were observed from daily precipitation greater than various thresholds (greater than 10 mm, 50 mm, and 100 mm rainfalls daily) for China as a whole. However, large areas of China experienced an increasing frequency of extreme amounts of heavy rainfalls (greater than 10 mm, 50 mm, and 100 mm rainfalls daily) after 1970's.

A statistically significant increasing trend is seen in Western Northwest China for the percent area of much more than normal rainfalls with a daily threshold above 10 mm, while North China had a decreasing trend.

In terms of days with daily precipitation greater than 10 mm decreasing trends are generally found with significant trends in Northeast and Southwest China. For rainfall days with daily rainfall above 50 mm, statistically significant increasing trends can be found in certain locations of China (Northeast, North, Northwest China). Statistically significant decreasing trends in the number of days with daily rainfall above 100 mm are apparent in much of China.

For rainfall intensity, China experienced a statistically significant positive trends, while three regions (South, East, and North China) also experienced significant trends. Zhai et al (1999) suggest the high increasing in rainfall intensity in these regions is due to the East Asian Monsoon. For the longest consecutive rain days, China experienced a statistically significant decreasing trend. All regions had decreasing trends with 7 out of the 8 regions being statistically significant at a 5% level.

In Italy, Brunetti et al. (2001) performed a study on 5 rainfall stations in northern Italy: Genoa (1833-1998), Milan (1858-1998), Mantova (1868-1997), Bologna (1879-1998) and Ferrara (1879-1996). Regional anomaly series were computed for the five stations on a seasonal and yearly basis. Anomalies included in the analysis were: number of days with precipitation greater than 1 mm, and average rain amount per rain day. In addition, anomalies were calculated for the proportion of daily precipitation falling in the following categories: 1.00-2.49 mm, 2.50 mm - 12.49 mm, 12.50 mm - 24.99 mm, 25.00 mm - 49.99 mm, 50.00 mm, and greater than 50 mm. . The non-parametric Mann-Kendall test was applied to the anomalies to detect any significant trends.

Brunetti found the average number of rain days over the five stations in the period of 1834-1998 having a more significant trend than total precipitation, on a yearly and seasonal basis. A positive increasing trend in precipitation intensity was detected causing an increase in the proportion of daily precipitation falling in the higher precipitation intervals (25 mm - 49.99 mm and greater than 50 mm). A decrease was observed in the precipitation falling in the lower intervals (0 to 12.49 mm).

In summary, statistical evidence (Karl et al, 1995; Karl and Knight, 1998; Groisman et al., 1999; Zhang et al, 1999) exists suggesting extreme and total precipitation totals are changing in recent

decades in the region of North America. To the author's knowledge, no tests have been performed on the different storm (5 min to 12 hour) durations of extreme rainfall. Therefore, in this thesis, trends are examined in the annual maximum (1-day event) for various durations for single sites and regional data sets.

2.4 Spatial Analysis

In most studies, the detection of trends are studied without taking into account the role of spatial correlation and ignoring its importance in statistical analysis (Douglas et al., 2000). Neglecting spatial correlation in trend detection is due to the requirement of independent observations in most trend tests. Spatial correlation (cross correlation) creates an overlap in information contained in each data point, meaning a trend found at a site will most likely be found at a nearby site in a spatially correlated region. Thus, correlation reduces the effective sample size of the data set. The presence of correlation also nullifies the assumption of independently and identically distributed (iid) variables which is required in statistical analysis. Therefore, the significance of the test statistic for trend detection must be determined by the development of an approximate statistical distribution (Douglas et al., 2000).

To detect observed cross correlation in data sets, two methods have been commonly used. The first utilizes the binomial distribution on a procedure developed by Livezey and Chen (1983) and the other uses the techniques of geostatistics.

2.4.1 Binomial Distribution

The fundamental question in using this approach is determining the probability that significant correlation at a 95% level can occur by chance, or (in terms of specific confidence level), what percent of area represented by significant correlations would be equalled or exceeded one out of twenty (5%) by accident (Livezey and Chen, 1983).

In terms of probability, the binomial distribution is used to describe situations where only two outcomes are possible. Therefore, this distribution can be applied in the design of overall significance tests where the two scenario's are test passed (probability equal to 0.05) and tests failed (probability equal to 0.95). Given a collection of independent tests, N, and a significance level of 95% (probability (p) equal to 0.05), the binomial distribution is expressed as

$$p_r = \frac{N!}{r!(n-r)!} p^r (1-p)^{n-r} \tag{2.5}$$

where, p_r is the probability of an event succeeding r times. The probability of an exact number succeeding events is computed using equation 2.5, and the cumulative probability greater than or equal to the exact number events ($P(r>r_o)$) can be computed as well. Linear interpolation is used to determine the threshold criterion, the number of significant tests, r_o, that will occur by chance for P=0.05. The value of r_o is compared with the significant tests found from the observed results, r. If r exceeds the value of r_o, then the region is spatially correlated.

Zhang et al. (2001) studied streamflow data which consisted of 151 basins for a 30-year period, 71 for a 40 year period, and 47 for a 50 year period, respectively. The researchers determined the trend and local significance for each basin separately. The percentage of basins where significant trend is detected was used as a measure of global significance. The significance of trend over the entire spatial field of observations was estimated by comparing the percentage of basins where significant trend was detected, to the percentage of trend would be expected to occur by chance (for a given significance level and number of degrees of freedom).

Douglas et al. (2000) analyzed flood and low flows for 3 major geographic regions and 9 hydrologic super regions (following Lettenmaier et al., 1994). Douglas et al. (2000) used the Livezey and Chen (1983) procedure to determine if a region has significant autocorrelation. Autocorrelation was found for each station in a region and compared to the number of significant tests that will be equalled or exceeded by chance 5% of the time. If the observed autocorrelation for a region was greater than what would occur by chance, then the region is significantly autocorrelated.

Douglas et al. (2000) compared the trend results from these regions by analysing two cases: with cross correlation (spatially dependent) and without cross correlation (spatially independent). Significance for regions that are spatially independent were found using analytical equations and the use of the normal distribution, while significance for spatially correlated regions were found by using a bootstrap procedure (discussed in Chapter 3) which creates an empirical cumulative distribution function. They found that many more trend tests would have been considered statistically significant if cross correlation was ignored. This emphasizes how misleading many trend tests have been in the past if spatial correlation existed in the data sets.

2.4.2 Geostatistical Analysis

Geostatistics is a set of statistical estimation techniques involving variables which vary in space (Kitanidis, 1993). Geostatistics is very popular in the mining industry, however, it has also found some applications in the field of hydrology and geophysics (de Marsily and Delhomme, 1989; Cressie, 1993). Possible applications of geostatistics include:

a) Averaging or integrating problems, such as taking measurements of precipitation at a number of rain gauges and estimating the mean annual precipitation at an unknown location and evaluating the accuracy of the estimate.

b) Inverse problem, such as taking measurements of hydraulic head at a number of wells and other information and estimating the values of transmissivity using a groundwater model.

These problems illustrate the common characteristics for the application of geostatistics. They involve the use of spatial variables, such as precipitation, moisture content, and water table elevation. Statistical techniques are then used to produce estimates of an unknown quantity with the known spatial variables and determining the reliability and the accuracy of the estimate.

The steps in a geostatistical analysis can be subdivided into two steps: structural analysis and best linear unbiased estimation (BLUE). Structural analysis is the selection of a model, or semivariogram, to describe spatial variability. It is based on the analysis of data and other information, such as experience with data at similar sites and geologic and hydrologic information. The selection of the variogram is an iterative process consisting of: (1) exploratory data analysis and the selection of a temporary model, (2) parameter estimation based on the semivariogram selected and (3) model validation or diagnostic checking (Kitanidis, 1993).

The variogram is the characterization of spatial autocorrelation in several directions and for various lag distances to obtain an experimental variogram (Daviau et al., 2000). The variogram is the difference between random variables at two different locations. If two stations are close together, the differences in the variables and variance should be small (high correlation). As the distance between station locations increases, differences in the variance becomes larger and larger, becoming less correlated. In geostatistics, the increase in variance as the distance between stations increase is called the range. Eventually, their will be a point where the data at different stations behave independently of each and the variance becomes constant, known as the sill. If the variables contain no range, meaning the plateau is reached instantly and the variogram is a horizontal line, then the variables have no dependency to each other.

The BLUE procedure deals with finding the estimate of a value ($\hat{z}$) of z at an unmeasured station (x_o) from known observations ($z(x_1).....z(x_n)$) from neighbouring locations by using a linear estimator such as :

$$\hat{z}(x_o) = \sum_{i=1}^{n} \lambda_i z(x_i) \qquad (2.6)$$

where λ are weights. The sum of all weights is usually 1 and are usually inversely proportional to some power of the distance between the measured and unmeasured stations. A more objective approach is to choose weights based on the variogram technique. If the variogram is approximately constant, then the weights should be approximately the same. However, if the variogram has a significant dip (or range) then larger weights should be selected for site's close to the unmeasured

location. A common approach is to use kriging techniques, a system of linear equations which are unbiased and have the smallest possible mean square error, to solve for the weights.

Adamowski and Bocci (2001) expressed the variance of the random time trend and flow residual variables in terms of semivariograms in order to capture the spatial dispersion in the regions analysed. The components taken from the semivariograms were used in kriging techniques to determined the weights and the regional time trend in 10 homogeneous regions containing 248 stations across Canada was determined.

Daviau et al. (2000) uses geostatistics to improve current methods for exploratory data analysis and parameter estimation in current regional flood frequency analysis for eastern and central Canada using 371 flow stations. Instead of point values, Daviau et al. (2000) used variograms to shape and size a proposed region based on the degree of spatial correlation. The at-site estimates were then obtained with the use of unbiased L-moments and kriging techniques (rather than regression) was performed to map a spatially correlated surface based on the at-site parameters. GIS was then used to measure the spatial association between the variables and to diagnose the homogenous regions for further refinement using spatial contrast measures.

Geostatistics was used in this analysis to analyse the spatial correlation in the region. Variograms were created to determine if a range existed in the precipitation field. Kriging techniques were not applied in this thesis since estimates were not needed at ungauged locations. The purpose of geostatistics in this thesis is to determine if a region is spatially independent or dependent, which would ultimately decide if the significance of the trend could be found using analytical equations and the normal distribution or if an empirical CDF would need to be created.

Chapter 3

THEORETICAL DEVELOPMENT

3.1 L-Moments

In extreme flood and precipitation analysis, Hosking and Wallis (1993) developed a procedure involving the grouping of sites with similar attributes and characteristics to form one homogeneous region. This procedure involves transforming the at-site data into L-moments, the assignment of sites into a region based on a discordancy measure, and testing if the region is indeed homogeneous by using a heterogeneity measure. In this thesis, homogeneous regions were delineated and validated using the techniques and methodology discussed below.

3.1.1 Theory of L-Moments

The method of L-moments estimates statistical properties of hydrological data and defined as linear combinations of a ranked data set (Wang, 1996) or estimated using probability weighted moments (PWM) defined by Greenwood et al. (1979) as

$$\beta_r = E\left\{x\left[F(x)\right]^r\right\} \tag{3.1}$$

where x is a random variable with a cumulative distribution function F. Hosking (1986, 1990)

defined the r-th L-moment of a random variable to be a linear combination of PWM's expressed as

$$\lambda_{r+1} = \sum_{k=0}^{r} p^*_{r,k}\beta_k \tag{3.2}$$

where

$$p^*_{r,k} = (-1)^{r-k}\binom{r}{k}\binom{r+k}{k} \tag{3.3}$$

For any distribution, Vogel and Fennessey (1993) showed the unbiased estimators b_r of the r-th order PWM , β_r, can be expressed as

$$b_r = \frac{1}{n}\sum_{j=1}^{n-r}\left[\frac{\binom{n-j}{r}}{\binom{n-1}{r}}\right]x_{(j)} \tag{3.4}$$

where n is the record length, and $x(j)$ is an ordered annual maximum observation. For r being 0, 1, 2, and 3, Equation 3.4 yields

$$\begin{aligned}
b_0 &= \frac{1}{n}\sum_{j=1}^{n} x_{(j)} \\
b_1 &= \sum_{j=1}^{n-1}\left(\frac{(n-j)}{n(n-1)}\right)x_{(j)} \\
b_2 &= \sum_{j=1}^{n-2}\left(\frac{(n-j)(n-j-1)}{n(n-1)(n-2)}\right)x_{(j)} \\
b_3 &= \sum_{j=1}^{n-3}\left(\frac{(n-j)(n-j-1)(n-j-2)}{n(n-1)(n-2)(n-3)}\right)x_{(j)}
\end{aligned} \tag{3.5}$$

An estimate of the sample L-moments (l_r) was employed using unbiased PWMs defined as

$$l_{r+1} = \sum_{k=0}^{r} b_r(-1)^{r-k}\binom{r}{k}\binom{r+k}{k} \tag{3.6}$$

where r equaling 0 to 3 will yield

$$\begin{aligned}\lambda_1 &= \beta_0 \\ \lambda_2 &= 2\beta_1 - \beta_0 \\ \lambda_3 &= 6\beta_2 - 6\beta_1 + \beta_0 \\ \lambda_4 &= 20\beta_3 - 30\beta_2 + 12\beta_1 - \beta_0\end{aligned} \tag{3.7}$$

in which λ_1 is a measure of location, and λ_2 is a measure of the dispersion. Hosking found it convenient to standardize L-moments of order 3 such that the r-th moment ratio is given by

$$\tau_r = \frac{\lambda_r}{\lambda_2} \tag{3.8}$$

where the third moment, τ_3, is a measure of skewness and is defined by the ratio of λ_3 to λ_2. The fourth moment, τ_4, is a measure of kurtosis and defined by the ratio of λ_4 to λ_2. The coefficient of variation, L-CV, is the ratio of λ_2 to λ_1.

3.1.2 Theoretical Properties of L-Moments

(i) Robustness

Robustness in a sample statistic occurs when its performance is unaffected by small changes in the tails of the distribution, meaning that the presence of outliers in data sets do not significantly affect the estimates of parameters.

Non-robustness in the method of moments is caused by the squaring and cubing of the data, giving heavier weight to large observations in the sample. It was found (Royston 1991) that L-moments are less sensitive to extreme outliers by using a non-parametric sampling technique. His work showed that different values of skewness and kurtosis were found when outliers and no outliers existed in the sub-samples, however, L-skewness and L-kurtosis values remained consistent around

the population value with the presence of outliers.

(ii) Bias

An sample statistics is unbiased when the estimated quantity and the expected value are equal. In using a non-parametric re-sampling technique, Royston (1991) discovered that L-moments can be much less biased than the ordinary method of moments. As skewness and kurtosis tend to decrease as the sample size decreases, their L-moments displayed no decreasing trend. Wallis (1989) used a parametric bootstrapping technique to demonstrate the ability of L-moments to be less biased than ordinary moments. In generating 100 samples using the EV I distribution with sample sizes ranging from 10, 25, 40, and 100, Wallis found L-moment estimates of skewness and kurtosis to be less biased, having a smaller variance and being normally distributed about their population values when compared to the conventional moments estimates.

3.1.3 Discordancy Measure

The discordancy measure developed by Hosking and Wallis (1993) is used to identify and remove sites containing properties which are irregular in comparison with others formed as one homogeneous region. The L-moments (L-CV, L-skewness, and kurtosis) of a proposed region are plotted in three dimensional space to form a cloud, as shown in figure 3.1. The center of the cloud was determined by taking the average values of L-CV and L-skewness for all sites and two concentric ellipses (major and minor axis) were constructed and selected to give the best fit to the data (determined by the sample covariance matrix of the sites' L-moments). Site's to be removed from the group exist beyond the outermost ellipse.

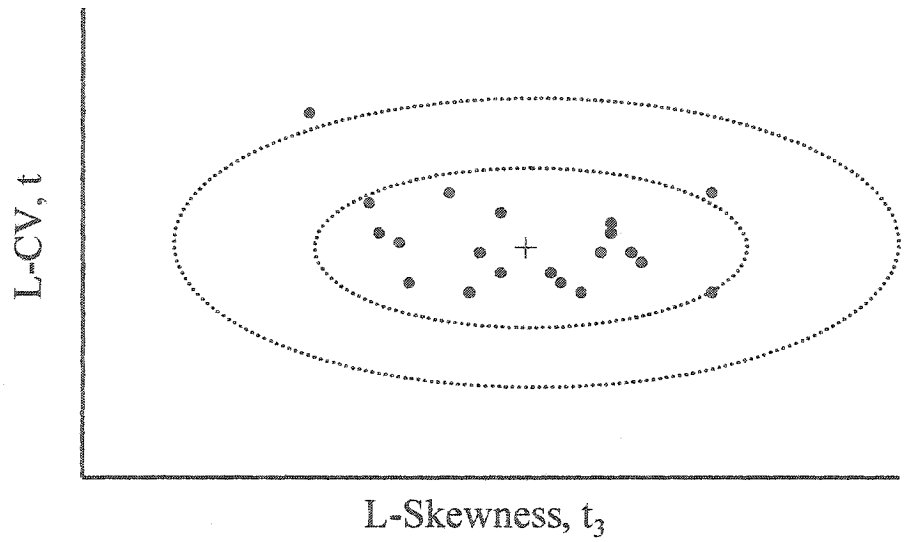

Figure 3.1: Definition sketch for the discordancy measure (after Hosking, 1997)

Let $u_i = [\tau^{(i)}, \tau_3^{(i)}, \tau_4^{(i)}]^T$ be a vector containing the L-moment ratios for site i (Hosking and Wallis, 1993), then the unweighted group average is defined as

$$\overline{u} = N^{-1} \sum_{i=1}^{N} u_i \tag{3.9}$$

The sample covariance matrix, S_i, is defined as

$$S_i = (N-1)^{-1} \sum_{i=1}^{N} (u_i - \overline{u})(u_i - \overline{u})^T \tag{3.10}$$

Equation's 3.9 and 3.10 are used to define the discordancy measure for site i as

$$D_i = \frac{1}{3}(u_i - \overline{u})^T S^{-1} (u_i - \overline{u}) \tag{3.11}$$

Site's which produce large values for D_i indicate a difference between the discordant site and the group as a whole. The threshold value for D_i is 3, meaning if a site exceeds this threshold it will be removed from the group. Hosking and Wallis mentioned that large values of D_i should be examined

regardless of the magnitude.

Hosking and Wallis suggest (1993) two uses for the discordancy measure: (i) applying the measure to a large amount of sites in a geographical region before the analysis commences. The idea is to flag sites with gross errors in their data sets which stand out from the other sites in the region. Errors can be caused in recoding the observed data or by man-induced changes, such as moving gages to different sites (Hosking and Wallis, 1993); (ii) to remove sites from a proposed group into a different group.

3.1.4 Homogeneous Tests for Regions

Hosking and Wallis (1993) developed a heterogeneity measure, H, to determine if a proposed region can be treated as homogeneous. The H measure compares the site variations in sample L-moments for the proposed region with what would be expected from a homogeneous region

To test the homogeneity of the data set, the at-site weighted standard deviation of the proposed region, V, is defined by (Hosking and Wallis, 1993):

$$V = \frac{\sum_{i=1}^{N} n_i \left(LCV^i - \overline{LCV} \right)^2}{\sum_{i=1}^{N} n_i} \tag{3.12}$$

A four parameter kappa distribution is used to simulate a large number of homogeneous regions by a Monte Carlo technique. The simulated regions have no serial or cross correlation. From the simulations, the mean (μ_v) and standard deviation (σ_v) from the homogeneous population are computed. The heterogeneity measure is computed by

$$H = \left(\frac{V - \mu_v}{\sigma_v} \right) \tag{3.13}$$

If H is less than 1, then the region is homogeneous; if H is greater than 1 but less than 2, then the region is possibly heterogeneous; if the region is greater than 2 then it is definitely heterogeneous. In order for the H statistic to have significance, Hosking and Wallis (1993) indicated that proposed regions must be based on site characteristics, such as geography and mean annual precipitation (MAP). In this thesis, the direction of trend (plus, minus, no trend) was used in the process of delineating homogeneous regions. Fortran subroutines created by Hosking (1991) allowed the computation of the discordancy and heterogeneity measures.

3.2 Trend Test

Natural and human-induced factors may produce gradual and instantaneous shifts or trends in a hydrological time series. A number of parametric and nonparametric tests for trends are available. One of the parametric tests to detect and estimate linear trends is the method of linear regression. However, linear regression requires some assumptions (such as normality of residuals, constant variance, and true linearity of the relationship) which often are not exactly met in practical applications. Alternatively, a non-parametric test can be used whereby no assumptions are required. Therefore, the nonparametric Mann-Kendall test for trend (Mann, 1945; Kendall, 1962) is used in this study (Maidment et al., 1993).

3.2.1 Linear Regression

In describing a trend, a simple linear regression model was used and is given by

$$y_t = \alpha + \beta t \qquad (t = 0, 1, 2, .. n) \tag{3.14}$$

where y_t is the annual maximum rainfall time series, α is the intercept, β is the slope (trend), and n is the length of the data. For illustration purposes, figure 3.2 presents the raw observed data for station 6151032 (Burketon) for a storm duration of 2 hours. It clearly indicates the presence of a

trend in the data.

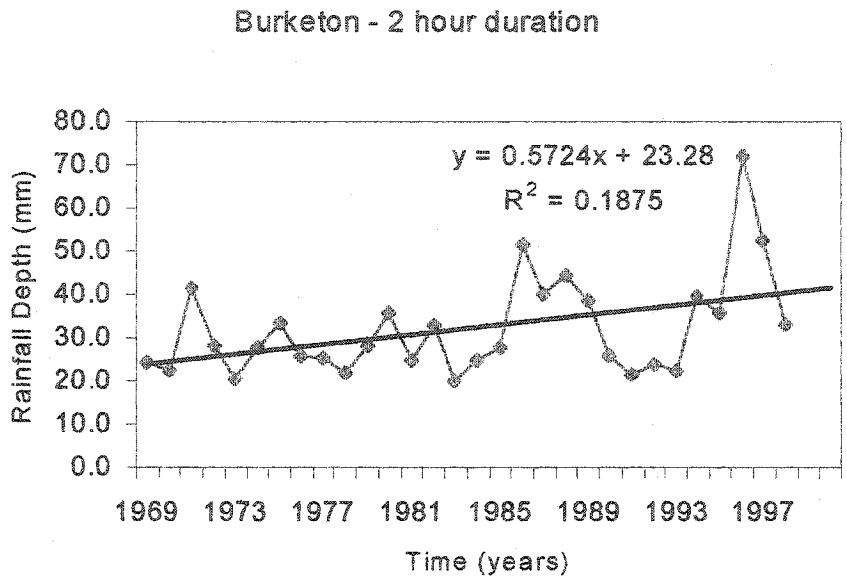

Figure 3.2: Raw data from station 6151032 (Burketon) fitted with a linear trend for a two hour storm

3.2.2 Single Sites

The significance of trend, β, was estimated using the non-parametric Mann-Kendall test (Mann, 1945; Kendall, 1975) at a 95% confidence interval. The Mann-Kendall test is applied to linear trends in this paper, however, it can also be applied to nonlinear tends (Maidment, 1993).

The trend test is applied to an annual extreme value time series, x_i, ranked from $i = 1,..., n-1$, and x_j is ranked from $j = i+1,...,n$. Each data point, x_i, is used as a reference point and is compared to all other data points (x_j) such that

$$sign(x) = \begin{cases} 1 & x_j > x_i \\ 0 & x_j = x_i \\ -1 & x_j < x_i \end{cases} \tag{3.15}$$

The Kendall's S statistic is calculated as

$$S = \sum_{i=1}^{n-1} \sum_{j=i+1}^{n} sign(x_j - x_i) \tag{3.16}$$

If the data is identically, independently distributed, the mean is zero and the variance for the S statistic can be defined by

$$\sigma^2 = \frac{n(n-1)(2n+5) - \sum_{i=1}^{n} t_i(i)(i-1)(2i+5)}{18} \tag{3.17}$$

The summation term in Equation 3.17 is only used if data values are tied in the series. The test statistic, Z_s, can be calculated as

$$Z_s = \begin{cases} (S-1)/\sigma & \text{for S} > 0 \\ (S+1)/\sigma & \text{for S} > 0 \\ 0 & \text{for S} = 0 \end{cases} \tag{3.18}$$

in which Z_s follows a standard normal distribution, with the critical value $Z_{\alpha/2}$. Equation 3.18 can be used for record lengths greater than 10, if the number of tied data is low (Kendall, 1962). The at-site significance level (p) can be obtained by using the test statistic in the cumulative distribution function for a standard normal variate (F_N), or

$$p = 2\left[1 - F_N(Z_s)\right] \tag{3.19}$$

If $|Z_s|$ is greater than $Z_{\alpha/2}$, where α denotes the significance level, then the trend is significant.

3.2.3 Regional Approach

The Mann-Kendall test statistic can be modified to analyze trends on a regional basis rather than individual sites. At a regional scale, Douglas et al. (2000) defined the regional average Kendall's S as

$$\overline{S}_m = \frac{1}{m}\sum_{K=1}^{m} S_K \tag{3.20}$$

where m is the number of stations in a region and S_K is the S statistic for the Kth station in that region. The mean of the regional statistic is zero and variance is given by

$$Var(\overline{S}_m) = \frac{n(n-1)(2n+5) - \sum_{i=1}^{n} t_i(i)(i-1)(2i+5)}{18m} \tag{3.21}$$

Equation 3.21 can be simplified to σ^2/m if the data is independent, where σ^2 is defined in Equation 3.17. Based on the assumption of iid data, the regional average S statistic should approximate zero for large regions, producing the following test statistic

$$Z_m = \frac{\overline{S}_m}{\sigma/\sqrt{m}} \tag{3.22}$$

where the test statistic Z_m can be used as a standard normal variate to determine the significance by comparing it with a tabulated critical value.

3.2.4 Serial Correlation

When trend is estimated by Equation 3.14, it is assumed that the data is uncorrelated and the confidence interval is sensitive to non-normality of the parent distribution (Sen, 1968). If the data has significant autocorrelation, then the Mann-Kendall test will suggest a significant trend in a time series which is actually random more often than detected by the significance level (von Storch and Navarra, 1995). In order to eliminate the effect of significant autocorrelation, the data is "pre-

whitened" before computing the trend as follows

$$W_t = x_t - \rho_1 x_{t-1} \tag{3.23}$$

where ρ_1 is the autocorrelation coefficient of order 1. The population autocorrelation (ρ_k) is defined by

$$\rho_{(k)} = \frac{\mathrm{cov}\big(x(t), x(t+k)\big)}{\mathrm{var}\, x(t)} \tag{3.24}$$

where the numerator in Equation 3.24 represents the covariance function of two observations k units of time apart. The population autocorrelation can be estimated by the serial autocorrelation (r_k) coefficient computed from the following equation

$$r_k = \frac{\sum (x(t) * x(t+k)) - \frac{1}{n-k} \sum x(t) * \sum x(t+k)}{\left(\sum x^2(t) - \frac{1}{n-k} \left(\sum x(t) \right)^2 \right)^{1/2} \left(\sum x^2(t+k) - \frac{1}{n-k} \left(\sum x(t+k) \right)^2 \right)^{1/2}} \tag{3.25}$$

where x is the rainfall, t is the time, and all summations are carried from t =1 and $t = n$-k. Equation 3.25 determines the degree of correlation between observations that are separated by k time units.

The array of autocorrelatrion coefficients ($\rho(1)$, $\rho(2)$....$\rho(n)$) graphed as ordinates against lag (k) produces the correlogram. Figure 3.3 illustrates a correlogram showing autocorrelation (ACF) for Windsor station for a 5 minute storm.

For the null hypothesis that $\rho_k = 0$ for lags greater than 1, the confidence limits for the correlogram is given by (Anderson, 1942)

$$-z_{1-\alpha/2} \frac{1}{\sqrt{n}} < \rho_k < z_{1-\alpha/2} \frac{1}{\sqrt{n}} \tag{3.26}$$

where ρ_1 is statistically significant if it exceeds the confidence interval shown in Equation 3.26.

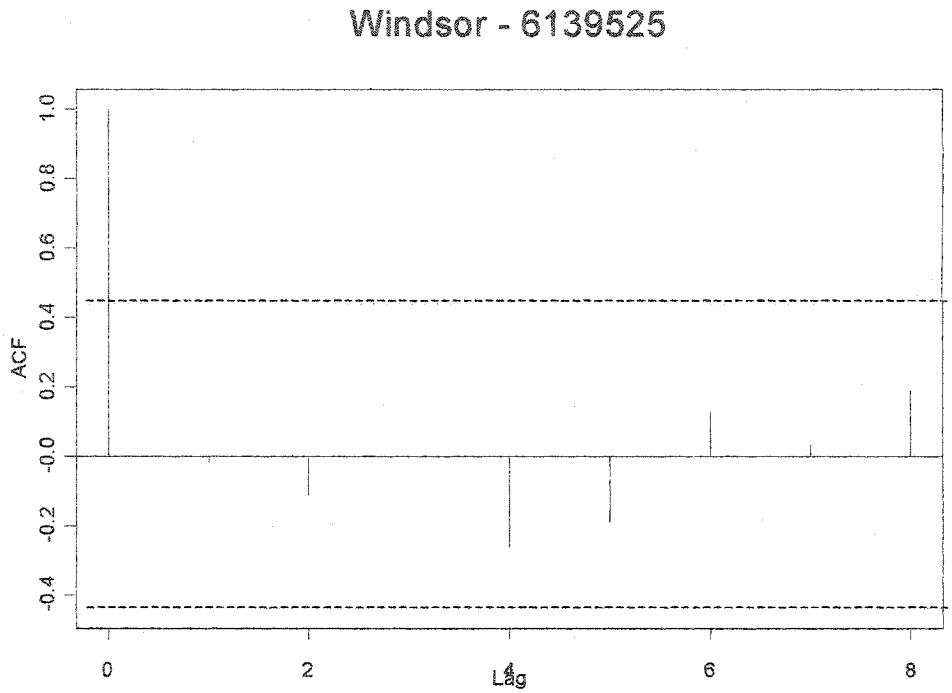

Figure 3.3: ACF with confidence interval for Windsor station for a 5 minute storm. Dashed lines indicate confidence interval at the 5 % level

3.3 IDF Relationships

To determine the affect of increasing trend on IDF estimates, the observed trend component was removed by using Equation 3.14 and shown by

$$x_r = \left(x_{obs} - x_t\right) + \alpha \tag{3.27}$$

where x_r is the time series with the trend component removed and x_{obs} is the observed rainfall data. Figure 3.4 shows the new time series with the trend component removed for the 2 hour storm duration in Burketon. The observed and the removed time series are used to determine the difference in IDF estimates produced at a given station.

IDF curves are often fitted with the Extreme Value Type I distribution developed by Gumbel (1954). To fit the raw AM data to the EV I distribution, the method of moments is often applied due to its simplicity and ease of implementation (Hogg and Carr, 1985). The distribution requires the first two moments, the mean and standard deviation, to be computed. The skewness is fixed in the EV I with a constant value of 1.14. The method of moment estimates for the parameters are

$$\hat{\alpha} = \frac{1.28}{s} \tag{3.28}$$

$$\hat{\beta} = \bar{x} - 0.45s \tag{3.29}$$

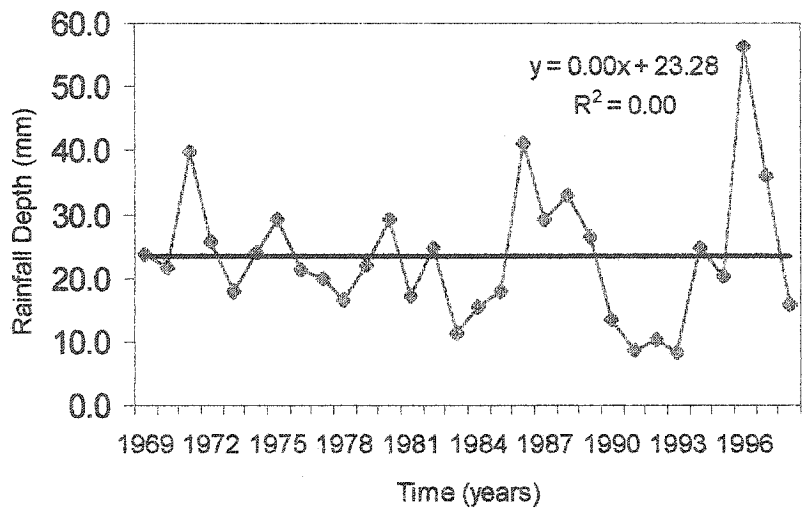

Figure 3.4: Station 6151032 (Burketon) rainfall series with the removal of the linear trend

where x bar and s denote the mean and standard deviation of the observed data set. Intensity of rainfall is fit to the Gumbel distribution by using the following equation

$$I = \beta - \frac{\ln\left(-\ln\left(1-\frac{1}{T}\right)\right)}{\alpha} \tag{3.30}$$

Rearranging equation 3.30 yields an equation to determine the return period (T), defined by

$$T = \frac{1}{1 - e^{-e^{\alpha(1-\beta)}}} \tag{3.31}$$

Equation 3.31 was used to determine the change of return period between the time series with and without trend for a given station and intensity.

3.4 Spatial Correlation and Field Significance

The methodologies discussed in section 3.2 applied to regions that were spatially independent. As mentioned in the previous section, for spatially significant data fields the variance of the *S* statistic cannot be applied. Therefore, observed spatial correlation must be detected in the data sets. Three measures were used to determine if a regional data set can be considered as correlated: (1) time series analysis; (2) L-moments; (3) geostatistics.

3.4.1 Time Series Analysis

The dependency between data sets from two sites in a region can be investigated with the use of cross correlation coefficients. The cross correlation coefficient can be defined as a function of the cross covariance function

$$\rho_{k,k_j} = \frac{E\left((x_i(t) - Ex_i)(x_j(t+k) - Ex_j\right)}{\left(\text{var}\, x_i\ \text{var}\, x_j\right)} \tag{3.32}$$

where x_i, x_j denote the annual maximum precipitation data with means Ex_i and Ex_j and variance x_i and x_j at station's K_i and K_j, respectively. The sample estimate of the cross correlation coefficient is

$$r_{K_i,K_j} = \frac{\sum_{t=1}^{n}\left(x_i(t)-\bar{x}_i\right)\left(x_j(t)-\bar{x}_j\right)}{\left(\sum_{t=1}^{n}\left(x_i(t)-\bar{x}_i\right)^2\right)^{1/2}\left(\sum_{t=1}^{n}\left(x_j(t)-\bar{x}_j\right)^2\right)^{1/2}} \tag{3.33}$$

The plot of sample cross correlation verses lag is the cross correlogram. Cross correlograms are often used to examine the dependency between two time series with one series leading or lagging the other by k units of time. The average cross correlation coefficient for a region can be computed from the following equation

$$\bar{r}_m = \frac{2\sum_{i=1}^{m-1}\sum_{j=i+1}^{m} r_{K_i,K_j}}{m(m-1)} \tag{3.34}$$

The regional variance for the S statistic defined in Equation 3.22 is only valid for data that is iid. For regions with high cross correlations coefficients, Equation 3.22 becomes invalid, therefore, an alternative approach must be taken to determine the variance and the significance of trend. Following the work of Salas-La Cruz (1972), Douglas et al (2000) showed that a region that is cross correlated has a variance of

$$Var(\bar{S}_m) = \frac{\sigma^2}{m}\left[1+(m-1)\bar{r}_m\right] \tag{3.35}$$

Therefore, the variance will increase for a spatially correlated region causing the significance of trend to decrease.

As an initial indicator, cross correlation coefficients were computed for a region to determine if it experiences a high correlation. Douglas et al. (2000) treated regions as spatially dependent when cross correlation coefficients exceeded 0.123, while Hosking (1997) treated regions as spatially dependent when correlation exceeded 0.2. The selection of the threshold value in determining if a region is spatially correlated or independent is quite subjective. Another problem with this

approach is that the coefficient does not incorporate space in the computation. These problems will be examined in the next two sub sections.

3.4.2 L-Moments

The method of L-moments is employed to determine if the data contained in a number of sites can be grouped together to form one homogeneous region. As mentioned earlier, the heterogeneity measure is used to verify proposed regions as homogeneous on the basis of the following relationship

$$H = \frac{(observed\ dispersion) - (mean\ of\ simulation)}{(standard\ deviation\ of\ simulations)} \tag{3.36}$$

In Hosking and Wallis' procedure, homogenous regions are delineated based on the mean and standard deviation of 500 simulated regions, containing no cross correlation, generated by the kappa distribution. In other words, positive H values suggest that regions are spatially independent, since they have similar dispersion to simulated regions that contain no cross correlation

Hosking (1997) indicates that negative H values can occur, indicating that there is less dispersion among at-site sample L-CV values than what would be expected from a homogeneous region. He indicates the most likely cause of H being negative is high positive correlation between the data values at different sites in a proposed region. If H<-2, a significant amount of cross correlation exists between the sites frequency distribution or a problem may exist with the data set that causes the sample L-CVs to be unusually close.

Regions that are significantly cross correlated are dependent on the average cross correlation coefficient, as shown in Equation 3.35. In terms of L-moments, high interstate dependence may cause the heterogeneity measure to be negative. In this thesis, these two factors are used in the decision process to determine if a region is spatially independent or dependent. To confirm these assumptions, the next section incorporates similarity of data with physical distance between sites

in a region

3.4.3 Geostatistics

A geostatistical approach is employed (Chilès and Delfiner, 1999) to investigate the spatial dispersion of the regionalized precipitation field. Variograms are plots of the autocorrelation function at various lags for a given direction (Isaaks and Srivastava, 1989). Since the available data is often sparse, the lags are often specified with tolerance for direction and distance. When the angular tolerance is omitted and only separation distance matters, the results is an omnidirectional variogram, which was used in this thesis.

The semivariogram plots the squared differences of rainfall observations between stations in a region, and can be calculated from

$$\gamma(h) = \frac{1}{2n(h)} \sum \left(K_i(x_i,t) - K_j(x_j,t) \right)^2 \tag{3.37}$$

where x_i and x_j are the annual maximum precipitation data at station location K_i and K_j for a time t, and $n(h)$ is the number of pairs (i,j) which are a distance h apart. A variogram of a random field is $2\gamma(h)$, however it not unusual to see $\gamma(h)$ referred to as the variogram (Kitanidis, 1993). The separation distance is determined using.

$$h = \left| l_i - l_j \right| = \sqrt{(long_i - long_j)^2 + (lat_i - lat_j)^2} \tag{3.38}$$

where l_i and l_j are location vectors composed of two components; the latitude (lat) and longitude (long), $|l_i - l_j|$ denote the norm or Euclidean distance between stations i and j in space, respectively.

Several types of models exist to model the semivariogram. The model chosen in this thesis is the spherical model (Brooker, 1991) which is illustrated in figure 3.5 and defined as

$$\gamma(h) = \begin{cases} 0 & h = 0 \\ C_o + C\left\{1.5\left(\frac{h}{a}\right) - 0.5\left(\frac{h}{a}\right)^3\right\} & 0 < h < a \\ C_o + C & h \geq a \end{cases} \qquad (3.39)$$

where C_o is the nugget effect representing a random measurement error. A pure nugget effect is a variogram which has a constant sill for any lag distance meaning no spatial correlation. $C_o + C$ is the sill, measuring half the maximum squared difference between pairs. The range, a, is the distance at which the variogram reaches the sill.

The correlation structure in a region vanishes when the separation distance, h, between stations is greater than the range; therefore, a region was labeled spatially correlated if (a) a range, or correlation, existed in the variograms for a region and (b) if the heterogeneity measure and cross correlation values suggested spatial correlation.

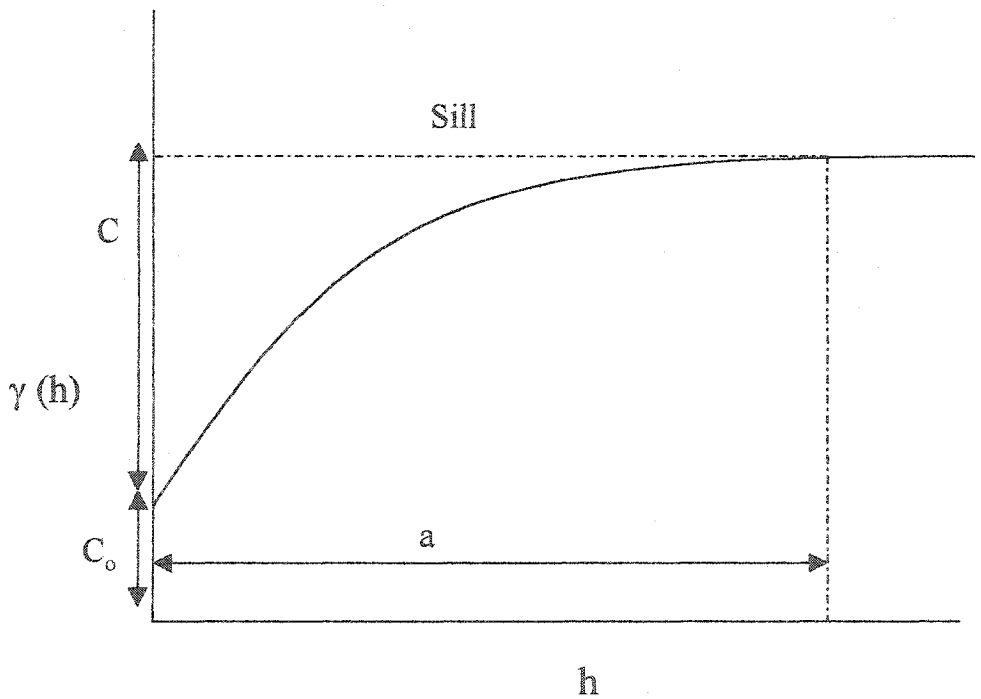

Figure 3.5: Definition sketch of a spherical variogram

3.5 Non-parametric Bootstrap

The bootstrap can be used (Efron, 1979) to estimate properties of a statistical parameter of interest (i.e. trend). In this thesis, the null hypothesis is for the data to show no trend, be serial independent and spatially correlated. A bootstrap sample is created from the observed data and bootstrap replicated are then formed to create an empirical CDF for the regional average Mann-Kendall statistic. Field significance is found by using the observed S computed by Equation 3.20 for the region.

The bootstrapping techniques are applicable to a single, homogeneous sample of data, denoted by $y_1,..., y_n$. An independent and identically distributed series, $Y_1,..., Y_n$, are generated by randomly sampling the homogeneous sample of data, and the probability distribution function (PDF) and CDF of the random sample are denoted by f and F, respectively. The sample is to be used to make interferences about a population characteristic, denoted by θ, using a statistic T. In this thesis, θ is the field significance of a spatially correlated region and the regional average Mann-Kendall S statistic is used as the test statistic T.

Two types of bootstrapping methods exist: parametric and non-parametric. Parametric bootstrapping is to be used when there is a known probability model where random samples are drawn from a specified statistical distribution. In the case of non-parametric bootstrapping, the data is not generated from any mathematical models, however, the assumption of random variables that are independent and identically distributed is retained. In this thesis, non-parametric bootstrapping was performed.

Bootstrapping was developed to answer the following problem: given a random sample $Y = Y_1, Y_2, ... Y_n$ from an unknown probability distribution F, estimate the sampling distribution of some random variable R on the basis of the observed data y. Efron (1979) defined the sampling distribution based on a parameter of interest, θ, and its estimate, $\hat{\theta}$

$$R(Y,F) = \hat{\theta} - \theta \tag{3.40}$$

There are four general steps in the non-parametric bootstrap procedure for a one sample problem (Efron, 1979):

1. To define the empirical distribution, which assigns equal probability (1/n) to each sample value y_j. The corresponding estimate of F (the unknown CDF of the random variable) is the empirical distribution function (EDF) $\hat{F}$, defined as

$$\hat{F}_y = \frac{\#\{y_j \le y\}}{n} \tag{3.41}$$

where $\#\{A\}$ means the number of times the event A occurs (Davidson et al. 1997). If there are repeats in the data, the EDF assigns probabilities proportional to the sample frequencies at each distinct observed value y (Davidson et al., 1997). The EDF plays a role of fitted model when no mathematical form is assumed for F.

2. With $\hat{F}$ fixed, draw a random sample of size n from original data set with replacement and calculate the statistic of interest on the bootstrap sample. That is

$$Y_1^*, Y_2^*, \ldots, Y_n^* \sim \hat{F} \tag{3.42}$$

where equation 3.42 is referred to as the bootstrap sample and

$$\hat{\theta} = \hat{\theta}\left(Y_1^*, Y_2^*, \ldots, Y_n^*\right) \tag{3.43}$$

equation 3.43 is the estimate of θ based on the sample data.

3. Approximate the sampling distribution of θ by repeating step 2 to create a large number (B) of bootstrap replicates

$$\begin{aligned}
\hat{\theta}^{*1} &= \hat{\theta}\left(Y_1^{*1}, Y_2^{*1}, \ldots, Y_n^{*1}\right) \\
\hat{\theta}^{*2} &= \hat{\theta}\left(Y_1^{*2}, Y_2^{*2}, \ldots, Y_n^{*2}\right) \\
&\cdots\cdots\cdots\cdots\cdots\cdots\cdots\cdots\cdots\cdots \\
\hat{\theta}^{*B} &= \hat{\theta}\left(Y_1^{*B}, Y_2^{*B}, \ldots, Y_n^{*B}\right)
\end{aligned} \tag{3.44}$$

which gives B new estimates of the statistic of interest, however, they are not entirely new since they are related to the original estimate $\hat{\theta}$

4. Use bootstrap replicates to create empirical CDF to determine properties of the statistic of interest, such as standard error of estimate, bias, confidence interval, and field significance in this thesis.

In this thesis, the expected value of the single site and regional average Kendall's S is zero, meaning the mean value of 0 is expected to occur for a corresponding probability of 0.5. In step 1 of the algorithm, the observed rainfall data was used for a single station to create the EDF. In step 2, the observed time series for the station was randomly re-sampled until no trend was evident (Kendall's S value of zero). In step 3, the randomly generated time series created in step 2 is the new bootstrapped sample, however, it still maintains the spatial structure of the observed time series. In step 4, a bootstrap replicate is generated from the bootstrap sample and a corresponding Mann-Kendall's S is produced. Steps 1 to 4 is repeated for each station in the region and the average S statistic is then found from the bootstrap replicates. The entire bootstrap procedure is repeated 5000 times. The 5000 regional average S statistics are then ranked in ascending order and given a non-exceedance probability (P) using the Weibull plotting formula given by

$$P = \frac{r}{B+1} \tag{3.46}$$

where r is the rank of the data and B was taken as 5000 in this analysis. The CDF is determined based on the plot of the regional average S's and their assigned probability. The observed regional S is used to determine the field significance for the region. Figure 3.6 shows an example of the bootstrap CDF for the central region for a 10 minute storm duration.

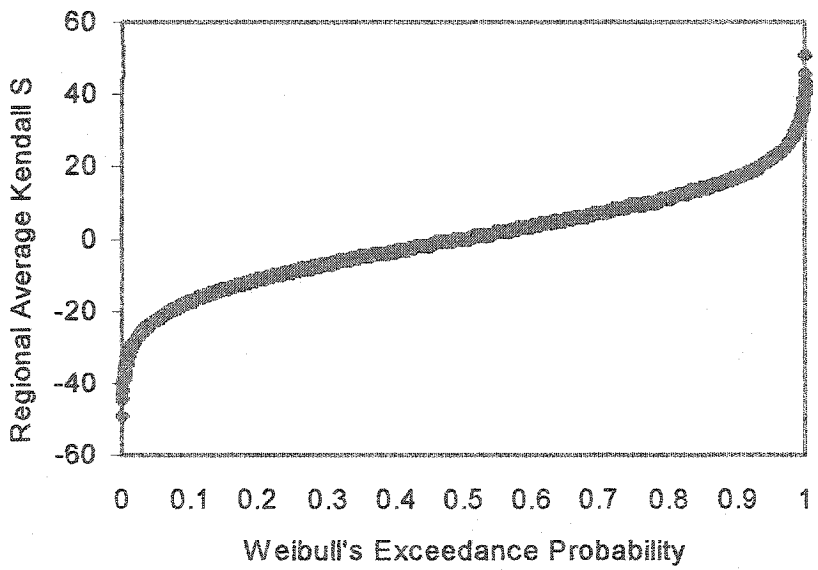

Figure 3.6: A bootstrapped cumulative distribution function for a 10 minute storm for the central region

Chapter 4

NUMERICAL ANALYSIS

4.1 Introduction

The determination of trends are investigated at various rainfall stations across the province of Ontario using the Mann-Kendall trend test (section 3.2.1). The procedure used for the single site analysis is shown in figure 4.1:

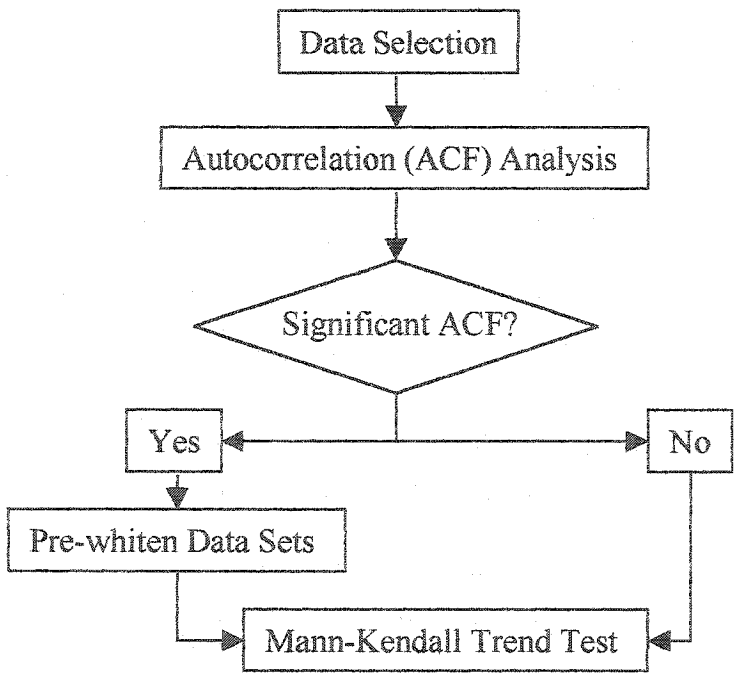

Figure 4.1: Flow chart outlining single site analysis

The test requires rainfall data to be time independent; therefore, data sets with significant ACFs were pre-whitened before applying the test (section 3.2.3). The significance of trend for different record lengths is examined to determine the impact of selecting a time frame for each site and duration. The results for the single site analysis is shown in section 4.3.

The results from the single site analysis influenced the study on the effect of trend on the return period. Various stations were selected across Ontario with increasing trend statistics. The linear trend component was removed from the observed rainfall time series and the difference in IDF estimates were computed. For a given intensity, the difference in return period was found between a station with and without the trend component, respectively. The flow chart can be seen in figure 4.2 and the results in section 4.4.

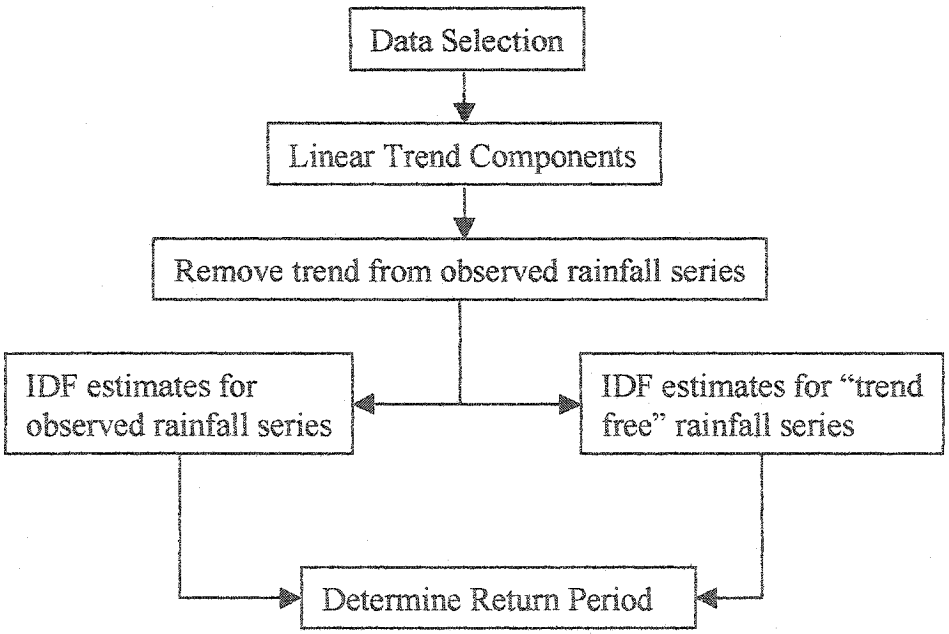

Figure 4.2: Flow chart for the effect of trend on IDF estimates and return period

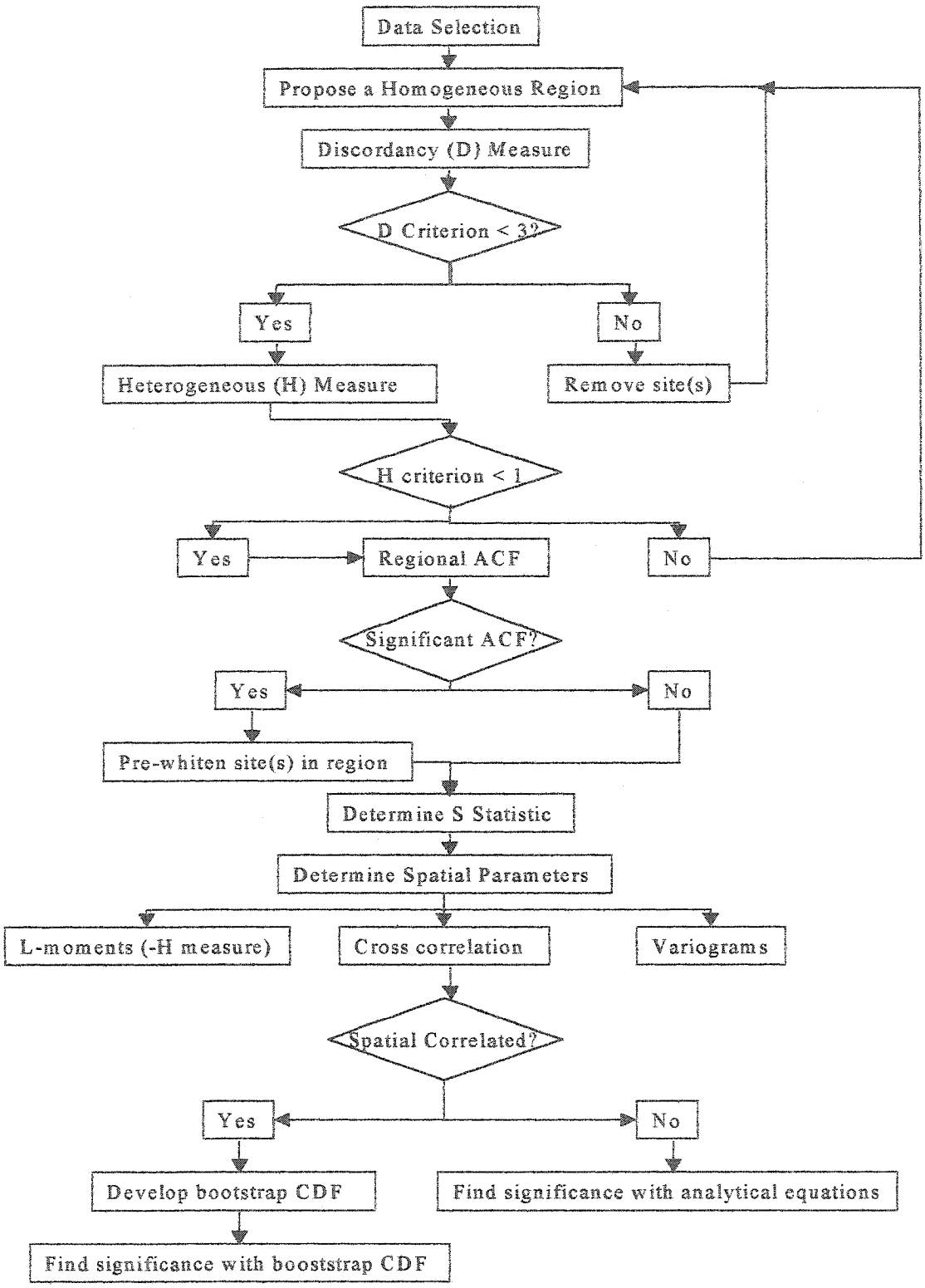

Figure 4.3: Flow chart outlining regional analysis

The procedure in the regional analysis is shown in figure 4.3. Rainfall stations are grouped together to form homogeneous regions by the method of L-moments, outlined in section 3.1 and results displayed in section 4.5. The regional average Kendall S statistic is employed (section 3.2.2) to determine trends at a regional scale, and the affect of significant ACF on the regional data sets are investigated (section 3.2.3). Each region is tested to detect significant spatial correlation (refer to section 3.4), which alters the test procedure in determining the significance of trend. A non-parametric bootstrapping technique (section 3.5) is applied to spatially correlated regions, while regions that are spatially independent utilize analytical equations. The results for the regional analysis is shown in section 4.6. The role of serial and spatial correlation in trend analysis is discussed in section 4.7.

4.2 Data Selection

The numerical analysis was performed on annual maxima rainfall series for storm durations of 5, 10, 15, an 30 minutes (typical times of concentration for small urban catchments) and 1, 2, 6, and 12 hours (typical times of concentration for larger rural watersheds) for the province of Ontario, Canada. The data base contains 149 sites with rainfall data ranging from 1905 to 1998. The data was obtained from the Atmospheric Environmental Services (AES) Branch of Environment Canada.

In the single site analysis, stations were selected based on the following criteria: suitable record length and current data sets. A minimum record length of 20 years was desired as well as data sets ending in the 1990's. Out of the 149 stations, 58% of the stations contain record lengths less than 18 years and/or record lengths not updated to the year 1988. These stations were eliminated and 63 stations remained and used in the analysis (figure 4.4). Record lengths ranged from 18 to 73 years and data sets ranged from 1926 to 1998, respectively. The majority of stations are in southern Ontario, which has a high population density and where most urban development activities take place. The station's name, identification number, record length, time period, and geographic location are listed in table C1 of Appendix C.

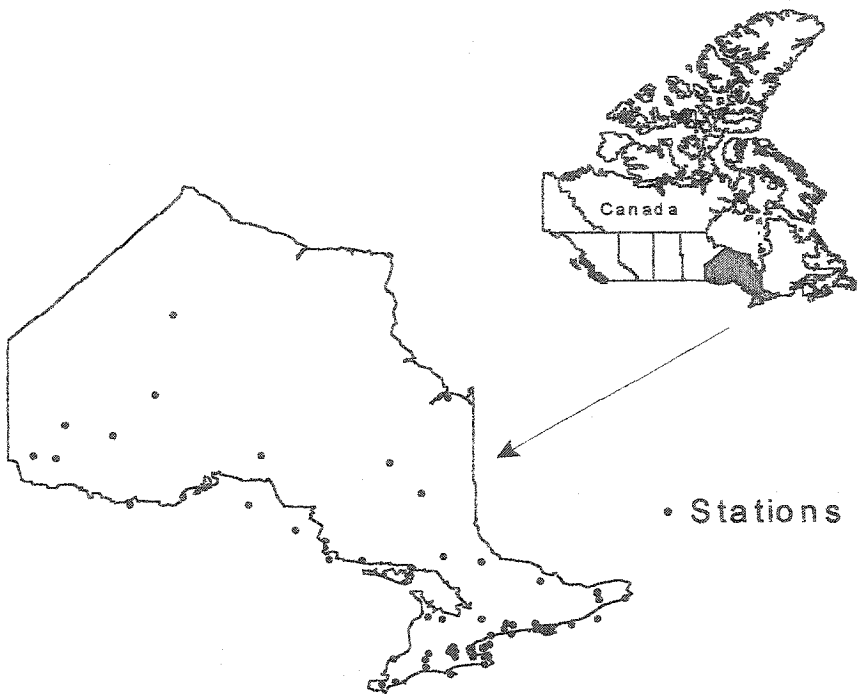

Figure 4.4: Station locations in the province of Ontario

Out of the 63 stations, a total of 15 have been chosen for the analysis on IDF estimates based on their year of record (current data), trend coefficient, and location to represent various regions across Ontario. The sites along with record length can be seen in table C2 in Appendix C. Five stations (Big Trout lake, Moosonee, Sudbury, Chalk River, Timmins) located in the geographically defined North region (North of 45°50') have records length ranging from 1952 to 1994. The Central region consists of 5 stations (Kingston, Orillia, Oshawa, Bowmanville, and Burketon) have records length ranging from 1961 to 1998, while the South region (South of 43° 50') have five stations (Delhi, Waterloo, Sarnia, Preston, and Port Colborne) with record lengths ranging from 1962 to 1998.

In the regional analysis, problems occur in selecting stations with the same time frame and a suitable record length. Table 4.1 displays the rainfall gauging network for the province of Ontario. Out of 149 stations, 52% have a record length less than 20 years and approximately 19% have a record length greater than 30 years. It was decided to use only stations with a minimum record length of 20 years or higher; however, out of the remaining stations, 18% have some missing data or are outdated (having no data recorded during the 1990s). As a result, these stations were eliminated from the analysis, which left only 44 stations. Furthermore, in a regional analysis, problems occur in selecting stations with the same time frame. Stations belonging to regions in the north (latitude greater than 46°) have record lengths beginning in 1971 and ending in 1990, while stations belonging to regions in the south have record lengths from 1976 to 1995 (figure 4.5), respectively.

Table 4.1: Data selection for study area

Storm Duration	Minimum Record Length < 20 year		Minimum Record Length = 20 year		Minimum Record Length = 25 year		Minimum Record Length = 30 year	
	Years of Record	Number of Sites	Years of Record	Number of Sites	Years of Record	Number of Sites	Years of Record	Number of Sites
5 minute	710	77	576	26	517	19	1029	27
10 minute	714	77	580	26	517	19	1033	27
15 minute	725	77	534	24	540	20	1070	28
30 minute	732	77	535	24	512	19	1103	29
1 hour	836	76	515	23	564	21	1111	29
2 hour	836	76	491	22	589	22	1110	29
6 hour	826	76	486	22	617	23	1077	28
12 hour	829	76	487	22	617	23	1078	28

A similar procedure was performed in selecting stations for the 25 year time frame. A total of 37 stations were used, however, the majority of stations are located in southern Ontario. Southern regions have record lengths beginning in 1971 to 1995, while regions in the North begin in 1966 and end in 1990. Table C3 displays the stations used in the 20 and 25 year regional analysis.

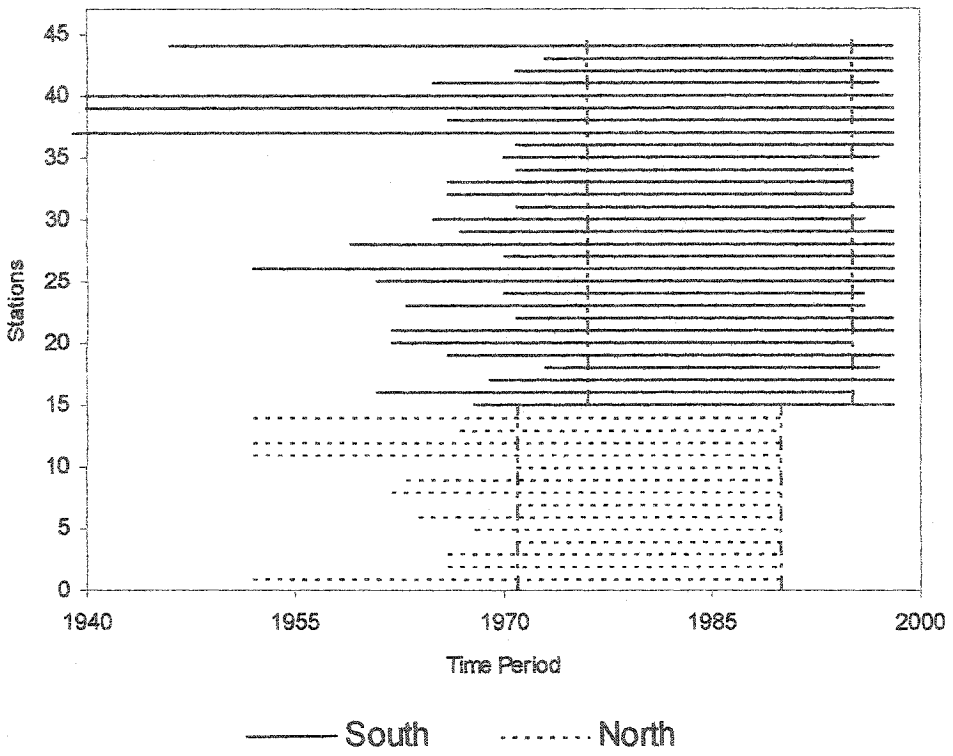

Figure 4.5: Time frame selection (vertical dashed lines) for 44 stations

4.3 Single Site Analysis

The impact of trends in data sets can ultimately affect the design of water resources projects. Increasing trend in annual extreme rainfall in the 1990's in comparison with data from previous decades may suggest that structures were designed for lower annual extremes. This section focuses on trends found in individual sites and its affects on IDF estimates.

4.3.1 Trend Determination

ACF coefficients for all durations and three stations are listed in table's A1 to A3 in Appendix A and significant results are shown in table 4.2. These tables were repeated for all 63 stations used in the single site analysis.

Table 4.2: Summary of significant autocorrelation

Station	Storm Duration	Record Length	Significance Level[a]	ACF lag 1[b]
Big Trout lake	10 minute	24	0.4001	0.4407
Bowmanville	15 minute	31	0.3520	0.3954
Bowmanville	30 minute	31	0.3520	0.4435
Brantford	10 minute	35	0.3313	0.3435
Brantford	15 minute	35	0.3313	0.3767
Burketon	1 hour	30	0.3578	0.4594
Burketon	2 hour	30	0.3578	0.4146
Kenora	6 hour	25	0.3920	-0.3984
North Bay	1 hour	27	0.3772	-0.3894
Owen Sound	12 hour	32	0.3465	0.4541
St Thomas	12 hour	73	0.2294	0.2662
Toronto Ellesmere	1 hour	29	0.3640	0.4095
Toronto Ellesmere	2 hour	29	0.3640	0.5186
Toronto Ellesmere	6 hour	29	0.3640	0.4215
Toronto Ellesmere	12 hour	29	0.3640	0.3760
Toronto Pearson Airport	15 minute	49	0.2800	0.3011
Toronto Pearson Airport	30 minute	49	0.2800	0.3005
Toronto Pearson Airport	1 hour	49	0.2800	0.2882
Toronto Pearson Airport	2 hour	49	0.2800	0.2883
Trenton	10 minute	33	0.3412	0.3439
Trenton	15 minute	33	0.3412	0.3610

[a] calculated using equation 3.26
[b] calculated using equation 3.25

The results show that 4.2% (21 out of a possible 504 tests) experience significant positive ACF, with 2 stations experiencing negative values. There is no apparent pattern with ACF values and geographic location of stations, however, two Toronto stations account for 38% of significant results. Nine significant ACF's were found for short duration storms in comparison with 12 found for long duration storms, indicating that no specific pattern is evident between ACF and storm duration.

It can be concluded (table 4.2) that some of the annual extreme rainfall series are time dependant; however, trends may be induced by climate change which in turn may cause serial correlation to occur. Due to the relatively low number of significant ACF's found, it may be possible that the apparent serial correlation may be a purely random effect. However, Shahin et al. (1993) indicate that purely random effects found in time series have an ACF equal to zero for all lags greater than 1 in the correlogram, which is not the results found in table 4.2. In addition 6 stations contribute to 76% of the significant ACF's, indicating a pattern that significant ACF has affected multiple durations of a station. Therefore, the autocorrelated data for stations listed in table 4.2 were pre-whitened.

An example of trends found for three stations can be seen in table's A4 to A6 in Appendix A. Trends for all durations and stations used in this analysis were determined, and a summary of stations with various durations experiencing significant trends at the 5% level are shown in table 4.3. Table A7 in Appendix A displays an additional 37 durations experiencing a trend significant at a 90% confidence interval. In total, 14% (69 durations) are experiencing a trend at a 90% level.

Out of the 69 durations, significant trends were found across the province of Ontario from Big Trout Lake to Windsor. Out of the 69 durations, 83% of the trends occur for multiple durations of a station indicating that trends occur for more than one duration for a site. It appears that shifts in the annual extreme time series is not specific to location in the province. In the north region, 16 significant trends were found out of a possible 160 tests (10%). Out of the 16 trends, 12 stations experienced significant positive trends suggesting an increase in extremes is occurring in the North, in comparison with 4 negative trends. In the south, 53 significant trends were recorded out of 344 trends (15.4%). Southern Ontario is generally experiencing negative trends, with 33 trends being negative, while 20 testing positive.

In terms of storm duration, short storms had 37 significant trends, while long duration storms had 32, respectively. The 15 minute storm had the most significant trends with 11, while the 10 minute and 6 hour storm had 10, respectively. It appears that all storm durations are susceptible to trends

Table 4.3: Sites with trends significance at a 5% level

Site	Station Number	Duration	Significance[a]
Big Trout Lake	6010738	5 minute	96.32
Big Trout Lake	6010738	15 minute	98.60
Kapuskasing	6073960	2 hour	99.22
North Bay	6085700	6 hour	96.82
Orillia	6115820	5 minute	99.52
Orillia	6115820	10 minute	96.66
Orillia	6115820	15 minute	97.16
Oshawa	6155878	30 minute	98.38
Oshawa	6155878	1 hour	95.38
Ottawa Airport	6106000	5 minute	97.04
Ottawa Airport	6106000	10 minute	98.50
Ottawa Airport	6106000	15 minute	99.00
Ottawa Airport	6106000	30 minute	98.44
Ottawa Airport	6106000	1 hour	98.92
Ottawa Airport	6106000	2 hour	96.78
Ottawa Airport	6106000	6 hour	97.58
Preston	6146714	10 minute	93.60
Preston	6146714	15 minute	97.02
Preston	6146714	30 minute	99.12
St Catherine	6137287	5 minute	99.62
St Catherine	6137287	30 minute	97.44
St Catherine	6137287	1 hour	99.64
St Catherine	6137287	2 hour	99.60
St Catherine	6137287	6 hour	97.70
Stratford	6148105	6 hour	95.92
Timmins	6076572	10 minute	96.28
Timmins	6076572	15 minute	97.78
Toronto Island Airport	6158665	10 minute	98.04
Toronto Island .Airport	6158665	15 minute	97.44
Toronto Pearson Airport	6158733	12 hour	96.30
Wiarton	6119500	6 hour	95.78
Wiarton	6119500	12 hour	97.34

[a] Calculated using equation's 3.16 and 3.19

Annual rainfall time series are usually a stationary process, meaning free from periodicity, shifts, and trends. However, external conditions may cause data to experience shifts, and trends. For instance, rapid industrialization may cause pollution levels to increase in neighbouring rivers, or a

depletion of forests (caused by fires) may cause an increase in surface runoff leading to an increase in water levels in a watershed (Salas, 1993). Similarly, global warming may be the possible cause of trends observed in the rainfall data sets, leading to changes in extremes as has been detected in this thesis (table 4.3).

4.3.2 Effect of Significant Autocorrelation

This section investigates the assumption of significant autocorrelation on the trend results. Trends at a 5% significance level are shown in table 4.4. Out of the 32 stations, 16 stations would remain significant at a 5% level if the data sets were pre-whitened. Table A7 in Appendix A reveals the results found for sites significant at a 90% confidence interval, and only 12 sites maintained a significant trend out of 37. In total, 12% of the stations and trends which were significant would be retained.

The results found in this study are similar with others research. In flood research, Douglas et al. (2000) pre-whitened significant ACFs found in low flows (due to high ACFs values) in the USA, however, maximum flood flows were left intact (no evidence of temporal correlation). Zhang et al. (1997, 2001) used an iteration scheme in a linear model to detect serial correlation because of its effect on the interpretation of the trend. This iteration scheme was applied to maximum flood flows and precipitation totals (summer, winter, etc) for Canada.

A temporal independent data sets is required in most statistical tests, as well as in the Mann-Kendal which is used test used in this thesis.

Table 4.4: Comparison of modified and Mann Kendall test on sites with significance at a 5% level

Site	Storm Duration	Modified Mann-Kendall Significance[a]	Mann-Kendall Significance[b]
Big Trout Lake	5 minute	86.16	96.32
Big Trout Lake	15 minute	92.75	98.60
Kapuskasing	2 hour	96.51	99.22
North Bay	6 hour	91.45	96.82
Orillia	5 minute	98.81	99.52
Orillia	10 minute	94.77	96.66
Orillia	15 minute	95.77	97.16
Oshawa	30 minute	95.83	98.38
Oshawa	1 hour	91.46	95.92
Ottawa Airport	5 minute	89.39	97.04
Ottawa Airport	10 minute	93.37	98.50
Ottawa Airport	15 minute	91.09	99.00
Ottawa Airport	30 minute	95.86	98.44
Ottawa Airport	1 hour	98.27	98.92
Ottawa Airport	2 hour	96.19	96.78
Ottawa Airport	6 hour	97.73	97.58
Preston	10 minute	97.90	97.20
Preston	15 minute	95.55	97.02
Preston	30 minute	98.60	99.12
St Catherine	5 minute	88.70	99.62
St Catherine	30 minute	78.93	97.44
St Catherine	1 hour	95.00	99.64
St Catherine	2 hour	99.14	99.60
St Catherine	6 hour	84.37	97.70
Stratford	6 hour	94.23	95.92
Timmins	10 minute	94.43	96.28
Timmins	15 minute	95.84	97.78
Toronto Island Airport	10 minute	96.07	98.04
Toronto Island Airport	15 minute	97.99	97.44
Toronto Island Airport	12 hour	92.31	96.30
Wiarton	6 hour	85.67	95.78
Wiarton	12 hour	81.14	97.34

[a] calculated using equation's 3.23, 3.16, and 3.19
[b] calculated using equation's 3.16 and 3.19

4.3.3. Comparison of Record Length

In order to examine whether the record length has an effect on trend analysis, several different time spans were investigated. Table 4.5 (a) and (b) displays the summary of trends found by using various record lengths for North and South Ontario, respectively. In the North, 14 and 9 stations were used to find trends with record lengths of 20 (1971 - 1990) and 25 years (1966 - 1990), respectively. In the South, three different time frames were used: 30 stations with a 20 year period beginning in 1976 to 1995; 28 stations with a 25 year period beginning in 1971 to 1995; and 17 stations with a 30 year period beginning in 1966 to 1995. The stations used for this analysis is listed in table C3 in Appendix C.

Table 4.5 shows the interpretation of trend would be quite similar if two different record lengths were used in the analysis. The overall percentage of trends found in the 20 and 25 year time frame for the North were comparable, with a 9.8% and 9.7% of stations experiencing significant trends at a 90% level. However, the 20 year time frame recorded more significant trends at a 95% level, with a percentage of 6.3% in comparison with a 2.8% in the 25 year time frame, respectively.

In southern Ontario, the majority of significant trends were found in the 25 year time frame, where 15.2% of sites experienced a significant trend at a 90% level. The results for the 20 year and 30 year time periods were comparable with 7.9% and 7.6% of stations experiencing trends, respectively. At a 95% significance level, the 25 year time frame also had the most significant trends at 6.3%, in comparison with 3.8% and 3.7% at a 20 and 30 year time frame, respectively.

Considering all significant trends at the 90% confidence interval (shown in table 4.5) detected in all record lengths for all stations, an equal amount of trends (nine) were found for short and long duration storms in the North, with 6 out of the 9 significant trends being significant at the 95% level for short duration storms. In the South, the majority of trends (58%) were also found in short duration storms in comparison with long duration storms (42%). Out of the 63 trends found, 68% of the significant trends at the 95% level occur during the short duration storms.

Table 4.5: Results of significant trends using different record lengths for

Storm	N = 20 years (1971 - 1990)[a]		N = 25 years (1966 - 1990)[b]	
Duration	90%	95%	90%	95%
5 minute	1	1	0	1
10 minute	1	1	0	0
15 minute	0	2	0	0
30 minute	0	1	1	0
1 hour	1	0	1	0
2 hour	1	0	2	1
6 hour	0	1	1	0
12 hour	0	1	0	0
Total	**4**	**7**	**5**	**2**

[a] 20 years: stations 14
[b] 25 years: stations 9

(a) North

Storm	N = 20 years (1976 - 1995)[c]		N = 25 years (1971-1995)[d]		N = 30 years (1966- 1995)[e]	
Duration	90%	95%	90%	95%	90%	95%
5 minute	1	3	4	3	0	1
10 minute	3	0	1	3	0	1
15 minute	1	1	1	3	0	1
30 minute	2	0	4	2	1	1
1 hour	0	1	6	0	2	0
2 hour	2	1	3	0	0	0
6 hour	1	2	0	2	1	1
12 hour	0	1	1	1	1	0
Total	**10**	**9**	**20**	**14**	**5**	**5**

[c] 20 years: stations 30
[d] 25 years: stations 28
[e] 30 years: stations 17

(b) South

As for sign of trend, the North experienced significant positive trends. At the 90% level, the 20 year period experienced 10 positive and 1 negative trend, with 7 of the positive trends being significant at the 95% level. The 25 year period was not as clear, with 3 positive and 4 negative trends being significant at the 10% level. The direction of trend for South Ontario was generally negative. Out of the 63 trends significant at the 90% interval, 46 were negative, 19 being significant at the 95% level. The majority of negative trends occurred at the 20 year time frame; the 25 and 30 year period

had a mixture of positive and negative trends throughout stations and no clear pattern was evident.

All record lengths used in this study were adequate in detecting trends, and a greater separation distance in record length should be investigated in the future. In terms of storm duration, all evidence concludes that short duration storms produce more significant results than long duration storms, possibly due to the difference in storm types (convective and frontal). Significant results found at the 5% level occurred more frequently in short duration storms, with 67% and 68% for the North and South regions, respectively. In terms of sign of trend, the North generally experienced positive trends, while the South experienced negative trends. The cause of this pattern was not investigated in this thesis.

4.4 Influence of Trend on Design Storms

4.4.1 Rates and Trends

The majority of slopes for all durations and stations are positive, indicating increases in annual extreme precipitation is being observed across the various regions in Ontario, as seen in table 4.6. The average rate (mm/hour) for the 5, 10, 15, 30 minute and 1, 2, 6, and 12 hour storms are as follows: 0.066, 0.092, 0.145, 0.195, 0.210, 0.206, 0.163, 0.169. It appears that higher rate increases are found in long duration storms.

It can be seen that the Moosonee station has the highest average slope increase with 0.39 mm/hour, while Oshawa, Burketon, and Sarnia had noticeable high rates of increase with 0.29, 0.23, and 0.20 mm/hour, respectively. The majority of stations with the highest average slope were found in the Central region, with 3 out of the 5 stations having the highest rates of increase from the 15 stations

Table 4.6: Rates and trends for: a) short duration storms

Stations	Storm Duration							
	5 minute		10 minute		15 minute		30 minute	
	Rate[a]	Z[b]	Rate	Z	Rate	Z	Rate	Z
Sarnia	0.068	0.831	0.000	0.257	0.054	0.455	0.175	0.751
Bowmanville	0.057	0.714	0.108	1.241	0.115	1.122	0.159	1.191
Burketon	-0.01	0.268	-0.008	0.000	0.081	0.339	0.203	1.392
Chalk River	0.053	0.964	0.116	1.306	0.144	1.335	0.117	0.949
Big Trout Lake	0.117	**2.087**	0.143	1.586	0.186	**2.456**	0.175	1.415
Kingston	0.024	0.541	0.037	1.020	0.026	0.768	0.044	0.541
Moosonee	0.107	1.347	0.107	1.269	0.203	*1.693*	0.349	*1.876*
Orillia	0.195	**2.818**	0.169	**2.127**	0.214	**2.192**	0.107	1.167
Oshawa	0.124	*1.933*	0.173	*1.840*	0.218	*1.914*	0.3	**2.402**
Port Colborne	0.020	0.149	-0.010	-0.43	0.027	0.059	0.017	0
Preston	0.108	*1.917*	0.267	**2.196**	0.364	**2.172**	0.514	**2.616**
Waterloo	0.101	1.345	0.188	*1.937*	0.278	*1.937*	0.360	1.503
Delhi	-0.03	-0.683	0.040	0.638	0.053	0.43	0.115	0
Sudbury	0.01	0	-0.057	-0.357	0.075	0.519	0.184	0.585
Timmins	0.047	1.635	0.108	**2.083**	0.139	**2.287**	0.109	*1.937*

b) long duration storms

Stations	Storm Duration							
	1 hour		2 hour		6 hour		12 hour	
	Rate	Trend	Rate	Trend	Rate	Trend	Rate	Trend
Sarnia	0.218	0.632	0.344	1.225	0.207	0.869	0.547	1.166
Bowmanville	0.223	1.531	0.224	*1.887*	0.294	1.411	0.254	0.969
Burketon	0.344	*1.749*	0.572	*1.660*	0.380	*1.767*	0.265	1.321
Chalk River	0.140	0.178	0.065	0.400	0.123	0.475	0.207	0.771
Big Trout	0.061	0.571	-0.044	0.298	-0.074	-0.348	0.262	1.463
Kingston	0.067	0.402	0.076	0.415	0.131	0.817	0.037	0.201
Moosonee	0.327	1.507	0.356	0.925	0.821	0.792	0.833	0.000
Orillia	0.075	0.646	0.138	0.667	0.037	0.188	0.007	-0.188
Oshawa	0.354	**2.046**	0.321	*1.876*	0.442	*1.933*	0.346	1.276
Port	0.078	0.148	0.056	0.030	0.005	0.756	0.074	1.423
Preston	0.460	1.356	0.265	0.654	-0.242	-0.818	-0.319	-0.397
Waterloo	0.351	1.205	0.164	0.375	-0.015	0.099	-0.211	-0.079
Delhi	0.102	0.311	0.089	0.222	0.096	0.237	0.287	0.133
Sudbury	0.275	1.200	0.391	*1.655*	0.192	0.974	-0.028	0.325
Timmins	0.080	1.537	0.076	0.544	0.050	0.206	-0.023	0.012

[a] Slope (B) from equation 3.14
[b] Calculated using equation 3.18
Bold: Significant at a 5% level
Italic: Significant at a 10% level

used for the analysis.

Trends detected by the Mann-Kendall test were used to indicate the direction of rates found by using linear regression (table 4.6). The trend statistics generally corresponded with the direction of slope (positive, negative or no trend), with 5% of the tests showing a difference between the trend statistic and rate. A total of 12 (10%) stations were found to be significant at the 5% level, respectively. An additional 16 tests are significant at the 10% level resulting in 23% of tests having a significance of 10% or lower.

In terms of short storm duration, an average trend coefficient of 1.06, 1.11, 1.31, 1.22 and 1.00 was found for the 5, 10, 15, 30, and 60 minute duration storm, respectively. Figure 4.6 illustrates the average rate of trend found for short and long duration storms and reveals that short duration storms show the most significant increasing trends. This is also shown by the fact that 9 out of the 16 significant tests at a 10% level, and 11 out of 12 significant trends at a 5% level are found in short duration storms.

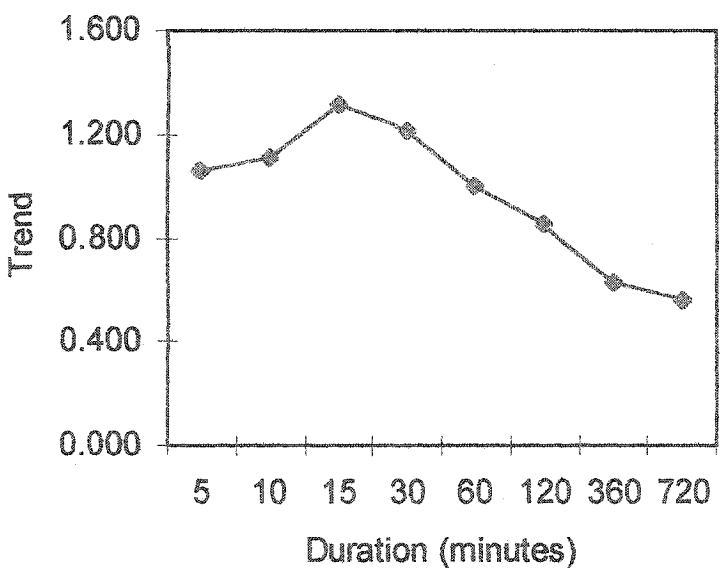

Figure 4.6: Average trend for short and long duration storms

Oshawa station had the highest average trend coefficient of 1.903, 2 and 5 tests being statistically significant at the 5 and 10% level, respectively. This average rating alone is statistically significant at a 10% level. Timmins had 2 and 1 significant trends at a 5 and 10% level, and the second highest trend coefficient of 1.28. Stations worth mentioning are Preston and Orillia having 3 trends significant at a 5 %level, Burketon having 3 significant at a 10% level, and Moosonee and Waterloo with 2 trends at a 10% level. In all, three out of the 5 stations in the Central region ranked in the top 5 out of 15 stations with the highest average trend coefficient.

4.4.2 The Effect of Trends on Design Storms

The percent difference in design storm estimates for trend and trend-free conditions for each station and return periods are given in table's A8 to A12. For a 2 year return period, design storm estimates for station time series with trend were on average 6 to 15.73% higher than the time series at a station with no trend, respectively. The highest percent increases were recorded for short storm durations, with the 15, and 30 minute storms recording 15.55 and 15.73 % increases, respectively. Only four stations (Sarnia, Sudbury, Delhi, and Kingston) did not record percent increases greater than 10 percent. Oshawa and Moosonee recorded percent differences in the magnitude of 23 and 22%, respectively.

As the return period increases to the 50 year event, the range of percent increase in design storm estimates with and without trend decreases, as shown in figure 4.7. The range of percent decrease for all durations for the 5, 10, 25, and 50 year return periods are: 4.79 to 12.70%; 4.2 to 11.5%; 3.7 to 10.4%; and 3.4 to 9.8%. The average percent increase in stations also decreases with return period. In the 2 year event, 10 stations had percent increases higher than 10 %; however the 5, 10, 25, and 50 year return periods had 6, 4, 3, and 3, respectively. Oshawa and Moosonee consistently had the highest differences in the two time series for all return periods.

The pattern of decreasing design storm estimates affected by trend with increasing return period is also related to the trend coefficient, as shown in figure 4.8. The highest average percent difference

in IDF estimates for all return periods occurs at the highest trend coefficient registered for the 15 and 30 minute storm durations, respectively

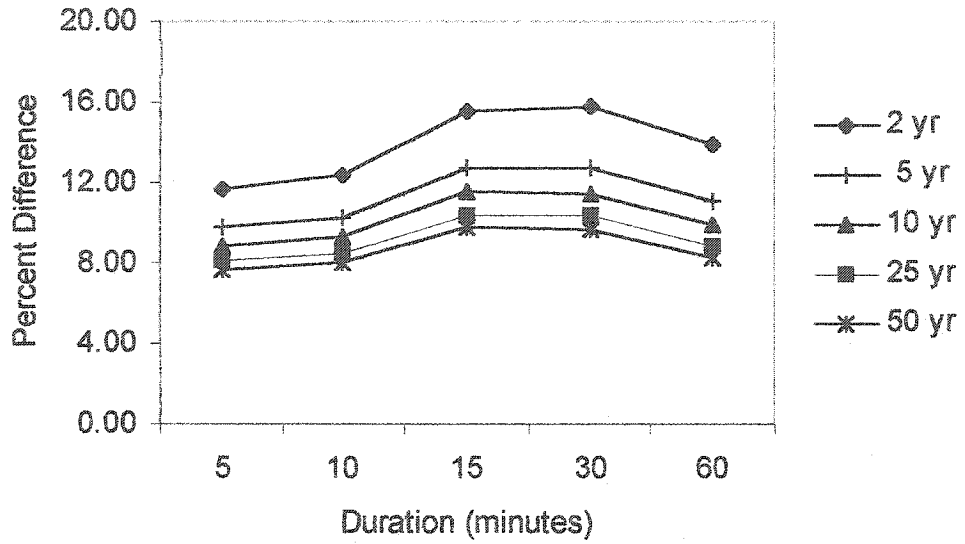

Figure 4.7: Percent difference in IDF estimates with and without trend

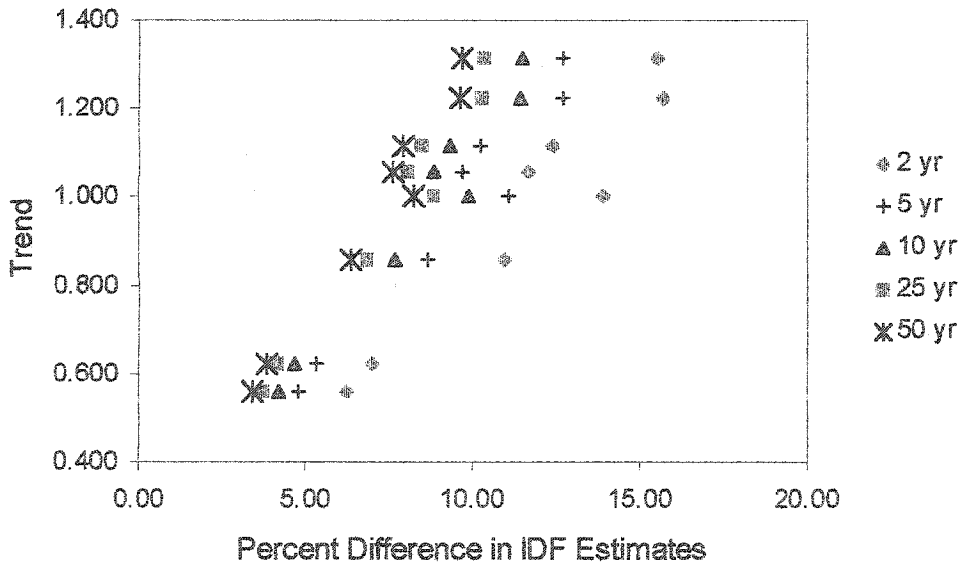

Figure 4.8 : Percent difference in IDF estimates with trend for various return period

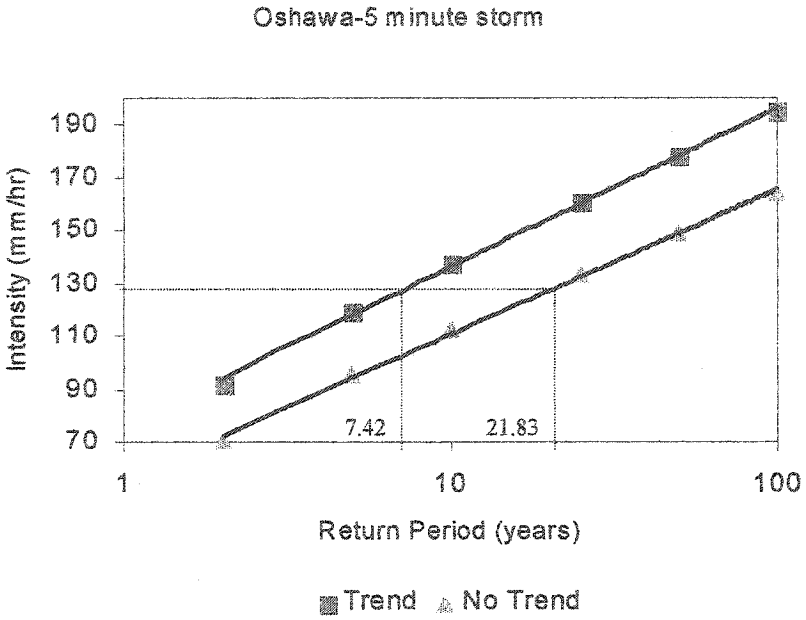

(a)

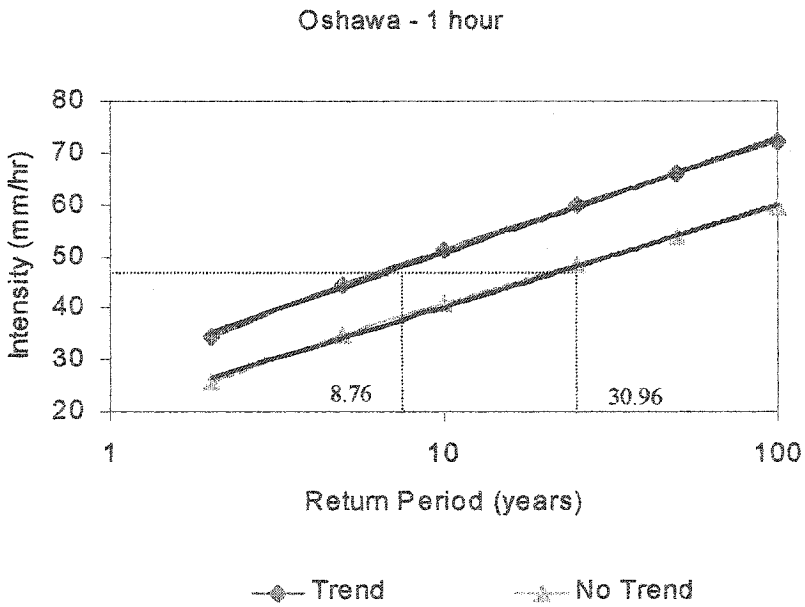

(b)

Figure 4.9: IDF curves with and without trend for Oshawa: a) a 5 minute storm duration and b) 1 hour duration

4.4.3 Return Period

The effect of trends on return period based on IDF estimates is illustrated for Oshawa for a 5 and 60 minute rainfall in figure 4.9. For a given intensity of 130 mm/hour, the 5 minute storm duration of Oshawa yields a return period of 7.42 (with trend) and 21.83 (without trend). For the 1 hour duration, the results show that the return period is 8.76 years (with trend) and 30.96 years (with no trend) for a constant intensity of 50 mm/hour. The difference in return period is quite significant indicating that presence of trends in rainfall observations increases the frequency of occurrences of extreme events. This is a very important finding, having a major implication in the engineering practice.

Figure 4.10 gives plots of rainfall intensity versus change in return periods due to trends and it illustrates that changes in the return period can be as high as 36 years for the 5 minute duration. The difference in return period decreases with increasing duration with the peak difference of 26 years found for the 1 hour storm.

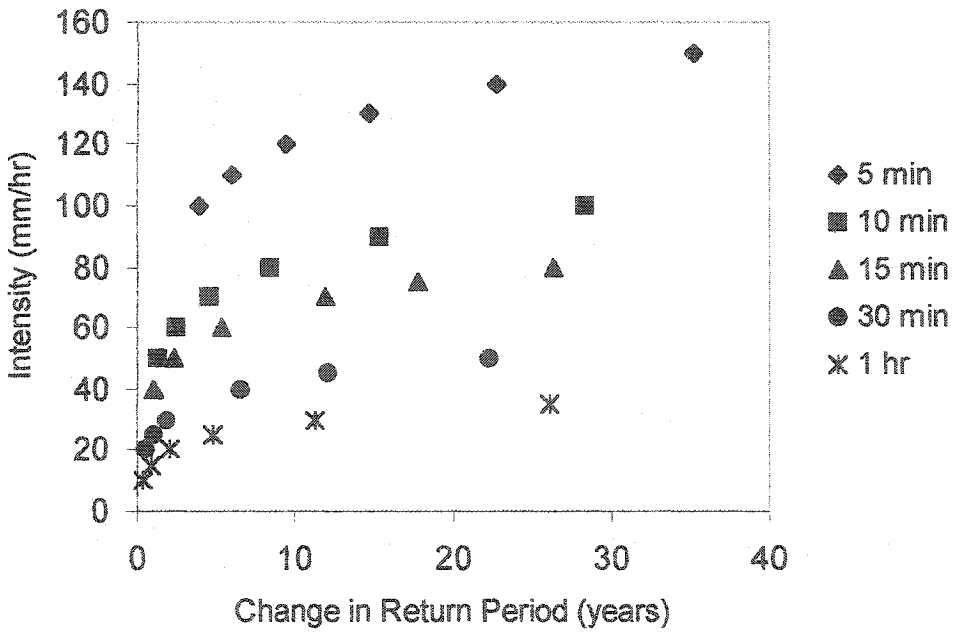

Figure 4.10: Intensity versus change in return period for short storm durations

4.5 Homogeneous Regions

An attempt is made to determine whether the trends in rainfall exhibit any regional pattern. Therefore, following single site analysis, a regional analysis was performed using homogeneous regions. Homogeneous regions can be defined as stations which have similar at-site characteristics, such as mean annual precipitation (MAP), hydrologic, physiographic, climatic variables, and trend direction. Schaefer (1990) analyzed annual precipitation data by grouping sites in Washington state with similar MAP. Aron et al. (1987) performed a study in Pennsylvania State, USA, in which IDF curves were developed using the Log Pearson 3 distribution for five geographically defined regions. There is no unique approach to the delineation of a homogeneous region. In this thesis, regions were formed first in terms of geographical location and MAP. In addition, if the majority of stations in a region had either predominantly positive or negative trends than this fact was also used in forming regions. In this thesis, regions were developed based on two time frames of 20 and 25 years of record.

As an example, table 4.7 displays six stations for a proposed homogeneous regions along with their geographic location, MAP totals and Kendall's S for a 20 year period and 10 minute storm duration. The stations are in close proximity to each other, generally located in the eastern region of Ontario near the St. Lawrence River. The mean MAP value for the six stations is 908.65 mm with a standard deviation of 32.05 mm, respectively. Kendall's S for each station indicates that all stations experience a negative trend component, suggesting that the region as a whole is receiving less extreme rainfall then in the past. Similar grouping procedure was performed for all station in Ontario for all durations and time frames and are displayed in figure 4.11.

Possible drawbacks for forming homogeneous regions in this study were the shortness of record lengths and sparse availability of stations. Homogeneous regions for one storm duration might not necessarily be homogeneous for another duration. It is possible that grouping of stations into homogeneous regions might correspond to different storm types such as convective (short duration), frontal (long duration), etc. Hosking (1997) indicates that if the region is not accepted as

homogeneous, then the proposed regions should be redefined. It is possible for a station to belong to different regions depending on the storm duration.

Table 4.7: Factors considered for delineation of regions

Station	ID	Location	MAP	Kendall's S
Trenton	6158875	St Lawrence	849.3	-34
Ottawa CDA	6106000	St Lawrence	909.9	-50
Ottawa Airport	6105976	St Lawrence	910.5	-60
Picton	6156533	St Lawrence	946.3	-19
Kemptville	6104025	St Lawrence	914.7	-35
Kingston	6104175	St Lawrence	921.2	-2

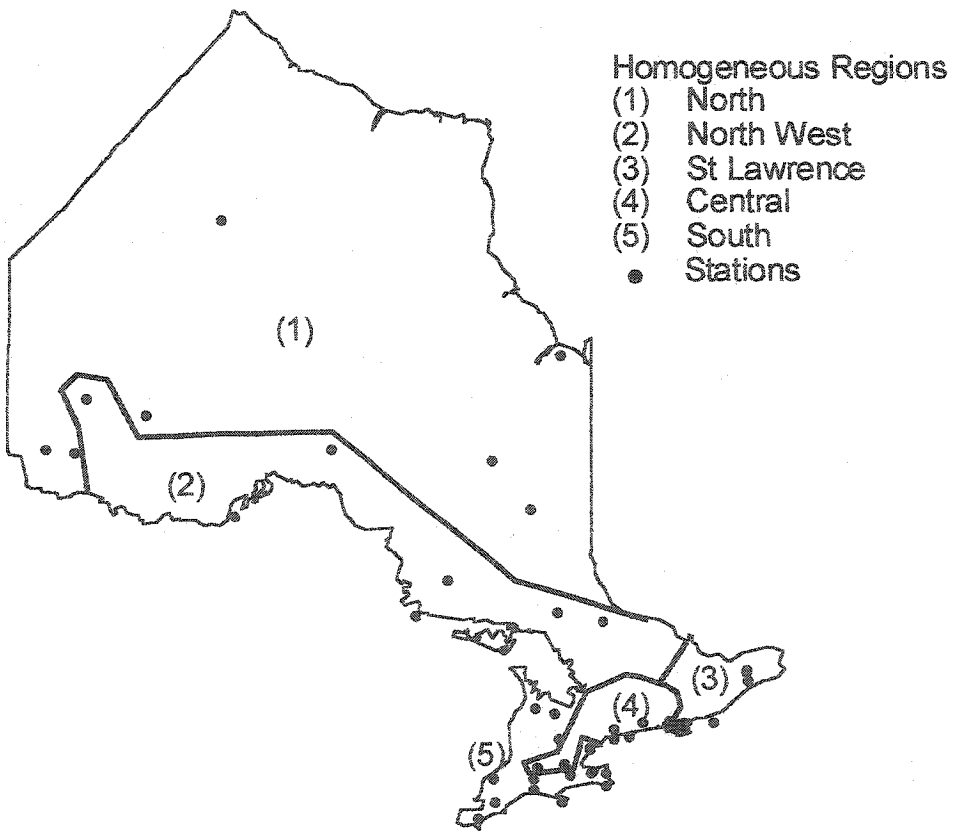

Figure 4.11: Station locations in the province of Ontario and homogeneous regions for a 5 minute storm duration (20 year period)

For the 20 year period, the 5, 10 minute and 1, 6 hour storm durations have five regions that are nearly identical to each other. These durations contain five regions: North (1), Northwest (2), St Lawrence (3), Central (4), and South (5), as shown in Figure 4.11 for the 5 minute duration rainfall. The 15 minute storm duration is similar to the durations mentioned above; however, there is only one North region. The 30 minute, 2, and 12 hour storms have similar regions where the North, Central, and South regions have been adjusted to satisfy homogeneous conditions. Figure B1 displays another example of a homogeneous region for the 20 year time frame in Appendix B. All storm durations were delineated as shown in Figure 4.12 and B1, respectively.

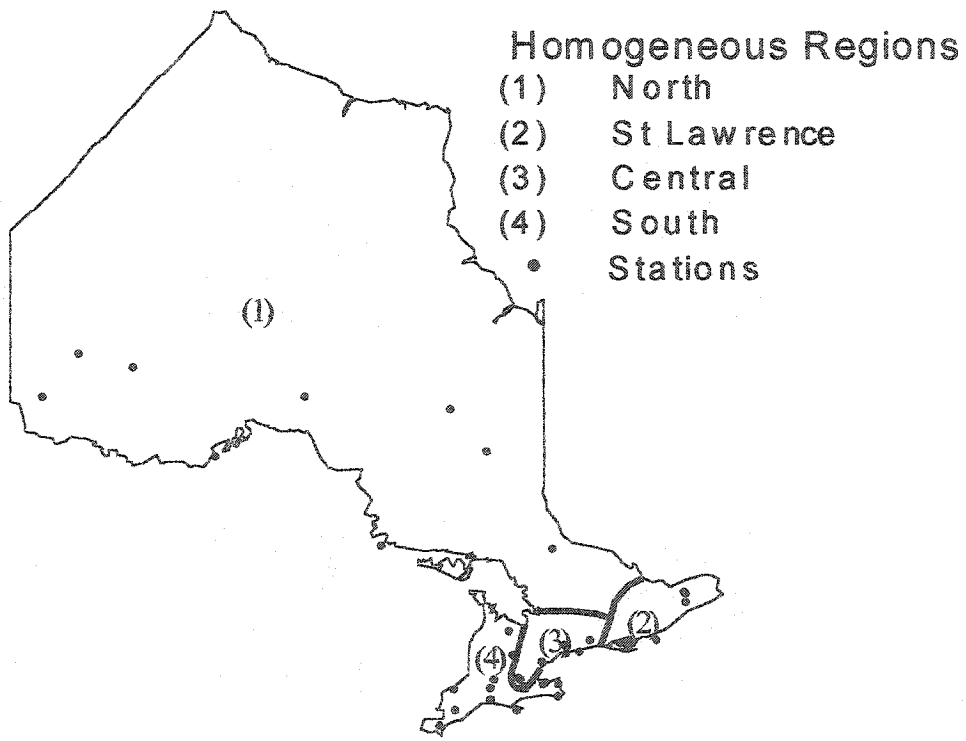

Figure 4.12: Homogeneous regions for a 5 minute storm for a 25 year time frame

For the 25 year period, the 5, 10 minute and 2, 6, and 12 hour storm durations have four regions that are nearly identical to each other. The four regions are: North (1), St. Lawrence (2), Central (3), and South (4), as shown in Figure 4.12 for the 5 minute duration rainfall. The 15 minute storm duration is similar to the durations mentioned above, however, the Central and South regions have been joined to form one region. The 30 minute storm duration has two regions in the North while the 1 hour storm have two regions in the South. These adjustments regions have been made to satisfy homogeneous conditions. Figure B2 in Appendix B displays another region for the 25 year time frame. All durations were delineated as shown in figure's 4.12 and B2, respectively.

Tables 4.8 and 4.9 show region size (number of stations) along with their corresponding heterogeneity and cross correlation values for a 20 and 25 year time period, respectively. Region sizes range from 4 to 17 stations, depending on location. There are more stations in southern Ontario, in comparison with the rest of the province. All homogeneous regions formed by site characteristics were accepted based on the at-site statistics for the 20 and 25 year time period. However, one region in the 25 year time frame has an H statistic of 1.08, meaning that it may be heterogenous. Some regions have heterogeneity values that are negative, implying the regions may be experiencing spatial correlation.

Table 4.8: Spatial analysis results for homogeneous regions with a 20 year time frame

Rainfall Durations	Homogeneous Regions	Number of Stations	Regional Average		Significant Lag-1[c]	Heterogeneity Measure H[d]
			r_m[a]	r_1[b]		
	North (1)	7	0.0166	0.0283	0	-0.02
	North West (2)	7	0.0662	-0.1449	0	0.03
5 minute	St Lawrence (3)	5	0.0821	0.0562	0	-0.18
	Central (4)	8	0.0958	-0.0157	0	0.15
	South(5)	17	0.0488	-0.0720	0	0.46
10 minute	North (1)	8	0.0199	0.0074	0	-0.21
	North West (2)	6	-0.0717	-0.1213	0	-0.13
	St Lawrence (3)	6	0.023	0.0844	0	-0.72
	Central (4)	8	0.0853	-0.0104	0	-0.99
	South (5)	16	0.0542	-0.0173	0	0.34
15 minute	North (1)	14	-0.0007	-0.0625	0	0.73
	St Lawrence (2)	6	0.0048	0.0843	1	-0.77
	Central (3)	8	0.0154	-0.0498	1	-0.92
	South (4)	16	0.0567	0.0472	0	-0.16
30 minute	North (1)	6	0.0149	0.0004	0	0.38
	North West (2)	8	0.0019	0.0043	0	0.45
	St Lawrence (3)	6	-0.0069	0.0366	0	-0.5
	Central (4)	14	-0.0173	-0.0027	1	0.2
	South (5)	10	0.0807	0.0205	0	0.84
1 hour	North (1)	7	-0.0152	0.0183	0	-0.74
	North West (2)	7	0.0234	0.0100	1	-0.06
	St Lawrence (3)	6	0.0493	-0.0570	0	-1.04
	Central (4)	7	0.0412	0.0203	0	0.93
	South (5)	17	0.0414	-0.0142	0	0.42
2 hour	North (1)	9	0.0130	-0.0484	1	-0.12
	North West (2)	5	0.0234	0.0606	0	0.76
	St Lawrence (3)	8	0.1057	-0.0831	0	-1.76
	Central (4)	11	-0.0094	0.0830	0	-0.52
	South (5)	11	0.0645	-0.0759	0	0.44
6 hour	North (1)	9	0.0207	0.0222	0	0.01
	North West (2)	5	0.0402	0.0265	0	0.55
	St Lawrence (3)	8	0.2115	-0.0540	0	-1.12
	Central (4)	8	0.1621	-0.0486	0	-0.12
	South (5)	14	0.0569	0.0264	0	0.17
12 hour	North (1)	9	0.0845	0.0434	2	0.99
	North Central (2)	5	0.0013	0.0618	0	0.75
	St Lawrence (3)	9	0.2750	-0.0583	0	-1.07
	Central (4)	9	0.0805	-0.1055	0	-0.54
	South (5)	12	0.1307	0.0941	1	-0.91

[a] Calculated by using equation 3.34

[b] The average autocorrelation coefficient (equation 3.25) for a region

[c] The number of significant autocorrelation detected in a region

[d] Calculated by using equation 3.13

Table 4.9: Spatial analysis results for homogeneous regions with a 25 year time frame

Rainfall Durations	Homogeneous Regions	Number of Stations	Regional Average r_m[a]	Regional Average r_1[b]	Significant Lag-1[c]	Heterogeneity Measure H[d]
	North (1)	9	-0.0308	-0.0134	0	0.59
	St Lawrence (2)	6	0.0388	0.0813	0	0.71
5 minute	Central (3)	9	0.066	-0.0622	0	0.89
	South (4)	13	0.021	0.0286	1	0.07
10 minute	North (1)	9	-0.0460	-0.0092	1	-0.33
	St Lawrence (2)	6	0.0412	0.1032	0	0.43
	Central (3)	9	0.1101	0.013	0	0.16
	South (4)	13	0.0228	0.0613	0	0.84
15 minute	North (1)	9	-0.0250	-0.0526	1	0.98
	Central (2)	12	0.0322	0.0621	2	0.38
	South (3)	16	0.0392	0.0811	0	0.84
30 minute	North (1)	5	-0.0525	-0.0849	0	0.28
	North West (2)	4	0.0027	0.0155	0	0.61
	St Lawrence (3)	6	0.0322	0.0331	0	0.15
	Central (4)	11	0.0197	0.09	1	0.93
	South (5)	11	0.042	0.0425	0	-1.05
1 hour	North (1)	9	-0.0047	-0.0732	1	-0.11
	St Lawrence (2)	10	0.0641	0.0184	0	-0.51
	Central (3)	8	0.0702	0.0031	0	0.41
	South Central (4)	5	0.0463	0.0951	0	1.08
	South (5)	5	0.0631	0.0525	0	-0.27
2 hour	North (1)	9	-0.0073	-0.0095	0	0.93
	St Lawrence (2)	7	0.1078	-0.0849	0	-1.01
	Central (3)	9	0.0630	0.0539	0	0.47
	South (4)	12	0.0717	0.0569	0	0.46
6 hour	North (1)	9	-0.0211	0.0497	1	-0.42
	St Lawrence (2)	7	0.2089	-0.0247	0	-1.23
	Central (3)	7	0.1589	-0.0114	0	-1.07
	South (4)	14	0.0551	0.0531	0	0.07
12 hour	North (1)	9	-0.0129	0.0627	1	0.34
	St Lawrence (2)	7	0.2633	-0.0744	0	-1.02
	Central (3)	7	0.2383	-0.0542	0	-1.13
	South (4)	14	0.1014	0.1208	1	-0.49

[a] Calculated by using equation 3.34
[b] The average autocorrelation coefficient (equation 3.25) for a region
[c] The number of significant autocorrelation detected in a region
[d] Calculated by using equation 3.13

4.6 Regional Analysis

4.6.1 Serial Correlation

Serial correlation indicates that the data is time dependent (not iid); however, the Mann-Kendall test requires the data to be iid. Therefore, when serial correlation was found to be significant, then the stations containing significant autocorrelation were pre-whitened (correlation was removed). Table 4.8 reveals that 8 out of a possible 352 data sets had a significant serial correlation value. As for the 25 year time frame, 10 out of a possible 296 datasets had a significant serial correlation value. Therefore, these stations were pre-whitened, while the remaining data for the other stations were left intact.

4.6.2 Spatial Correlation

Spatial correlation is expected to occur if stations are relatively close together, thus experiencing similar hydrological and climatic conditions. Table's 4.8 and 4.9 show observed spatial correlation for each region for the 20 and 25 year time frame, respectively. A few regions experience negative correlation values that are near zero, implying spatial independence. Regions with significant spatial correlation were detected by the method of L-moments indicated by negative H values. From the two tables and figure 4.13, it can be observed that the correlation coefficients ranging from 0 to 0.09, with corresponding heterogeneity values generally lie between 0 and 1, while cross correlation coefficients exceeding an approximate value of 0.09 produced generally negative values. Therefore, the spatial correlation was present.

From table 4.8, the following regions may be significantly correlated for the 20 year time frame: St Lawrence for the 5 minute, 1 hour, 2 hour, 6 hour, and 12 hour storm duration; Central for the 5 minute, 10 minute, 6 hour, and 12 hour storm duration; and the South 30 minute, and 12 hour storm durations. As for the 25 year period shown in table 4.9, the following regions may be experiencing spatial correlation: South regions with 30 minute, 1, and 12 hour; St Lawrence with 1, 2, 6, and 12

hour storm durations; and Central regions with 6, and 12 hour storm durations.

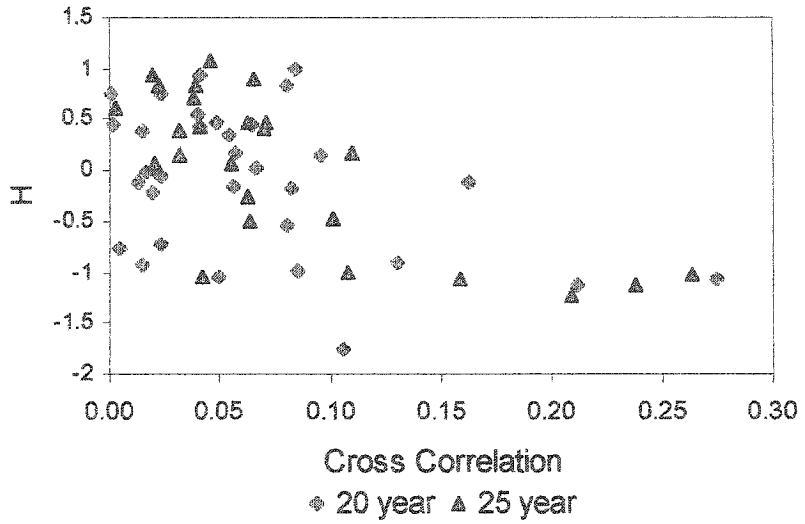

Figure 4.13: Relationship between heterogeneity measure (H) and cross correlation coefficients for all time frames

The possibility of spatial correlation occurring for various durations in the St Lawrence and Central regions is not surprising considering these regions are the smallest in terms of geographical distance. The South regions contain the largest amount of neighboring stations which may be responsible for spatial correlation to occur. The North regions are the largest in terms of geographical distance between stations having very few stations; therefore, it is reasonable to assume that stations existing in this region do behave independently of each other. Long durations storms have the majority of regions which may be spatial correlation.

Spatial correlation was further examined with the use of variograms. Figure 4.14 (a) illustrates a variogram for the St Lawrence region for a 2 hour region and 20 year time frame indicating a relationship between the separation distance of the stations and the variance. The heterogeneity measure and cross correlation for this region is -1.76 and 0.1057, respectively. All three techniques indicate that the region is spatial correlated. Figure 4.14 (b) shows the South 5 minute region where range is non-existent, and the correlation among stations behave independently of each other. The

heterogeneity and cross correlation values for this region are 0.46 and 0.0488, suggesting that all three techniques conclude that the region is not significantly correlated. Each assumption of a spatial correlated region was examined by the same procedure performed for all regions and durations for both time frames. Two additional variograms (figure's B3 to B6) for each time frame can be seen in Appendix B. However, variograms were computed for all regions and time frames in this thesis.

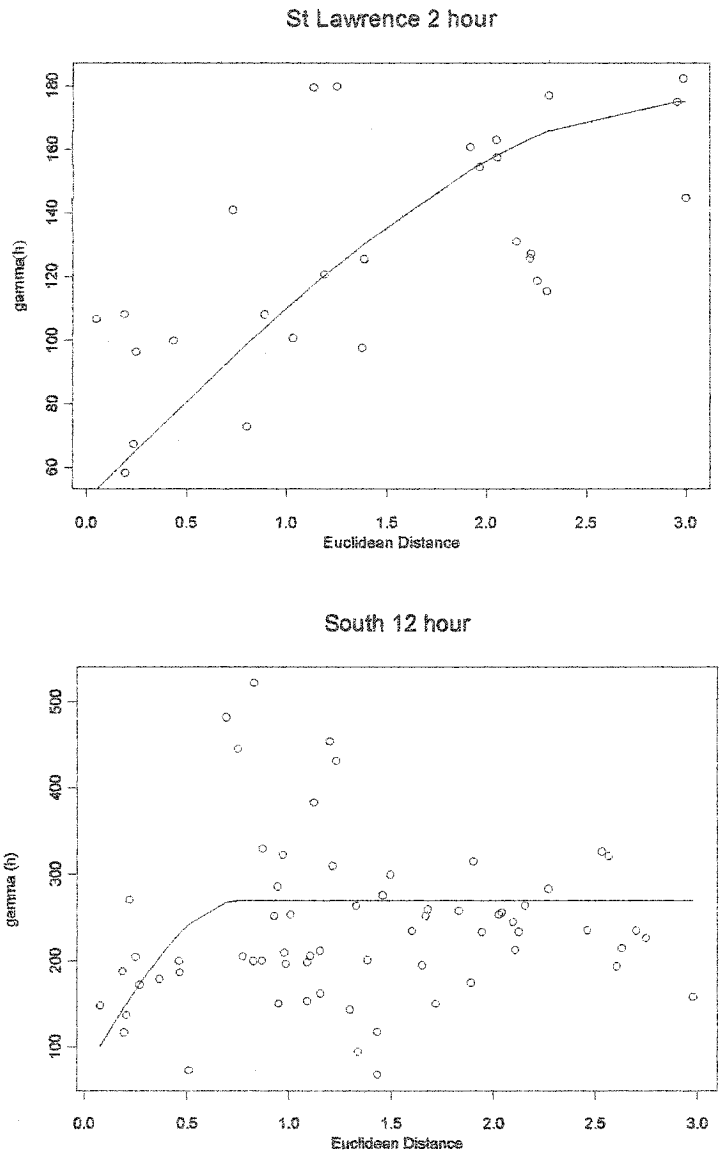

Figure 4.14: Spatial variations for regions: (a) St Lawrence 2 hour and (b) South 5 minute. Solid lines indicate fitted variogram models.

4.6.3 Regional S Statistic

Table 4.10 shows the results of the trend tests for homogeneous regions that are serial and spatially independent for a 20 year time frame. The trend results include the reduction of the variance caused by the occurrence of tied data. Significant trends are apparent in short storm durations, with 6 out of the 8 regions showing significance in the 5 and 10 minute storms, respectively. Only 3 significant trends were observed in the remaining storm durations. Four significant trends were positive while 5 were negative. This shows that different patterns of trends are observed for different regions and storm durations in Ontario.

The North (1) region experienced positive trends for all durations, and significant trends were found in four of the durations. The St Lawrence regions experienced negative trends for all durations and significant trends were found for the 5 , 10, and 15 minute storm durations. The South region for the 5, and 10 minute storm experienced significant negative trends, and all trends in the South regions, with the exception of the 2 hour duration, were negative. The five regions labeled Central for the 15, 30 minute and 1, 2, and 12 hour storms had positive trends, but none statistically significant at the 5% level.

Seven regions were assumed to be spatially dependent based on the cross correlation coefficient, heterogeneity measure, and empirical variograms. The bootstrap method was employed to create an empirical CDF to determine the significance of trends. Table 4.11 reveals that no regions experienced a statistically significant trend. The highest observed spatial correlation was found in the St Lawrence region for a storm duration of 2, 6, and 12 hour, and in the Central Region for the 5, 10 minute and 6 hour durations. The Central and St Lawrence regions maintained their positive and negative trend as found for spatial independent regions in Table 4.10. Bootstrap CDF's (figure's B8, B9) for two additional durations for a 20 year time frame are displayed in Appendix B. However, bootstrap CDF's were computed for all spatially significant regions, and the results incorporated in the analysis.

Table 4.10: Trends found for regions that were serial and spatially independent for a 20 year time frame

Rainfall Duration	Homogeneous Region	Number of Stations	S avg[a]	Z_m[b]	Significance[c]	Rate[d]
5 min	North (1)	7	29.14	2.52	98.81[x]	0.0831
	North West(2)	7	-18	-1.57	88.27	-0.0681
	St Lawrence (3)	5	-40	-2.92	99.64[x]	-0.1825
	South (5)	17	-25.59	-3.51	99.95[x]	-0.093
10 min	North (1)	8	21.88	2.02	95.66[x]	0.0706
	North West (2)	6	-20.67	-1.64	89.99	-0.0975
	St Lawrence (3)	6	-33.33	-2.66	99.21[x]	-0.2194
	South (5)	16	-19.56	-2.58	99.02[x]	-0.1274
15 min	North (1)	14	8.07	0.99	67.81	0.0213
	St Lawrence (2)	6	-25.33	-2.02	95.69[x]	-0.2530
	Central (3)	8	13.13	1.21	77.32	0.1169
	South (4)	16	-14.69	-1.93	94.63	-0.1189
30 min	North (1)	6	10.83	0.86	61.23	0.1060
	North West (2)	8	3.5	0.32	25.34	-0.0202
	St Lawrence (3)	6	-24	-1.91	94.40	-0.2929
	Central (4)	14	11.57	1.42	84.35	0.1095
	South (5)	10	-15.5	-1.60	88.99	-0.1374
1 hour	North (1)	7	7.71	0.67	49.42	0.1025
	North West (2)	7	6.14	0.53	40.26	-0.1018
	St Lawrence (3)	6	-20.33	-1.63	89.62	-0.3001
	Central (4)	7	16.71	1.44	84.96	0.2211
	South (5)	17	-9.71	-1.30	80.78	-0.0798
2 hour	North (1)	9	21.22	2.08	96.23[x]	0.2732
	North West (2)	5	-22.2	-1.61	89.29	-0.3674
	Central (4)	11	1.45	0.16	12.46	0.0215
	South (5)	11	3.82	0.41	31.94	0.0025
6 hour	North (1)	9	23.22	2.28	97.71[x]	0.4400
	North West (2)	5	-24	-1.74	91.85	-0.4395
	South (5)	14	-9.71	-1.18	76.25	-0.1443
12 hour	North (1)	9	4.56	0.45	34.38	0.0699
	North Central	5	15	1.09	72.43	0.3654
	Central (4)	9	5.78	0.56	42.73	0.1929

[a] Calculated using equation 3.20
[b] Calculated using equation 3.22
[c] Calculated using equation 3.19
[d] Slope (B) from equation 3.14
[x] Significant at 5 % level

Table 4.11: Trends for regions that were serial independent and assumed spatially correlated for a 20 year time frame

Rainfall Durations	Homogeneous Regions	Number of Stations	S avg[a]	Bootstrap Probability[b]	Significance[c]	Rate[d]
5 min	Central (4)	8	22	0.9505	0.901	0.0869
10 min	Central (4)	8	10.89	0.7894	0.5788	0.0583
2 hour	St Lawrence (3)	8	-15.375	0.1282	0.7436	-0.2512
6 hour	St Lawrence (3)	8	-24.875	0.0311	0.9378	-0.4798
	Central (4)	8	22.63	0.9525	0.905	0.3254
12 hour	St Lawrence (3)	9	-18.77	0.0837	0.8326	-0.4042
	South (5)	12	-17.16	0.1023	0.7954	-0.3261

[a] Calculated using equation 3.20
[b] Computed by empirical CDF procedure for each region (section 3.5), as shown in figure 3.6
[c] Calculated from figure 3.6
[d] Slope (B) from equation 3.14

Table 4.12 shows the results of the trend tests for the regions that are serial and spatially independent for a 25 year time frame. As in the 20 year time frame, significant trends are found in short storm durations, with 4 out of the 5 regions showing significance in the 5 and 10 minute storms, respectively. Significant trend was observed in the 2 hour storm duration. Three significant trends were negative while 2 were positive.

The North regions experienced a mixture of positive (3 durations) and negative (5 regions) trends, however, none significant at the 5% level. The St Lawrence regions experienced negative trends for all 4 durations and significant trends were found for the 5 , and 10 minute storm durations. The Central regions experienced all positive trends in short and long duration storms with significant trends found in the 5 minute, and 2 hour storm durations, respectively. The South regions experienced negative trends for short duration storms (5, 10, 15, 30) while long duration storms (1, 2, and 6 hour) had positive trends, with the 10 minute storm having a significant trend.

As shown in table 4.13, seven regions were spatially dependent based on the spatial analysis. Two regions, Central for 5 minute, and 6 hour were found to have significant positive trends. The St Lawrence regions experienced negative trends for all durations, while the Central and South regions were all positive. Bootstrap CDF's (figure's B9 to B10) for two additional durations for the 25 year time frame are listed in Appendix A. Bootstrap CDF's were computed for all spatially significant regions in the 25 year time frame and results included in the analysis.

Table 4.12: Regions found to serially and spatially independent for the 25 year time frame

Rainfall Duration	Homogeneous Region	Number of Stations	S avg[a]	Z Statistic[b]	Significance[c]
	North (1)	9	1.56	0.11	0.0879
5 minute	St Lawrence (2)	6	-45	-2.59	0.9905[X]
	Central (3)	9	43.44	3.06	0.9978[X]
	South (4)	13	-22.46	-1.93	0.9465
	North (1)	9	-19.89	-1.40	0.8379
10 minute	St Lawrence (2)	6	-34.17	-1.96	0.95[X]
	South (4)	13	-23.92	-2.03	0.958[X]
	North (1)	9	-9.78	-0.69	0.5101
15 minute	Central (2)	12	11	0.90	0.63
	South (3)	16	-14.69	-1.38	0.8339
	North (1)	5	-8.4	-0.44	0.3404
	North West (2)	4	-5.5	-0.26	0.2029
30 minute	St Lawrence (3)	6	-17.17	-0.99	0.6754
	Central (4)	11	22.91	1.79	0.9258
	South (5)	11	-6.82	-0.53	0.4045
	North (1)	9	-9.67	-0.68	0.5032
1 hour	St Lawrence (2)	8	-19.5	-1.29	0.8034
	Central (3)	10	10.5	0.78	0.5653
	South Central(4)	5	20.4	1.07	0.7135
	South (5)	5	24.4	1.27	0.7977
	North (1)	9	3.67	0.26	0.2034
2 hour	Central (3)	9	35.33	2.48	0.9869[X]
	South (4)	12	10.33	0.84	0.5988
	North (1)	9	-3.89	-0.27	0.2153
6 hour	South (4)	14	8.64	0.76	0.5509
12 hour	North (1)	9	8.44	0.59	0.4466

[a] Calculated using equation 3.20
[b] Calculated using equation 3.22
[c] Calculated using equation 3.19
[X] Significant at 5 % level

Table 4.13: Regions found to be spatially correlated for the 25 year time frame

Rainfall Duration	Homogeneous Region	Number of Stations	S avg[a]	Z Statistic[b]	Significance[c]
10 min	Central (3)	9	38.44	0.989	0.978[X]
2 hour	St Lawrence (2)	7	-12	0.2383	0.5234
6 hour	St Lawrence (2)	7	-19	0.1316	0.7368
	Central (3)	7	43.43	0.9927	0.9854[X]
12 hour	St Lawrence (2)	7	-13.86	0.2077	0.5846
	Central (3)	7	22.57	0.9042	0.8084
	South (4)	14	8.71	0.6916	0.3832

[a] Calculated using equation 3.20
[b] Computed by empirical CDF procedure for each region (section 3.5), as shown in figure 3.6
[c] Calculated from figure 3.6
[X] Significant at 5 % level

4.7 Comparison of Tests

In past studies (Zhai et al., 1999; Plummer et al., 1999), authors ignored the role of serial and spatial correlation in trend analysis. However, they still used trend tests violating the assumption that the data to be iid. The effects of serial and spatial correlation on the interpretation of the trend is explored in this section. Figure's B11 to B13 in appendix B show additonal durations for stations in both time frames. However, comparison's for all durations and stations were performed.

Figure 4.15 compares the field significance of raw and pre-whitened data for regions with a storm duration of 15 minutes for a 20 year time frame. Positive serial correlation removes a portion of the trend. From the nine regions that are found to be significant, the assumption of serial dependency would reduce the total significance to four regions. As for the 25 year time frame, out of the 7 significant trends, only 4 regions would be significant at a 5% level.

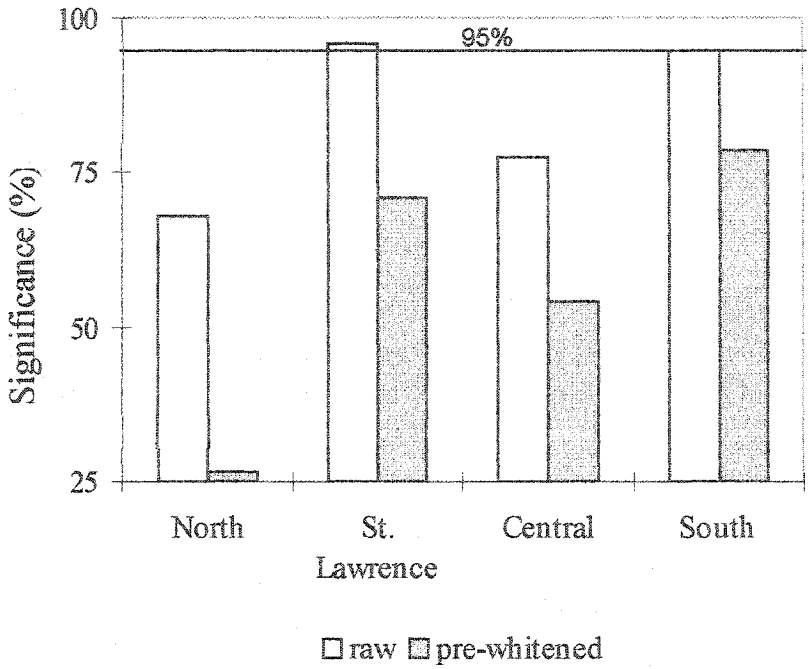

Figure 4.15: Comparison of raw and pre-whitened data for the 15 minute storm duration for a 20 year period for regions that are serial and spatially independent. Line at 5% level.

Figure 4.16 compares field significance of regions that are spatially correlated (as given in table 4.11) with the assumption of spatial independence for a 20 year time frame. The bootstrapping technique was used for spatial correlation, while the Mann-Kendall procedure was used for spatial independence. Three region would have experienced significant trends if spatial correlation was ignored. As for the 25 year time frame, all 7 regions would have experienced a decrease in trend interpretation. However, the two original significant trends found (table 4.13) remain significant in both procedures. This is due to the high regional positive trends found in the Central regions, respectively. Thus, it is important to accurately determine if a region is spatially correlated or independent. The differences between the two cases is generally 10 % for the annual maximum precipitation.

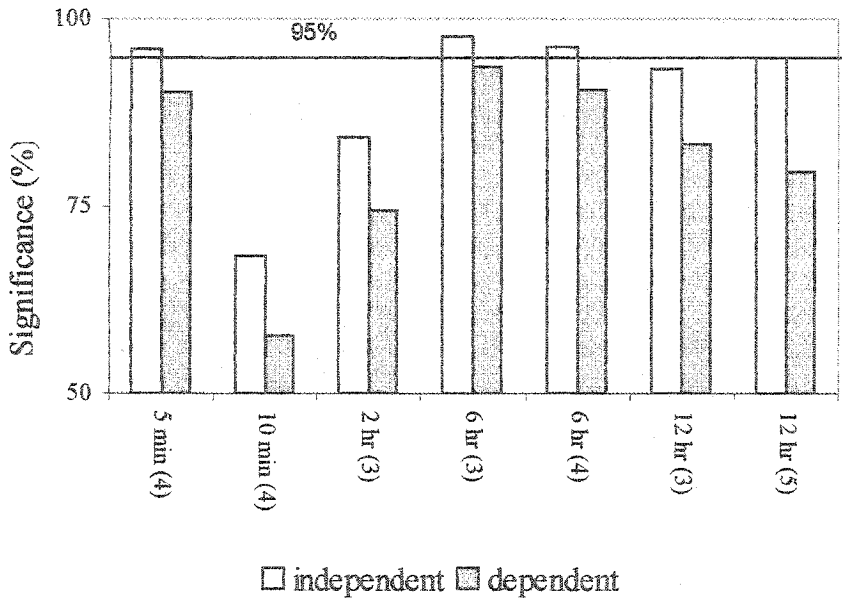

Figure 4.16: Comparison of spatially correlated (dependent) regions with the assumption of spatial independence. Correlated regions for each duration is listed in table 4.11 for the 20 year period.

Chapter 5

CONCLUSIONS

5.1 Conclusions

The following are conclusions made from the results of this study:

1.1 Trends have been detected in various stations across the province of Ontario for all storm durations. Trends were predominantly found for short duration storms, with significant increases generally occurring in northern Ontario, whereas significantly decreases generally found in southern Ontario.

1.2 Significant autocorrellation was detected in a small number of stations in single site (4.2%) and regional analysis (2.3%) of annual extreme rainfall time series.

1.3 Significant increases in design storm frequency have been detected in IDF estimates with stations experiencing increasing trends, in comparison with the same station with the trend removed. The rainfall series with trend causes the return period to be shorter than if trends were not accounted for.

1.4 Homogeneous regions were delineated for 8 storm durations and two time frames. Homogeneous regions for one storm duration might not necessarily be homogeneous for another duration. It is possible that grouping of stations into homogeneous regions might correspond to different storm types such as convective (short duration), frontal (long duration). The introduction of trend detection in homogeneous region delineation is original and was found to be a very significant contribution of this research.

1.5 Spatial correlation was detected by calculating cross correlation between stations, L-moments, and variograms. Spatial correlation was strongest with stations within close proximity of each other. Approximately 19% of the regions tested were spatially correlated.

1.6 Significant trends were observed in regional data sets, notably in short durations storms. The North regions generally experienced positive and negative trends for different time frames. The St Lawrence regions experienced negative trends for all durations and significant trends were found. The Central regions had positive trends, and the South region generally experienced negative trends. In total, 22% of regions tested were significant at the 5% level.

1.7 It was demonstrated, that presence of positive serial correlation removes a portion of the trend. Serial dependency would reduce the total number of significant regions used in this thesis.

1.8 The assumption of spatial dependency in regional data sets also reduces the significance of trend

1.9 This study demonstrates that different areas of the Province of Ontario show different trends and tendencies in extreme precipitation. There seems to be no simple trend description possible for all rainfall stations and durations.

5.2 Recommendations

1.1 Since significant trends have been detected in this research in design storms, it is therefore recommended that further study is warranted in order to evaluate more fully the practical significance of trends in design storms as applied in engineering projects.

1.2 It might be useful to conduct a similar study using Geographical Information System (GIS) which would facilitate more rigorous regional analysis

1.3 Since some stations have incomplete records, it would be very important for climate research studies to maintain them, especially in Northern Ontario.

Chapter 6

BIBLIOGRAPHY

1) Adamowski K, Bougadis J. Detection of trends in annual extreme rainfall. *28th Annual Meeting of the Canadian Geophysical Union*, Banff, Alberta, May 18-21, 2002.

2) Adamowski K, Bougadis J. Regional estimation of temporal trends in rainfall. *5th International Conference on Hydro-science and Engineering*, Warsaw, Poland, September, 2002.

3) Adamowski K, Bougadis J. Detection of trends in annual extreme rainfall. *Journal of Hydrological Processes*, (in press).

4) Adamowski K, Bougadis J. Influence of trend on short durations design storms. Submitted to the Journal of the Canadian Water Resources, 2003.

5) Adamowski K, Bocci C. 2001. Geostatistical regional trend detection in river flow data. *Journal of Hydrological Processes* **15**: 3331-3341.

6) Adamowski K, Pilon PJ, Alila Y. 1997. Regional short duration rainfall intensity- duration-frequency formula for Canada. In *Proceedings of International Workshop on Rainfall in Urban Area*, Pontresina, Switzerland, 4-7 December, pp 1-2.

7) Acreman MC, Sinclair CD. 1986. Classification of drainage basins according to their physical characteristics: An application for flood frequency analysis in Scotland. *Journal of Hydrology* **84:** 365-380.

8) Alexander GN, Karoly A, Sust AB. 1969. Equivalent distributions with application to rainfall as an upper bound to flood distributions. *Journal of Hydrology* **9**: 322-373.

9) Alila Y. 1994. A regional approach for estimating design storms in Canada. Ph.D Thesis, University of Ottawa, Department of Civil Engineering.

10) Anderson RL. 1942. Distribution of the serial correlation coefficient. *Annals of Mathematical Statistics* **13**: 1-13.

11) Aron G, Wall DJ, White EL, Dunn CN. 1987. Regional rainfall intensity-duration-frequency curves for Pennsylvania. *Water Resources Research* **12**(2): 1563-1569.

12) Bard, E. 2002. "Climate Shock: abrupt changes over millennial time scales." *Physics Today*, Vol. 55, No. 12.

13) Benson MA. 1962. Evolution of methods for evaluating the occurrence of floods. U.S. Geological Survey Water Supply Paper, 1550-A.

14) Bobee B, Robitaille R. 1977. The use of the Pearson Type III and the Log-Pearson Type III distributions revisited. *Water Resources Research* **13** (2): 427-443.

15) Booker PI. 1991. *A Geostatistical Primer*. World Scientific Publishing Co. Pte. Ltd: Singapore.

16) Bruce, J.P., Burton, I., Egener, I.D.M. and Theleb, J. 2002. Investigation of the potential municipal impacts and adaptation measures envisioned as a result of climate change. GCSI-Global change strategies International Inc.

17) Brunetti BM, Buffoni L, Maugeri M, Nanni T. 2000: Precipitation intensity trends in northern Italy. *International Journal of Climatology* **20**: 1017-1031.

18) Buishand TA. 1989. Statistics of extremes in climatology. *Statistica Beerlandica* **43**: 1-30.

19) Burn DH. 1988. Delineation of groups for regional flood frequency analysis. *Journal of Hydrology* **104**: 345-361.

20) Burn DH. 1989. Cluster analysis as applied to regional flood frequency. *Journal of Water Resources Planning and Management* **26**: 2257-2265.

21) Chilès JP, Delfiner P. 1999. *Geostatistics: Modeling Spatial Uncertainty*. John Wiley & Sons: New York.

22) Chowdhury JU, Stedinger JR, Lu L. 1991. Goodness-of- fit tests for regional generalized extreme value flood distributions. *Water Resources Research* **27**: 1765-1776.

23) Cressie NAC. 1993. *Statistics for Spatial Data, Revised Edition.* John Wiley & Sons: New York.

24) Dai A, Trenberth KE, Karl TR. 1997. Hydrological control of diurnal temperature range. *Geophysical Research Letters*, in press.

25) Dalrymple T. 1960. Flood frequency analysis. U.S. Geological Survey Water Supply, Paper 1543-A

26) Daviau JL, Adamowski K, Patry GG. 2000. Regional flood frequency analysis using GIS, L-moment and geostatistical methods. *Journal of Hydrological Processes* **14:** 2731-2753.

27) Davidson AC, Hinkley DV. 1997. *Bootstrap Methods and Their Application.* Cambridge University Press.

28) de Coursey DG. 1973. Objective regionalization of peak flow rates. In *Floods and Droughts, Proceeding of the Second International Symposium in Hydrology*, Fort Collins, Colorado, edited by E.L. Koelzer, V.A. Koelzer, and K. Mahmood, pp. 395-405. Water Resources Publications, Fort Collins, Colorado.

29) de Marsily G, Delhomme JP. 1989. Geostatistics: from mining to hydrology. Université de Paris IV, Proc. Nat'l Conf. Hydraulic Eng., *American Society of Civil Engineers*: 659-666.

30) Douglas EM, Vogel RM, Kroll CN. 2000. Trends in flood and low flows in the United States: impact of spatial correlation. *Journal of Hydrology* **240**: 90-105.

31) Efron B. 1979. Bootstrap methods: another look at the jackknife. *Annals of Statistics* 7(1):1-26.

32) Farhan YI. 1984. Regionalization of surface water catchments in east bank of Jordan. In *Proceedings of the Symposium "Problems in Regional Hydrology"*, University of Freiburg.

33) Farmer EE, Fletcher JE. 1972. Rainfall Intensity-Duration-Frequency Relations for the Kasatch Mountains of Northern Utah. *Water Resources Research* **8**(1): 266-271.

34) Fill HD, Stedinger JR. 1995. Homogeneity tests based upon Gumbel distribution and a critical appraisal of Dalrymple's test. *Journal of Hydrology* **166**: 81-105.

35) Gilbert RO. 1987. Statistical methods for environmental pollution monitoring. Von Nastrand Reinhold Vo.: New York.

36) Gingras D, Adamowski K. 1993. Homogeneous region delineation based on annual flood generation mechanisms. *Hydrological Sciences Journal* **38**(2): 103-121

37) Gingras D, Adamowki K, Pilon P. 1994. Regional flood equations for the provinces of Ontario and Quebec. *Water Resources Bulletin* **30**(1): 55-66.

38) Greenwood JA, Landwehr TA, Matalas NC, Wallis JR. 1979. Probability weighted moments: Definition and relation to parameters of several distributions expressible in inverse forms. *Water Resources Research* **15**: 1049-1054.

39) Groisman PY, Legates DR. 1995. Documenting and detecting long-term precipitation trends: where we are and what should be done. *Climatic Change* **31**: 601-622.

40) Groisman PYa, Karl TK, Easterling DR, Knight RW, Jamason PF, Hennessy KJ, Suppiah R, Page CM, Wibig J, Fortunak K, Razuvaev VN, Douglas A, Førland E, Zhai PM. 1999. Changes in the probability of heavy precipitation: important indicators of climatic change. *Climatic Change* **42**: 243-283.

41) Gruza G, Rankova E. 1999. Indicators of climate change for the Russian Federation. *Climatic Change* **42**: 219-242.

42) Gumbel EJ. 1954. *Statistics of Extremes*. Columbia University Press: New York.

43) Gupta V. 1970. Selection of frequency distribution. *Water Resources Research* **6**(4): 1193-1198.

44) Guttman NB, Wallis JR, Hosking JRM. 1992. Regional temporal trends of precipitation quantiles in the US. *Research Report RC 18453 (80774)*, IBM Research Division, Yorktown Heights, NY.

45) Guttman NB, Hosking JRM, Wallis JR. 1993. Regional precipitation quantile values for the Continental United States computed from L-moments. *Journal of Climate* **6**: 2326-2340.

46) Hanssen-Bauer I, Førland EJ. 1994. Homogenizing long Norwegian precipitation series. *Journal of Climate* **7**: 1001-1013.

47) Hazen A. 1924. Discussion on theoretical frequency curves and their application to engineering problems. Transactions of the *American Society of Civil Engineers* **87**: 143-173.

48) Heino R, Brázdil R, Førland E, Tuomenvirta H, Alexandersson H, beniston M, Pfister C, Rebetez M, Rosenhagen G, Rösner S, Wibig J. 1999. Progress in the study of climatic extremes in Northern and Central Europe. *Climatic Change* **42**: 151-181.

49) Hennessy KJ, Suppiah R, Page CM. 1998. Australian rainfall changes, 1910-1995. *Australian Meteorological Magazine* (in press).

50) Hershfield AM. 1961. Rainfall frequency atlas of the United States for durations from 30 minutes to 24 hours and return periods from 1 to 100 years. *Technical Paper No. 40*, U.S Weather Bureau, Washington, DC.

51) Hogg WD, Carr DA. 1985. Rainfall Atlas for Canada. Atmospheric Environment Services, Environment Canada.

52) Hogg WD, Louie PYT, Nitsoo A, Milewska E. 1997. Gridded water balance climatology for the Canadian Mackenzie Basin GEWEX study area. In *Proceeding of Workshop on "The Implementation of the Arctic Precipitation Data Archive (APDA) at the Global Precipitation Climatology Centre (GPCC)"*, Offenbach, Germany, 10-12 July 1996, WMO/TD-No .804, pp. 47-50.

53) Hosking JRM. 1986. The theory of probability weighted moments. *Research Report RC12210*, IBM, Yorktown Heights, N.Y.

54) Hosking JRM. 1990. L-moments: Analysis and estimation of distributions using linear combinations or order statistics. *Journal of the Royal Statistical Society Series B* **52**: 105-124.

55) Hosking JRM. 1991. Fortran routines for use with the method of L-moments, version 2. *Research Report RC17097*, IBM Research Division, Yorktown Heights, N.Y., 1991.

56) Hosking JRM, Wallis JR. 1993. Some statistics useful in regional frequency analysis. *Water Resources Research* **29**(2): 271-281.

57) Hosking JRM, Wallis JR. 1997. *Regional Frequency Analysis: An Approach Based on L-moments.* Cambridge University Press.

58) Intergovernmental Panel on Climate Change (IPCC). 1996. *Climate Change 1995: The Science of Climate Change. The Second IPCC Scientific Assessment.* J.T. Houghton, L.G. Meira Filho, B.A. Callendar, N. Harris, A. Kattenburg, and K. Maskell, Eds., Cambridge University Press N.Y., pp. 362.

59) Intergovernmental Panel on Climate Change (IPCC). 1998. *The Regional Impacts of Climate Change.* R. Watson, M. Zinyowere, R. Moss, and R. Dokkien, Eds., Cambridge University Press N.Y., pp. 517.

60) International Research Institute (IRI) for climate prediction. Columbia University, Annual Report, 2002-2001.

61) Isaaks EH, Srivastava RM. 1989. *An Introduction to Applied Geostatistics.* Oxford University Press Inc: Toronto.

62) Karl TR, Knight RW. 1995. Trends in high-frequency climate variability in the twentieth century. *Nature* **377**: 217-220.

63) Karl TR, Knight RW, Easterling DR, Quale RG. 1996. Indices of climate change for the United States. *Bulletin of American Meteorological Society* **77** : 279-292.

64) Karl TR, Knight RW. 1998. Secular trends of precipitation amount, frequency, and intensity in the United States. *Bulletin of American Meteorological Society* **79**: 231-241.

65) Karl RK, Easterling DR. 1999. Climate Extremes: Selecting Review and Future research directions. *Climatic Change* **42**: 309-325.

66) Keeping ES. 1966. Distribution-free methods in statistics. Statistical Methods in Hydrology, *Proceedings of Hydrology Symposium No. 5*, McGill University, Montreal, Canada.

67) Kendall MG. 1962. *Rank Correlation Methods*. 3rd ed. Hafner Publishing Company: New York.

68) Kitanidis P K. 1993. Geostatistics, Chapter 20 in *Handbook of Hydrology*, Edited by D. R. Maidment, MacGraw-Hill, New York, pp. 20.1-20.39

69) Klemes V. 1987. Hydrological and Engineering Relevance of Flood Frequency Analysis, in Hydrological Frequency Modeling, edited by V.P. Singh, 1-18.

70) Kumar KK, Deshpande NR, Kumar KR. 1997. Long-term changes in the heavy rainfall events over India. In *Workshop Proceedings on Indices and Indicators for Climate Extremes*, Asheville, NC. Sponsors, GCOS/CLIVAR and WMO.

71) Lambert SJ. 1996. Intense extratropical Northern Hemisphere winter cyclone events: 1899-1991. *Journal of Geophysical Research* **101**: 21319-21325.

72) Landwehr JM, Tasker RD, Jarret RD. 1979. Probability weighted moments compared with some traditional techniques in estimating Gumbel parameters and quantiles. *Water Resources Research* **15**(5) : 1055-1064.

73) Lavery BM, Joung G, Nicholls N. 1997. An extended high-quality historical rainfall dataset for Australia. *Australian Meteorological Magazine* **46**: 27-38.

74) Lettenmaier DP, Wood EF, Wallis JR. 1994. Hydro-climatological trends in the continental United States, 1948-1988. *Journal of Climate* 7: 586-607.

75) Livezey RE, Chen WY. 1983. Statistical field significance and its determination by Monte Carlo techniques. *Monthly Weather Review* **111**: 46-59.

76) Lough JM. 1993. Variations of some seasonal rainfall characteristics in Queensland, Australia: 1921-1987. *International Journal of Climatology* **13**: 391-409.

77) Lough JM. 1997. Regional indices of change: Queensland, Australia. In: *CLIVAR/GCOS/WMO Workshop on indices and indicators for climate extremes*, Asheville, NC, USA, June 3-7.

78) Lu LH, Stedinger JR. 1992. Sampling variance of normalized GEV/PWM quantile estimators: Formulae, confidence intervals, and a comparison. *Journal of Hydrology* **138**: 223-245.

79) Maidment, D.R. (editor in chief). *Handbook of Applied Hydrology*. McGraw-Hill Inc, 1993.

80) Mann HB. 1945. Non-parametric tests against trend. *Econometrica* **13**: 245-259.

81) Matalas NC, Wallis JR. 1973. Eureka! It fits a Pearson Type III distribution. *Water Resources Research* **9**(2): 281-289.

82) Matalas NC, Slack JR, Wallis JR. 1975. Regional skew in search of a parent. *Water Resources Research* **11**: 815-826.

83) Moore DS, McCabe GP. 1993. *Introduction to the Practice of Statistics, 2nd ed.* W.H Freeman and Company, USA, pp. 854.

84) National Environmental Research Council, *Flood Studies Report,* vol.1, London, 1975.

85) Nicholls N, Kariko A. 1993. East Australian rainfall events: interannual variations, trends and relationships with the southern oscillation. *Journal of Climate* **6**: 1141-1152.

86) Nicholls N. 1995. Long-term climate monitoring and extreme events. *Climatic Change* **31**: 231-245.

87) Nicholls N, Gruza G, Jouzel J, Karl TR, Ogallo L, Parker D. 1996. Observed climate variability and change. In: *IPCC 1995. The Second IPCC scientific assessment of climate change,* J.Houghton, and L.Meira Filho, Eds, Cambridge University Press.

88) Pearson CP. 1991a. New Zealand regional flood frequency analysis using L-moments. *Journal of Hydrology (New Zealand)* **28**: 2-10.

89) Pearson CP. 1991b. Regional flood frequency for small New Zealand basins. 2 Flood frequency groups. *Journal of Hydrology (New Zealand)* **30**: 77-92.

90) Pilon PJ, Adamowski,K. 1992. The value of regional information to flood frequency analysis using the method of L-moments. *Canadian Journal of Civil Engineering* **19**: 137-147.

91) Pilon PJ, Alila Y, Adamowski K. 1991. Regional analysis of Annual maxima precipitation using L-moments. *Atmospheric Research Journal* **27**: 81-92.

92) Plummer N, Salinger MJ, Nicholls N, Suppiah R, Hennessy KJ, Leighton RM, Trewin B, Page CM, Lough JM. 1999. Changes in climate extremes over the Australian region and New Zealand during the twentieth century. *Climate Change* **42**: 183-202.

93) Ross RJ, Elliott WP. 1996. Tropospheric water vapor trends over North America: 1973-1993. Submitted to *Journal of Climate.*

94) Royston P. 1991. Which measures of skewness and kurtosis are best. *Statistics in Medicine* **10**: 1-11.

95) Salas JD. 1993. Analysis and Modeling of Hydrological Time Series, Chapter 19 in *Handbook of Hydrology*, Edited by D. R. Maidment, MacGraw-Hill, New York, pp. 20.1-20.39

96) Salas-La Cruz JD. 1972_Information content of the regional mean. In *Proceedings of the International Symposium on Uncertainties in Hydrological and Water Resource Systems*, vol. 2, University of Arizona, Tucson. December 11-14.

97) Salinger MJ, Mullen AB. 1996. CLIMPACTS 95/96: Variability of monthly temperature and rainfall patterns in the historical record, *NIWA Report AK96051*, pp. 21.

98) Schaefer MG. 1990. Regional analyses of precipitation annual maxima in Washington State. *Water Resources Research* **26**(1): 119-131.

99) Sen PK. 1968. Estimates of the regression coefficient based on Kendall's tau. *Journal of the American Statistical Association* **63**: 1379-1389.

100) Shahin M, Van Oorschot HJL, De Lange SJ. 1993. *Statistical Analysis in Water Resources Engineering*. A.A. Balkema Publishers: Netherlands.

101) Singh, VP. 1992. *Elementary Hydrology*. Prentice Hall, Englewood Cliffs, NewYork.

102) Sneyers R. 1977. L'intensite maximale des precipitation en Belgique. Publication Serie B **86**, Bruxelles (in French).

103) Sneyers R. 1978. L'influene du relief sur les valeurs extremes de l'intensite et la duree des precipitations en Belgique. 15 Int. Tag f.alp. Meterogie, Grindwald, 19-23, September, 281-283 (in French).

104) Sneyers R. 1990. On the statistical analysis of series of observations. *Technical Note 143*, WMO-No. 415, pp. 192.

105) Stedinger JR, Tasker GD. 1985. Regional hydrologic analysis 1-ordinary, weighted, and generalized least squares compared. *Water Resources Research* **21**(9): 1421-1432.

106) Suppiah R, Hennessy KJ. 1996. Trends in intensity and frequency of heavy rainfall in tropical Australia and links with southern oscillation. *Australian Meteorological Organization* **45**: 1-17

107) Trenberth KE, Shea DJ. 1996. Atmospheric circulation changes and links to changes in rainfall and drought, 7th conference in climate variations, American Meteorological Society, Long Beach, CA. J14-J19.

108) Uppala S. 1978. Extreme distribution functions for daily and monthly precipitation in Finland. *Geophysica* **15**(1).

109) Vogel RM, Fennessey NM. 1993. L-moment diagrams should replace product moment diagrams. *Water Resources Research* **29**(6): 1745-1752.

110) von Storch H, Navarra A (Eds). 1995. Analysis of climate variability - Applications of statistical techniques. Springer-Verlag: Berlin, 334.

111) Wallis JR, Matalas NC, Slack JR. 1974. Just a moment! *Water Resources Research* **10**(2): 211-219.

112) Wallis JR. 1989. Regional frequency studies using L-moments. *Research Report RC 14597*, IBM.

113) Wang QJ. 1996. Direct sample estimators of L-moments. *Water Resources Research* **32**(12): 3617-3619.

114) Watt WE, Nozdryn-Plotnicki MJ. 1980. Rainfall frequency analysis for urban design. Proceedings Canadian Hydrology Symposium, National Research Centre, Ottawa, Ontario, Canada, 34-52.

115) White EL. 1975. Factor analysis of drainage basins properties: Classifaction of flood behavior in terms of basin geomorphology. *Water resources Bulletin* **11**: 676-687.

116) World Meteorological Organization (WMO). 1981. Selection of distribution types for extreme precipitation. *Operational Hydrology Report No. 15*, WMO-No. 560, Geneva, Switzerland.

117) Wiltshire SE. 1985. Grouping basins for regional flood frequency analysis. *Hydrological Sciences Journal* **30**: 151-159.

118) Wiltshire SE. 1986a. Regional flood frequency analysis I: Homogeneity statistics. *Hydrological Sciences Journal* **31**: 321-333.

119) Wiltshire SE. 1986b. Regional flood frequency analysis II: Multivariate classification of drainage basins in Britain. *Hydrological Sciences Journal* **31**: 335-346.

120) Wu B, Goodridge JD. 1974. On the selection of probability distributions for hydrologic frequency analysis. Paper presented at *American Geophysical Union* fall annual meeting.

121) Wurtele MG, Roe LM. 1978. Fisher-Tippet Representations of extreme rainfall and temperature data. Transactions EOS, *American Geophysical Union* **59**(12): 1603.

122) Yu B, Neil TD. 1993. Long-term variations in regional rainfall in the south-west of Western Australia and the difference between average and high intensity rainfall. *International Journal of Climatology* **13**: 77-88.

123) Zhai P, Eskridge R. 1997. Atmospheric vapor over China. *Journal of Climate* **10**: 2643-2652.

124) Zhai P, Sun A, Ren F, Liu Z, Gao B, Zhang Q. 1999. Changes of climate extremes in China. *Climatic Change* **42**: 203-218.

125) Zhang X, Vincent LA, Hogg WD, Niitsoo A. 2000. Temperature and precipitation trends in Canada during the 20th century. *Atmospheric Ocean* **38**(3): 395-429.

126) Zhang X, Harvey KD, Hogg WD, Yuzyk TR. 2001. Trends in Canadian Streamflow. *Water Resources Research* 37(4):987-998.

127) Zwiers, F.W. and Kharin, V.V. 1998. "Change in the extremes of climate simulated by CCC GCM2 under CO2 Doubling." *Journal of Climate*, 11 (9) :2200-2222.

APPENDIX A

Tables

Table A1: Autocorrelation Coefficients (ACF) for Atikokan Station

Storm Duration	ACF[1] N = 22 years[2]
5 minute	-0.2263
10 minute	-0.1759
15 minute	-0.3411
30 minute	-0.2104
60 minute	-0.0141
2 hour	0.0471
6 hour	0.1608
12 hour	-0.0356

[1] calculated using equation 3.25
[2] significance level calculated to be 0.4179 using equation 3.26 for a record length (N) of 22 years

Table A2: Autocorrelation Coefficients (ACF) for Big Trout Lake Station

Storm Duration	ACF[1] N = 20 years[2]	N = 24 years[2]
5 minute	0.0603	0.2417
10 minute	0.2714	**0.4407**
15 minute	0.2181	0.3958
30 minute	0.4100	0.3245
60 minute	0.3106	0.3494
2 hour	0.0725	0.0880
6 hour	-0.0207	-0.0058
12 hour	-0.0272	0.0477

[1] calculated using equation 3.25
[2] significance level calculated to be 0.4383 and 0.4000 using equation 3.26 for a record length (N) of 20 and 24 years, respectively

Table A3: Autocorrelation Coefficients (ACF) for Bowmanville Station

Storm Duration	ACF[1] N=20 years[2]	N = 25 years[2]	N=31 years[2]
5 minute	-0.2730	-0.2486	-0.1691
10 minute	0.3220	0.3156	0.1894
15 minute	**0.5504**	**0.4923**	**0.3954**
30 minute	**0.6331**	**0.5096**	**0.4435**
60 minute	0.1517	0.0787	0.0511
2 hour	0.3592	0.3167	0.2505
6 hour	0.2512	0.3565	0.3244
12 hour	0.3142	0.3464	0.3472

[1] calculated using equation 3.25
[2] significance level calculated to be 0.4383, 0.3920, and 0.3520 using equation 3.26 for a record length (N) of 20, 25, and 31 years. respectively

Table A4: Mann-Kendall's S and Z Statistic for Atikokan Station

Storm Duration	Record Length = 22 years	
	S^1	Z_s^2
5 minute	-43	-1.1853
10 minute	-37	-1.0151
15 minute	-9	-0.2258
30 minute	-26	-0.7052
1 hour	-39	-1.0724
2 hour	-34	-0.9309
6 hour	-2	-0.0282
12 hour	0	0.0000

[1] Calculated using equation 3.16
[2] Calculated using equation 3.18

Table A5: Mann-Kendall's S and Z Statistic for Big Trout Lake Station

Storm Duration	Record Length = 20 years		Record length = 24 years	
	S^1	Z_s^2	S^1	Z_s^2
5 minute	22	0.6830	85	**2.0872**
10 minute	29	0.9089	61	1.5857
15 minute	36	1.1355	100	**2.4556**
30 minute	23	0.7142	58	1.4147
1 hour	12	0.3569	24	0.5705
2 hour	-5	-0.1300	13	0.2979
6 hour	-8	-0.2282	-15	-0.3478
12 hour	14	0.4218	60	1.4635

[1] Calculated using equation 3.16
[2] Calculated using equation 3.18

Table A6: Mann-Kendall's S and Z Statistic for Bowmanville Station

Storm Duration	Record Length = 20 years		Record Length = 25 years		Record Length = 31years	
	S^1	Z_s^2	S^1	Z_s^2	S_1	Z_s^2
5 minute	21	0.6492	31	0.7008	43	0.7141
10 minute	41	1.2985	46	1.0515	74	1.2413
15 minute	38	1.2017	4	0.0701	17	0.2856
30 minute	27	0.8452	0	0.0000	29	0.4999
1 hour	30	0.9419	64	1.4722	91	1.5306
2 hour	29	0.9089	83	*1.9156*	112	*1.8869*
6 hour	41	1.2985	91	**2.1025**	84	1.4109
12 hour	24	0.7462	58	1.3312	58	0.9689

[1] Calculated using equation 3.16
[2] Calculated using equation 3.18

Table A7: Sites with Significance Levels of Trend Between 5% and 10%

Site	Station Number	Storm Duration	Significance[1]
Bowmanville	6150830	2 hour	94.08
Burketon	6151042	6 hour	94.08
Earfalls	6012198	15 minute	92.86
Fergus S.D.	6142400	6 hour	92.04
Greenwood	6153020	5 minute	90.42
Kapuskasing	6073960	1 hour	92.42
Kapuskasing	6073960	6 hour	93.16
Landsdowne	6014350	12 hour	94.18
Moosonee	6075425	15 minute	90.94
Moosonee	6075425	30 minute	93.94
Niagra Falls	6135638	10 minute	94.78
Niagra Falls	6135638	15 minute	94.76
North Bay	6085700	12 hour	93.66
Oshawa	6155878	5 minute	94.68
Oshawa	6155878	10 minute	93.42
Oshawa	6155878	15 minute	94.44
Oshawa	6155878	2 hour	93.94
Oshawa	6155878	6 hour	94.68
Ottawa Airport	6106000	12 hour	90.84
Owen Sound	6115820	30 minute	94.24
Owen Sound	6115820	1 hour	90.84
Peterborough	6166450	12 hour	90.30
Peterborough A.	6166418	5 minute	91.46
Preston	6146714	5 minute	94.48
Slate Island	6047810	5 minute	91.40
St Catherine	6137287	10 minute	94.74
St Catherine	6137287	12 hour	91.80
Sudbury	6068150	2 hour	90.20
Timmins	6076572	30 minute	94.72
Toronto	6158350	6 hour	93.58
Toronto	6158350	12 hour	94.56
Waterloo	6149387	10 minute	94.72
Waterloo	6149387	15 minute	94.72
Wiarton	6119500	2 hour	93.5
Windsor	6139525	10 minute	93.34
Windsor	6139525	60 minute	94.08
Windsor	6139525	12 hour	93.22

[1] Calculated using equation 3.19

APPENDIX B

Figures

Figure B1: Homogeneous regions for a 10 minute storm for a 20 year time frame

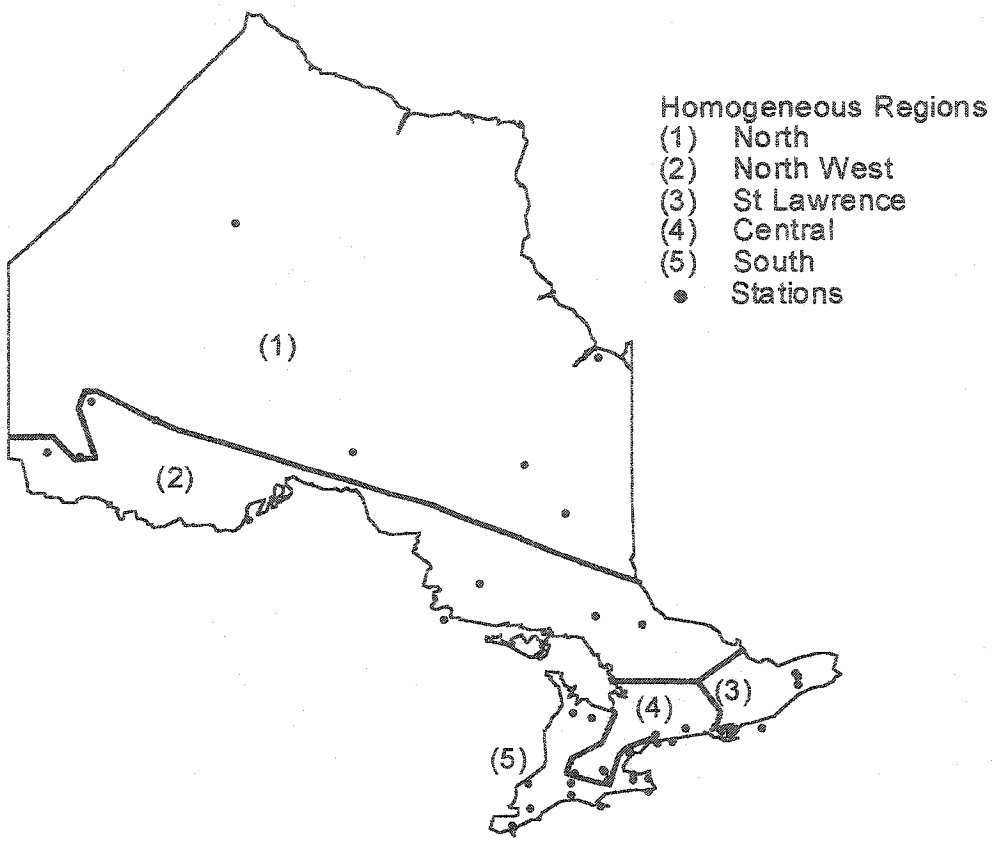

Figure B2: Homogeneous regions for a 10 minute storm for a 25 year time frame

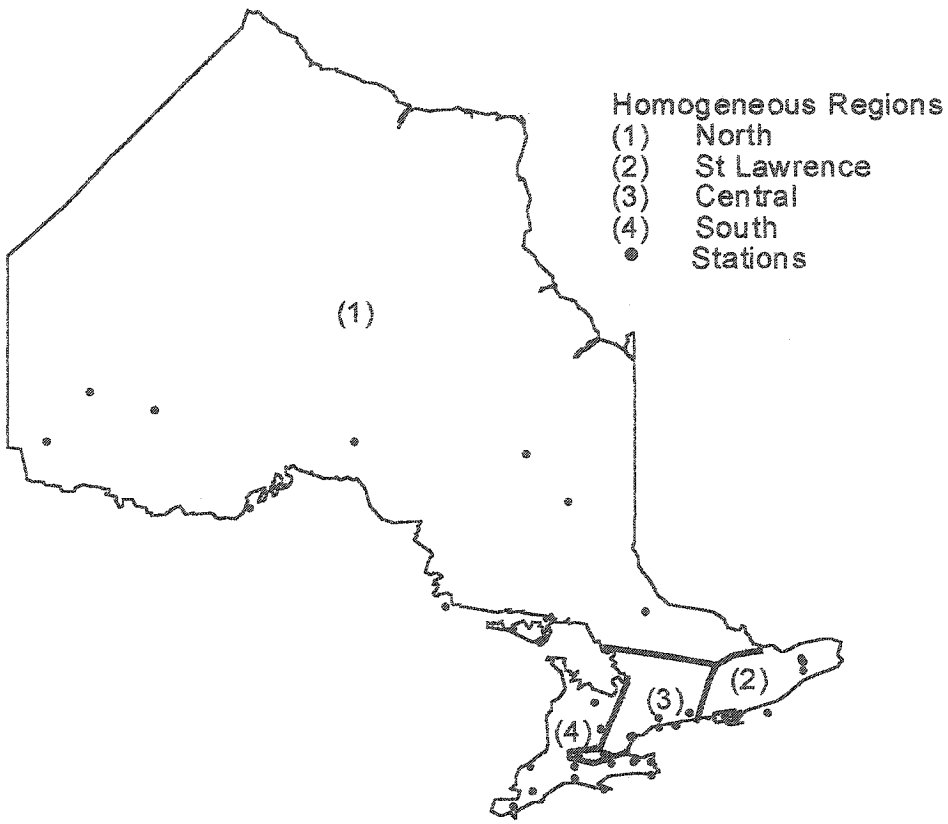

Figure B3: Spatial variations for North 5 minute region (20 year period). Solid lines indicate fitted variogram models.

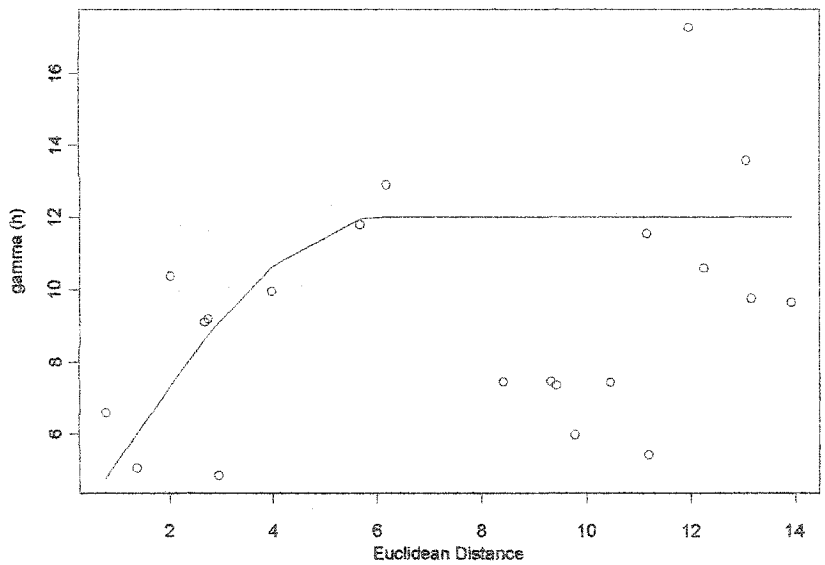

Figure B4: Spatial variations for South 15 minute region (20 year period). Solid lines indicate fitted variogram models.

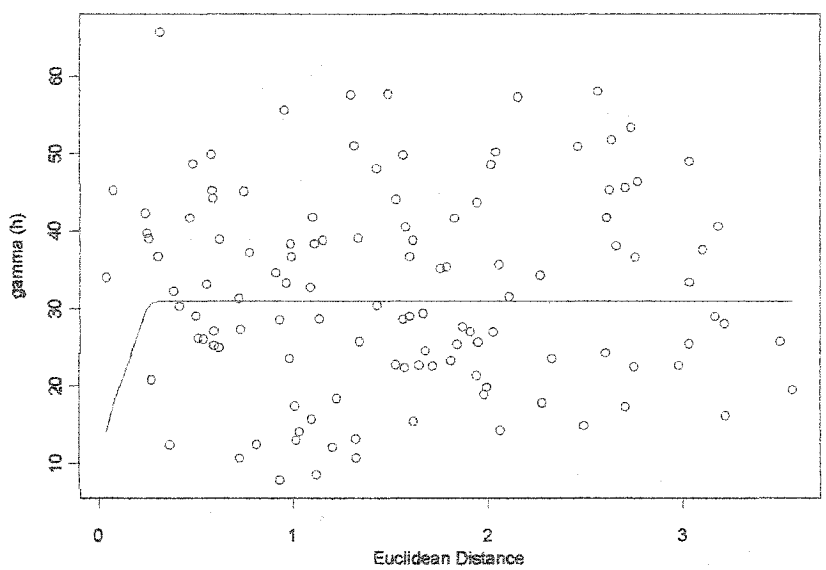

Figure B5: Spatial variations for St Lawrence 2 hour region (25 year period). Solid lines indicate fitted variogram models..

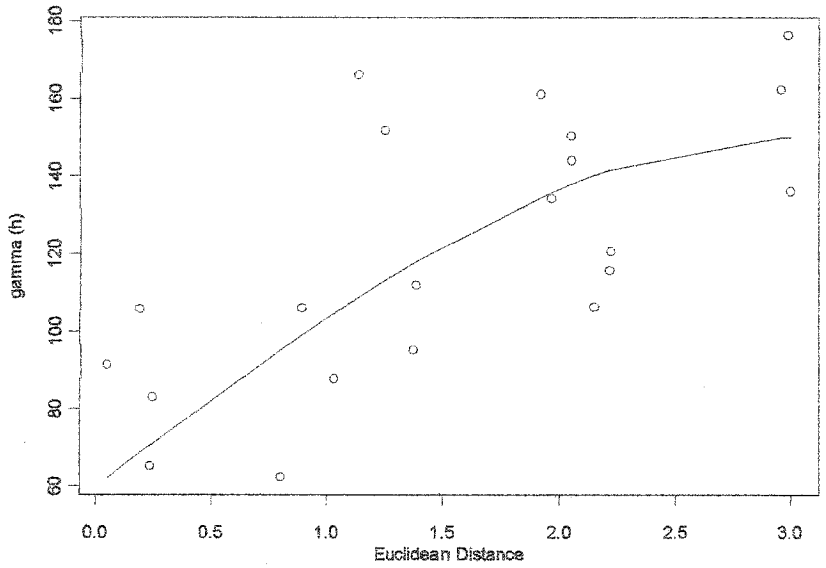

Figure B6: Spatial variations for North 6 hour region (25 year period). Solid lines indicate fitted variogram models

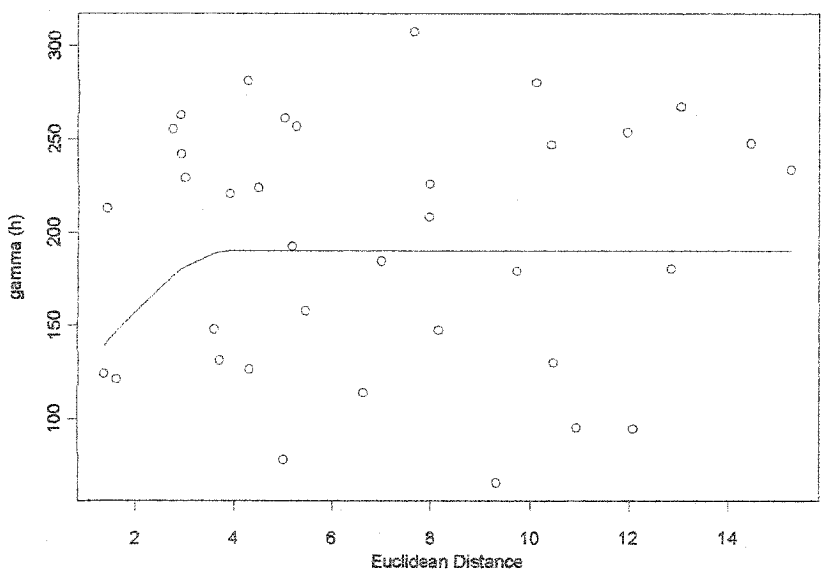

Figure B7: A bootstrapped cumulative distribution function for a 5 minute storm (20 year period) for the Central region.

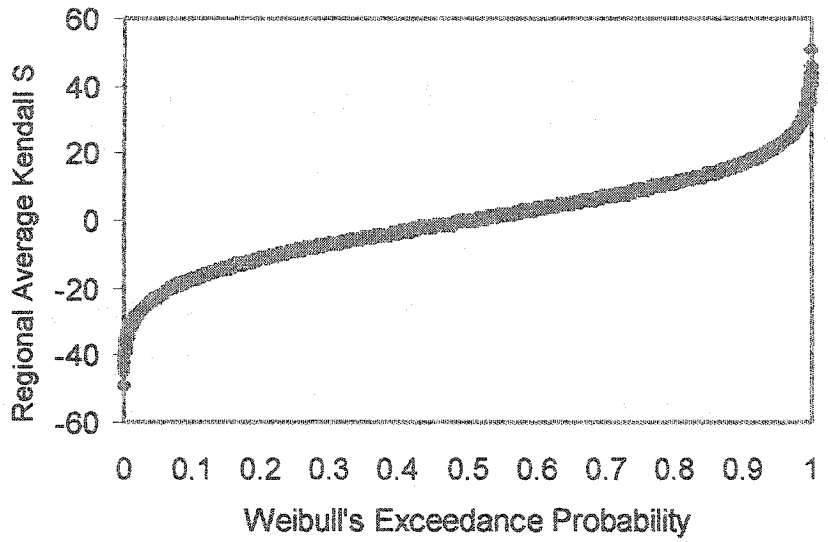

Figure B8: A bootstrapped cumulative distribution function for a 2 hour storm (20 year period) for the St Lawrence region.

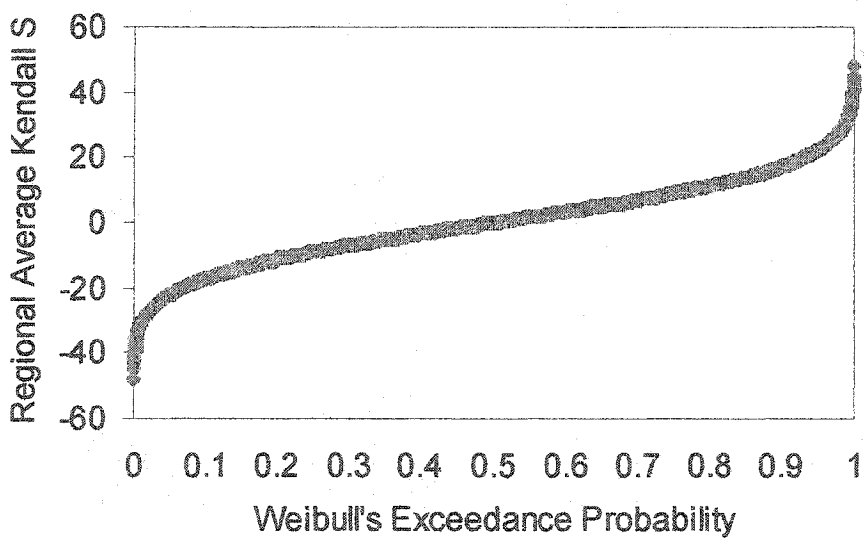

Figure B9: A bootstrapped cumulative distribution function for a 10 minute storm (25 year period) for the Central region.

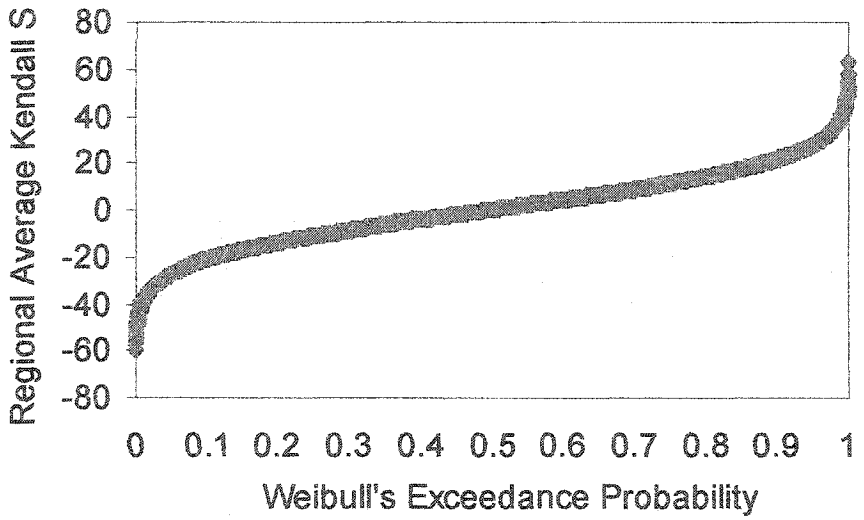

Figure B10: A bootstrapped cumulative distribution function for a 2 hour storm (25 year period) for the St Lawrence region.

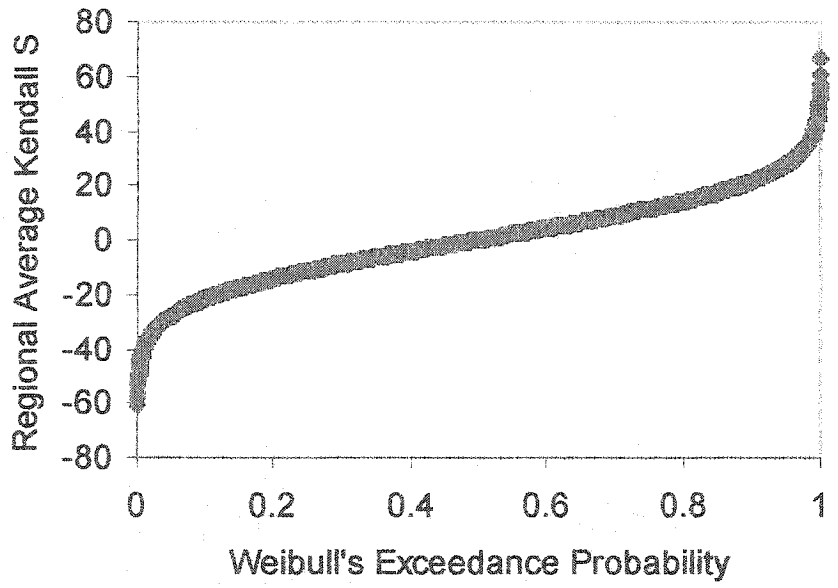

Figure B11: Comparison of raw and pre-whitened data for the 5 minute storm duration for a 20 year period for regions that are serial and spatially independent. Line at 5% level.

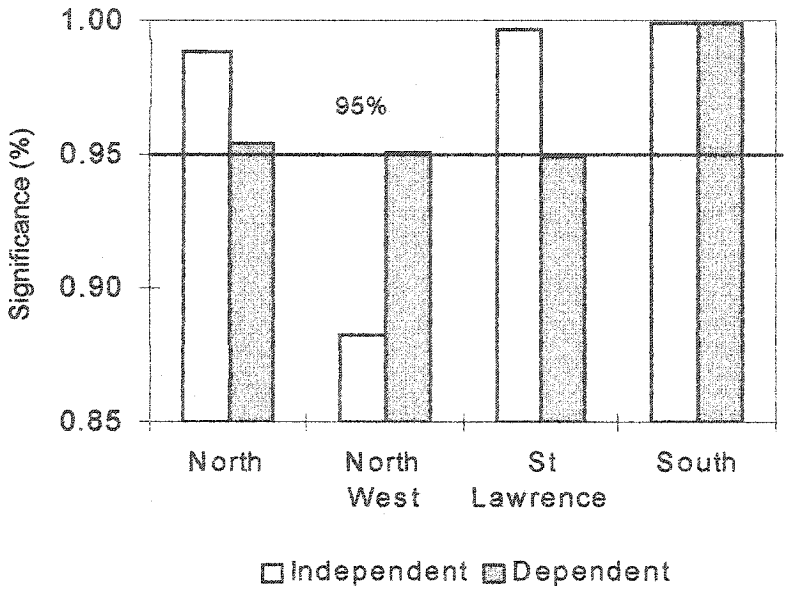

Figure B12: Comparison of raw and pre-whitened data for the 10 minute storm duration for a 25 year period for regions that are serial and spatially independent. Line at 5% level.

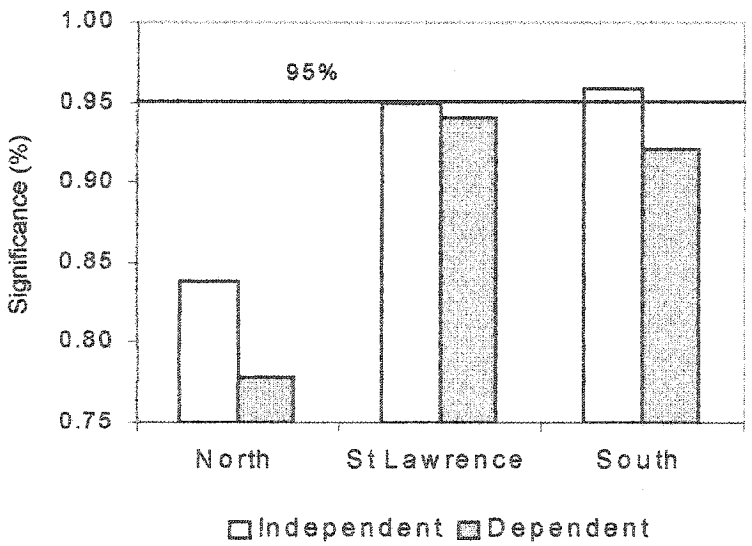

Figure B13: Comparison of spatially correlated (dependent) regions with the assumption of spatial independence. Correlated regions for each duration is listed in table 4.15 for the 25 year period.

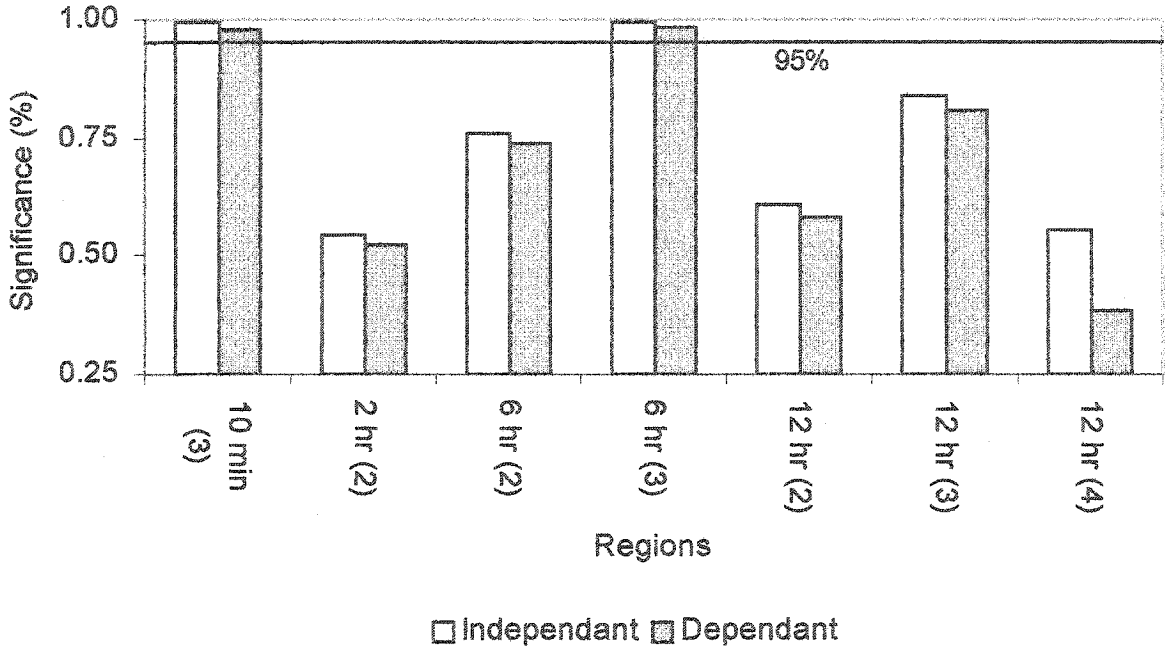

APPENDIX C

Rainfall Stations

Table C1: Stations used in the analysis

Station	ID	Record	Period	Latitude	Longitude
Atikokan	6020379	22	1967 - 1988	48°°45'	91°°37'
Big Trout Lake	6010738	24	1967 - 1990	53°°50'	89°°52'
Bowmanville	6150830	31	1968 - 1998	43°°55'	78°°40'
Brantford	6140954	35	1961 - 1995	43°°08'	80°°14'
Brockville	6100971	24	1967 - 1990	44°°36'	75°°40'
Burketon	6151042	30	1969 - 1998	44°°02'	78°°48'
Campbellford	6151137	25	1973 - 1997	44°°18'	77°°48'
Caribou Island	6041221	23	1966 - 1988	47°°20'	85°°50'
Cental Patricia	6016525	37	1953 - 1989	51°°27'	90°°13'
Chalk River	6106400	34	1961 - 1994	45°°59'	77°°26'
Chatham	6131415	33	1966 - 1998	42°°23'	82°°12'
Cornwall	6101901	37	1957 - 1993	45°°02'	74°°48'
Delhi CDA	6131982	34	1962 - 1995	42°°52'	80°°33'
Ear Falls	6011298	39	1952 - 1990	50°°38'	93°°13'
Elora	6142285	22	1970 - 1991	43°°39'	80°°25'
Fergus Shan	6142400	31-37	1962(68) - 1998	43°°44'	80°°20'
Geraldton	6042716	39	1952 - 1990	49°°47'	86°°56'
Greenwood	6153020	23	1970 - 1992	43°°54'	79°°04'
Guelph	6143069	37	1954 - 1990	43°°33'	80°°13'
Hamilton A	6153194	28	1971 - 1998	43°°10'	79°°56'
Hamilton RBG	6153300	34	1963 - 1996	43°°17'	79°°53'
Kapuskasing	6073960	25	1966 - 1990	49°°24'	82°°26'
Kemptville	6104025	27	1970 - 1996	45°°00'	75°°38'
Kenora	6034075	25	1966 - 1990	49°°47'	94°°22'
Kingston	6104175	38	1961 - 1998	44°°14'	76°°29'
Landsdowne	6014350	18	1971 - 1988	52°°14'	87°°53'
Lindsay	6164432	24	1965 - 1988	44°°21'	78°°44'
London	6144475	47	1952 - 1998	43°°02'	81°°09'
Mississaggi	6055210	20	1971 - 1990	46°°26'	83°°23'
Moosonee	6075425	23	1968 - 1990	51°°16'	80°°39
Niagra Falls	6135638	26	1965 - 1990	43°°08'	79°°05'
North Bay	6085700	27	1964 - 1990	46°°19'	79°°28'
Orillia	6115820	27	1965 - 1991	44°°37'	79°°25'
Oshawa	6155878	29	1970 - 1998	43°°52'	78°°50'
Ottawa CDA	6105976	40	1959 - 1998	45°°23'	75°°43'
Ottawa Int"l A	6106000	32	1967 - 1998	45°°19'	75°°40'
Owen Sound	6116132	32	1965 - 1996	44°°35'	80°°56'
Peterborough	6166450	28	1976 - 1992	44°°17'	78°°19'
Peterborough A	6166418	28	1971 - 1998	44°°14'	78°°21'
Picton	6156533	30	1966 - 1995	44°°01'	77°°08'
Port Colborne	6136606	34	1964 - 1997	42°°53'	79°°15'

Table C1: (continued)

Station	ID	Record	Period	Latitude	Longitude
Preston	6146714	25	1971 - 1995	43°°23'	80°°21'
Rawson Lake	6036904	20	1971 - 1990	49°°39'	93°°43'
Sarnia	6127514	28	1970 - 1997	43°°00'	82°°19'
Sault Ste Marie	6057593	29	1962 - 1990	46°°29'	84°°30'
Sioux Lookout	6037775	28	1963 - 1990	50°°07'	91°°54'
Slate Island	6047810	23	1967 - 1989	48°°37'	87°°00'
St Catherine	6137287	28	1971 - 1998	43°°12'	79°°15'
St Thomas	6137362	73	1926 - 1998	42°°77'	81°°10'
Stratford	6148105	33	1966 - 1998	43°°22'	81°°00'
Sudbury	6068150	20	1971 - 1990	46°°37'	80°°48'
Thunderbay	6048261	39	1952 - 1990	48°°22'	89°°19'
Timmins	6076572	39	1952 - 1990	48°°28'	81°°16'
Toronto	6158350	59	1940 - 1998	43°°40'	79°°65'
Toronto Ellesmere	6158520	29	1966 - 1994	43°°46'	79°°16'
Toronto Island A.	6158665	24	1971 - 1994	43°°38'	79°°24'
Toronto Old Weston	6158764	22-25	1966 - 1987(90)	43°°39'	79°°28'
Toronto Pears. A	6158733	49	1950 - 1998	43°°40'	79°°61'
Toronto Shelbourne	6158406	28	1966 - 1993	43°°39'	79°°21'
Trenton	6158875	33	1965 - 1997	44°°07'	77°°32'
Waterloo	6149387	28	1971 - 1998	43°°27'	80°°23'
Wiarton	6119500	25	1973 - 1998	44°°45'	81°°06'
Windsor	6139525	53	1946 - 1998	42°°16'	82°°58'

Table C2: Station data for IDF estimates and return period

Station	Station ID	Latitude	Longitude	Record Length	Period
Big Trout Lake	6010738	53°°50'	89°°52'	24	1967-1990
Bowmanville	6150830	43°°87'	78°°24'	30	1968-1998
Burketon	6151042	44°°02'	78°°48'	30	1969-1998
Chalk River	6106400	45°°59'	77°°26'	34	1961-1994
Delhi	6131982	42°°52'	80°°33'	34	1962-1995
Kingston	6104175	44°°14'	76°°29'	38	1961-1998
Moosonee	6075425	51°°16'	80°°39'	23	1968-1990
Orillia	6115820	44°°37'	79°°25'	27	1965-1991
Oshawa	6155878	43°°83'	78°°94'	29	1970-1998
Port Colborne	6136606	42°°85'	79°°15'	34	1964-1997
Preston	6146714	43°°24'	80°°25'	25	1971-1995
Sarnia	6127514	43°°00'	82°°18'	28	1970-1997
Sudbury	6068150	46°°37'	80°°48'	20	1971-1990
Timmins	6076572	48°°34'	81°°22'	39	1952-1990
Waterloo	6149387	43°°29'	80°°31'	28	1971-1998

Table C3: Stations and time frames for regional analysis

Station	Identification Number	Record Length[1]				
		1966-1995	1971-1995	1976-1995	1966-1990	1971-1990
Big Trout Lake	6010738					x
Bowmanville	6150830		x	x		
Brantford	6140954	x	x	x		
Burketon	6151042		x	x		
Campbellford	6151137			x		
Chatham	6131415	x	x	x		
Delhi CDA	6131982	x	x	x		
Ear Falls	6011298				x	x
Fergus Shan Dam	6142400	x	x	x		
Geraldton	6042716				x	x
Hamilton A	6153194		x	x		
Hamilton RBG	6153300	x	x	x		
Kapuskasing	6073960				x	x
Kemptville	6104025		x	x		
Kenora	6034075				x	x
Kingston	6104175	x	x	x		
London	6144475	x	x	x		
Mississaggi	6055210					x
Moosonee	6075425					x
NorthBay	6085700				x	x
Oshawa	6155878		x	x		
Ottawa CDA	6105976	x	x	x		
Ottawa Int"l A	6106000		x	x		
Owen Sound	6116132	x	x	x		
Peterborough A	6166418		x	x		
Picton	6156533	x	x	x		
Port Colborne	6136606	x	x	x		
Preston	6146714		x	x		
Rawson Lake	6036904					x
Sarnia	6127514		x	x		
Sault Ste Marie	6057593				x	x
Sioux Lookout	6037775				x	x
St Catherine	6137287		x	x		
St Thomas	6137362	x	x	x		
Stratford	6148105	x	x	x		
Sudbury	6068150					x
Thunderbay	6048261				x	x
Timmins	6076572				x	x
Toronto	6158350	x	x	x		
Toronto Pears. A	6158733	x	x	x		
Trenton	6158875	x	x	x		
Waterloo	6149387		x	x		
Wiarton	6119500			x		
Windsor	6139525	x	x	x		

[1] x indicates availability of data for a station and periods used in regional analysis

APPENDIX D

COMPUTER PROGRAMS

Program D1: Mann-Kendall Test Statistic

```
# this program calculates the Mann-Kendall Statistic S for Ottawa CDA(6105976) at a
# significance level (alpha) of 5%.

station<-6105976
alpha<-.05

#functions: sgn - assigning +1,-1, or 0 for the Mann-Kendall test; flow - displays the data as a
#nx2 matrix (time and rainfall data); naord - omits any NA at the beginning of the data.

sgn<-function(x){ if (x>0){-1} else if (x==0){0} else{1}}
flow<-function(stn){lawr[lawr$stnid==stn ,c("year","five.min")]}
ord<-function(stn){flow(stn)[order(flow(stn)["year"]),]}
naord<-function(stn){na.omit(ord(stn))}

#length of rainfall series (p); W is the rainfall data separated from the flow matrix.

W<-function(stn){naord(stn)[1:n(stn),"five.min"] }
p<-function(stn){length(W(stn))}

#calculate M-K statistic

aux_rep(1,p(station))%o%W(station) - W(station)%o%rep(1,p(station))
aux2_aux[col(aux)<row(aux)]
psum<-sapply(aux2,sgn)
sum(psum)

#Displays results
cat("The S variable is ",sum(psum),"\n")
```

D2: Modified Mann-Kendall Test

```
# this program calculates the Mann-Kendall Statistic S for Kingston (6104187) at a
# significance level (alpha) of 5%.

station<-6104175
alpha<-.05

##functions: sgn - assigning +1,-1, or 0 for the Mann-Kendall test; flow - displays the data as a
#nx2 matrix (time and rainfall data); naord - omits any NA at the beginning of the data.
```

```
sgn<-function(x){ if (x>0){1} else if (x==0){0} else{-1}}
flow<-function(stn){south20reg[south20reg$stnid==stn ,c("year","five.min")]}
ord<-function(stn){flow(stn)[order(flow(stn)[,"year"]),]}
naord<-function(stn){na.omit(ord(stn))}

# Determines the autocorrelation of the time series and selects the first order (lag 1)
#autocorrelation.

corr<-function(stn){acf(ord(stn)[,"five.min"],plot=F)}
lag1<-function(stn){corr(stn)$acf[[2]]}

#length of rainfall series (p); W is the rainfall data separated from the flow matrix and a #the
series with the first order autocorrelation removed.

W<-function(stn){naord(stn)[2:n(stn),"five.min"]- lag1(stn)*naord(stn)[1:(n(stn)-1),"five.min"]}
p<-function(stn){length(W(stn))}

#calculate M-K statistic
S<-0

aux_rep(1,p(station))%o%W(station) - W(station)%o%rep(1,p(station))
aux2_aux[col(aux)<row(aux)]
psum<-sapply(aux2,sign)
sum(psum)

#Displays the results
cat("The S variable is ",sum(psum),"\n")
```

D3: Variograms

```
#This program computes an omnidirectional variogram for the north region, 20 year time frame.
#It calculates the variogram of gamma_b + gamma_s of rainfall data over all time

#A file called ERIOD contains all stations and geographic location with in Ontario.  Stations
#belonging into a region are selected from the ERIOD file with their time frame, longitude, and
#latitude, respectively.

stations<-c(6,7,9,10:14)
tframe<-1971:1990
loc<-eriod[c(stations),c("latitude","longitude")]

#Opens up the spatial module which exist in S-Plus to fit the observed data to a linear, gaussian,
```

```
#or exponential variogram

var.fun<-function(gamma,distance,range,sill){ gamma- exp.vgram(distance, range=range,sill=sill)}
vargs.fun<-function(gamma,distance,range,sill){ gamma-gauss.vgram(distance, range=range,
sill=sill)}
varlin.fun<-function(gamma,distance,slope){gamma-linear.vgram(distance, slope=slope)}

#Omits any NA at the beginning of the data.  NAs throughout the time series were replaced by
#an average.  N function is the length of the rainfall series; W is the rainfall data for a station in
#the defined region. Datpiece is the rainfall data along with the stations number for all stations
#in a region, assembled into a matrix.

data<-function(stn){northg[northg$STNID==stn, c("year","ten.min")]}
ord<-function(stn){data(stn)[order(data(stn)[,"year"]),]}
naord<-function(stn){na.omit(ord(stn))}
n<-function(stn){dim(naord(stn))[[1]]}
W<-function(stn){naord(stn)[1:n(stn),"ten.min"] }
datpiece<-sapply(stations,W)

# Computes the gamma variable of the datpiece matrix

p.jul<-function(i){data.matrix((datpiece[,i]-datpiece[,(i+1):dim(datpiece)[[2]]])^2)}
ps.jul<-function(i){apply(p.jul(i),2,sum,na.rm=T)}
gammabs<-0

for (i in 1:(length(stations)-1)){
      nacount<-apply(apply(p.jul(i),2,is.na),2,sum)
      good<-length(tframe) - nacount
      g<-ps.jul(i)/(2*good)
      cat("",g,"\n")
      gammabs<-append(gammabs,g)
      #cat(round(gammabs,3),"\n")}

# The separation distance is computed as a euclidean distance and matched with its
#corresponding gamma variable

gammabs<-gammabs[-1]
distvec<-dist(as.matrix(loc))
vjul<-cbind(distvec,gammabs)
dimnames(vjul)<-list(NULL,c("distance","gamma"))
vjul<-as.data.frame(vjul)
vj<-vjul[order(vjul["distance"]),]
```

```
#Various optimum fitting variograms

#optvj.lin<-nls(~varlin.fun(gamma,distance,slope),data=vj, start=list(slope=.4))
#optvj.exp<-nls(~var.fun(gamma,distance,range,sill),data=vj, start=list(range=1,sill=2))
#optvj.gau<-nls(~vargs.fun(gamma,distance,range,sill),data=vj, start=list(range=1,sill=2))

#Output of a plot of the semivariogram

plot(vj$distance,vj$gamma,xlab="Space lag (years)",ylab="V_ij")
title("semivariogram")
#lines(vj$distance, linear.vgram(vj$distance,slope=optvj.lin$parameters["slope"]))

lines(vj$distance, spher.vgram(vj$distance,range=4,sill=15,nugget=2))
```

D4: Bootstrap Algorithm

```
#this program calculates the Mann-Kendall Statistic S and bootstrap replicates for Oshawa

options(object.size=9e6)

#mean of the average S statistic must have a mean of zero, therefore, the while loop is used to
#satisfy this condition.

while(sum(psum)!=0) {

#functions: sgn - assigning +1,-1, or 0 for the Mann-Kendall test; flow - displays the data as a
#nx2 matrix (time and rainfall data); naord - omits any NA at the beginning of the data.

station<-6158875
sign<-function(x){ if (x>0){-1} else if (x==0){0} else{1}}
flow<-function(stn){south20reg[south20reg$stnid==6158875,c("year","five.min")]}
ord<-function(stn){flow(stn)[order(flow(stn)["year"]),]}
naord<-function(stn){na.omit(ord(stn))}

#length of rainfall series (p); W is the rainfall data separated from the flow matrix.

W<-function(stn){naord(stn)[1:n(stn),"five.min"]}
p<-function(stn){length(W(stn))}

# The rainfall series was re-sampled (called a) and assigned a variable called JJ to be used to
#determine the kendall S statistic.
a_sample(W(stn), replace=T)
```

```
JJ_a
cat("samples",a,"\n")
cat("samples",JJ,"\n")

#calculate M-K statistic with the re-sampled rainfall series

psum<-0
aux_rep(1,p(station))%o%JJ - JJ%o%rep(1,p(station))
aux2_aux[col(aux)<row(aux)]
psum<-sapply(aux2,sign)
sum(psum)

#if the re-sampled rainfall time series has a S of zero, then the loop is broken and the bootstrap
#procedure takes place with the next commands.  If the re-sampled S is not zero, then the
#procedure is repeated until the re-sampled rainfall series is zero.

cat("the sum of psum is",sum(psum),"\n")
}

#the bootstrap function is called doug.  The aux2 matrix contained the nested for loop required
#in the Mann-Kendall S statistic.  The bootstrap time series having an average S of zero is re-
#sampled 5000 times (B) and the S values for each sample is stored.

doug<-function(rain){
psum<-sapply(aux2,sign)
sum(psum)}

temp_bootstrap(aux2, doug, B = 5000,  trace = T, assign.frame1 = T, save.indices = T)
```